From the Department of Neurophysiology

of the Centre for Biomedicine und Medical Technology Mannheim

of the Medical Faculty Mannheim

Director: Prof. Dr. med. Rolf-Detlef Treede

Mechanisms of heat-gated nociception in primary and dorsal horn sensory neurons of the rat.

Inauguraldissertation

zur Erlangung des

Doctor scientiarum humanarum

der Medizinischen Fakultät Mannheim

der Ruprecht-Karls-Universität zu

Heidelberg

vorgelegt von

Paulina Nuñez-Badinez

aus

Santiago de Chile

2018

Dekan: Prof. Dr. med. Sergij Goerdt
Referent: Prof. Dr. med. Rolf-Detlef Treede

to my beloved husband to be

TABLE OF CONTENTS

ABBREVIATIONS

AC-DC	Alternating Current/Direct Current	DNA	Deoxyribonucleic Acid
AMH	A-fiber Mechano Heat nociceptor	DPG	German Physiological Society
ANOVA	Analysis Of Variance	DRG	Dorsal Root Ganglion
AP	Action Potential	E001	Extracellular solution
cAMP	cyclic Adenosine Monophosphate	EC_{50}	Half maximal effective concentration
CBTM	Centre of Biomedicine and Medical Technology Mannheim	EEG	Electroencephalography
CLVM	Caudal Ventrolateral Medulla	EFIC	European Federation of Pain
CMH	C-fiber Mechano Heat nociceptor	FBS	Fetal Bovine Serum
CNS	Central Nervous System	FCS	Fetal Calf Serum
CV	Conduction Velocity	FURA	Fura-2-acetoxymethyl ester
DAAD	German Academic Exchange Service	GABA	Gamma-Aminobutyric Acid
DAMGO	(D-Ala^2, N-Me-Phe^4, Gly-ol)-enkephalin	GDP	Guanosine Diphosphate
DGSS	German Pain Society	GFP	Green Fluorescent Protein
DIC	Differential Interference Contrast	GPCR	G protein–coupled receptor
DMEM	Dulbecco's Modified Eagle Medium	GTP	Guanosine Triphosphate
DMSO	Dimethyl sulfoxide	HCN	Hyperpolarization-activated cyclic nucleotide–gated

HEK293	Human Embryonic Kidney 293 cells	MEM	Modified Eagle Medium
HT	High Threshold	MOR	µ-Opioid-Receptor
HTM	High Threshold Mechanosensitve	NaCl	Sodium Chloride
HTMR	High Threshold Mechanoreceptor	NaOH	Sodium Hydroxide
i.d.	inner diameter	Nd:YAG	Neodymium-doped Yyttrium Aluminium Garnet
i.p.	intraperitoneal	NS	Nociceptive Specific neuron
i.v.	intravenous	NT	non-transfected
IASP	International Association for the Study of Pain	NTS	Nucleus Tractus Solitarius
IL	Interleukin	o.d.	outer diameter
ISI	Inter Stimulus Interval	PAG	Periaqueductal Grey matter
KCl	Potassium Chloride	PBS	Phosphate Buffered Saline
L4	Lumbar 4	PI	Percentage of Inhibition
LEP	Laser Evoked Potentials	PKA	Protein Kinase A
LPb	Parabrachial area	PS	Pregnenolone Sulphate
LS	Laser Sensitive	RA	Rapidly Adapting
LTM	Low Threshold Mechanosensitive	RF	Receptive Field
LTMR	Low Threshold Mechanoreceptor	RNA	Ribonucleic Acid

ROI	Region of Interest	TRPM3	Transient Receptor Potential channel subfamily M member 3
rpm	rotation per minute	TRPV1	Transient Receptor Potential channel of the Vanilloid receptor type, subtype 1
RT	Room Temperature	TTL	Transistor-transistor logic
RTX	Resiniferatoxin	VMpo	posterior part of the Ventro-Medial nucleus
SA	Slowly Adapting	VPI	Ventro-Postero-Inferior nucleus
SEM	Standard Error of the Mean	VPL	Ventro-Postero-Lateral nucleus
SII	Second somatosensory cortex	WDR	Wide Dynamic Range
SP	Substance P	WT	wild type
TG	Trigeminal Ganglion		

1   INTRODUCTION

1.1   Nociception and Pain

1.1.1   Definitions

The International Association for the Study of Pain (IASP) defined *pain* as "an unpleasant sensory and emotional experience associated with actual or potential tissue damage, or described in terms of such damage". Moreover, they defined *nociception* as "the neural process of encoding noxious stimuli", noticing that: "Consequences of (this) encoding may be autonomic (e. g. elevated blood pressure) or behavioral (motor withdrawal reflex or more complex nocifensive behavior)", and "pain sensation is not necessarily implied"[3].

While it is possible from the first definition to understand that pain – being a sensory and emotional experience – involves brain processing, it is also possible from the second definition to infer that it occurs before signals reach the brain and, therefore, "pain sensation is not necessarily implied". Then again, nociception and pain could be understood as two different parts of the same phenomena, nociception occurring in a first place, and pain as a result. Although this is often in fact the case, nociception and pain may occur separately from each other as well, in which "pain may be experienced in the apparent absence of a stimulus and there may be activity in nociceptors in the absence of pain"[3]. The concept of pain, in spite of the validity of this definition, is still under debate[4].

Figure 1 depicts the somatosensory pathways for non-noxious and noxious stimuli. When potentially damaging (so called noxious) stimuli of different types (thermal, mechanical or chemical) are present at the terminals of the sensory neurons (which are located at the skin or innervating tissues) at a degree that reaches the threshold of sensory transduction molecules located at those terminals, then nociception begins. The transduction molecules open and change the local membrane potential and depolarize, which in turn elicits action-potential propagation along the peripheral neuron, passes the soma of the neuron (located either at the dorsal root (DRG) or trigeminal ganglia (TG)), and reaches the dorsal horn of the spinal cord, synapsing with a dorsal horn neuron. Finally, dorsal horn neurons integrate and propagate the received noxious signals and transmit them to higher brain areas through the spinothalamic tract to the thalamus, and once the electric signal reaches specific areas in the brain, stimuli are perceived as being painful[5, 6].

1.2   Primary sensory neurons

Primary sensory neurons are remarkably long cells present in the peripheral nervous system, with cell bodies located at the TG and DRG and their axons grouped together along peripheral nerves that innervate the head and the rest of the body (such as skin, articulations and viscera). At peripheral nerves these neurons are arranged into a heterogeneous population of different axon calibers, determined by its fiber diameter and myelination degree, which provides them with different conduction velocities. Based on these anatomical and functional criteria, the primary afferent fibers can be categorized into three different classes[5]: Large, myelinated cutaneous afferents, known as Aβ-fibers, are rapidly conducting low-threshold mechanoreceptors which normally respond to innocuous stimuli (like touch or hair movement) applied to the skin, muscle and joints. Fine myelinated and unmyelinated afferents,
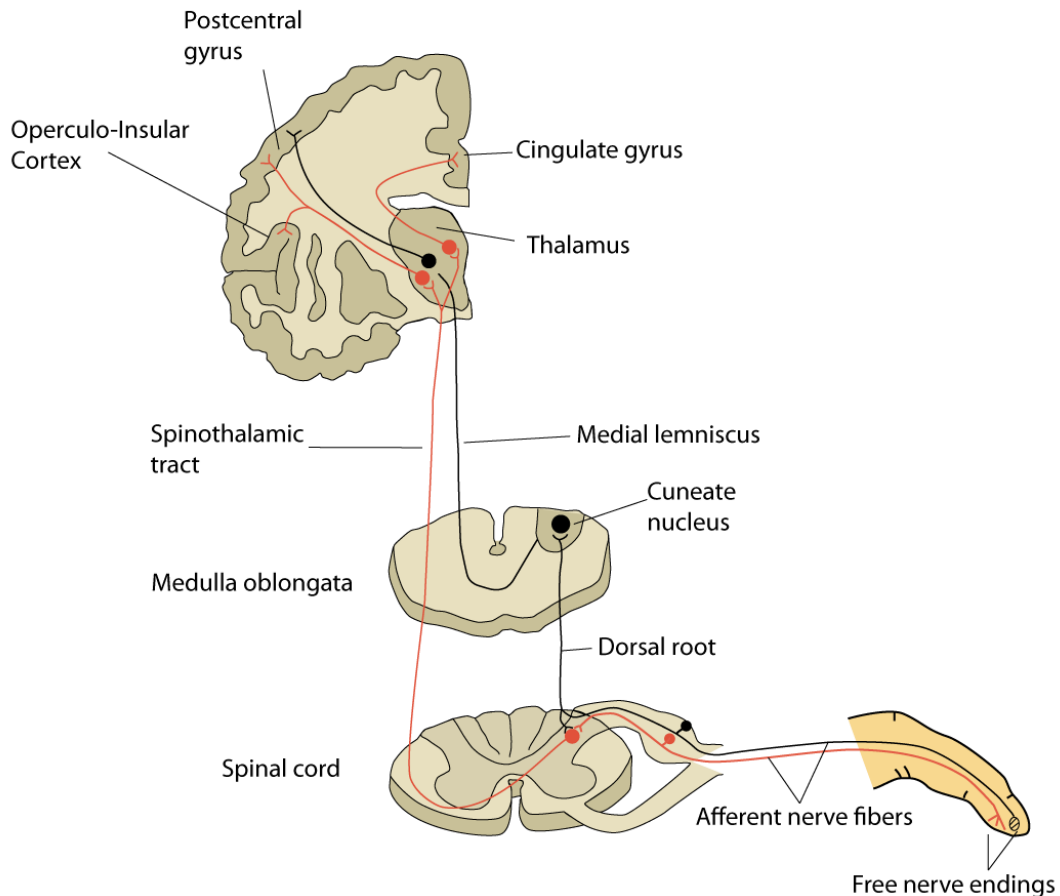
Figure 1: Somatosensory system. Tactile and proprioceptive systems (in black) project via large fibers in the peripheral nerve, the dorsal columns of the spinal cord and the medial lemniscus in the brainstem. Nociceptive and thermoreceptive systems (in red) project via small fibers in the peripheral nerve and via the spinothalamic tract in the spinal cord and brainstem. Both pathways project via VPL to the primary sensory cortex and via VPI to the secondary somatosensory cortex. In addition, the nociceptive and thermoreceptive systems project via VMpo to the dorsal insula. VPL:ventro-postero-lateral nucleus; VPI: ventro-posteroinferior nucleus; VMpo: posterior part of the ventromedial nucleus. Modified from [2].

known as Aδ-fibers and C-fibers, are medium and small diameter fibers that conduct noxious stimuli at intermediate and slower velocities, compared to Aβ fibers. Most of the Aδ-fibers and C-fibers are nociceptors or thermoreceptors[5, 7] and respond to noxious stimulation. Among nociceptors innervating the skin, Aδ- and C-fibers can be further classified depending on their responsiveness to the different noxious modalities[8]. Aδ- fibers that normally respond only to noxious mechanical stimuli and to noxious heat (53 °C) under sensitization are defined as A fiber mechano-heat nociceptor (AMH) type I, and Aδ- fibers that normally respond to both noxious mechanical and noxious thermal stimuli (over 46 °C) are called AMHs type II. The latter also responds to noxious chemical substances, but they are only present on hairy skin[9].

Due to its polymodal quality, AMH fibers are similar to C-fiber mechano-heat nociceptors (CMHs), since both are able to respond to a wide range of noxious mechanical stimulation as well as noxious heat and noxious chemicals. The difference is simply that the latter are present in both hairy and glabrous skin and have different anatomical and conduction properties. The receptive fields of CMHs are usually be-

tween 1-2 mm in diameter[8] and those areas colocalize for each modality[10]. There is evidence that some C fiber nociceptors preferentially respond to one stimulus modality, and therefore polimodality is widely distributed among different degrees on CMHs[8, 11]. C-fiber nociceptors can be further sub-classified into two groups: one group is able to express and secrete neuropeptides, like substance P, and are called peptidergic C-fibers, while the others do not express neuropeptides and are called nonpeptidergic C-fibers.

Primary afferents terminate in the dorsal horn of the spinal cord with a defined distribution pattern (Figure 2) determined by their functional class[7, 12]. Aβ tactile and their afferents end mainly in lamina III-V, with some extension to lamina II. Aδ hair follicle afferents arborize on either side of the border between lamina II and lamina III, and Aδ nociceptors end mainly in lamina I, with some giving branches to lamina V and X. Peptidergic primary afferents (which also include some Aδ nociceptors) arborize mainly in lamina I and lamina IIo, with some fibers penetrating more deeply, whereas most non-peptidergic C fibers form a band that occupies the central part of lamina II[7, 12].

All primary afferents use glutamate as their principal fast transmitter and therefore have an excitatory action on their postsynaptic targets[7].

1.2.1 Heat-activated ion channels in primary sensory neurons

In sensory neurons, detection and transmission of heat stimuli requires the co-ordinated activity of many different ion channels: background and voltage-gated K^+ channels are thought to ensure negative voltage over the plasma membrane when the stimulus is absent, voltage-gated Na^+ channels are thought to generate action potentials when a certain voltage threshold is crossed, and one or more depolarizing ion channels that are thought to open in response to heat such that the action potential threshold can be reached [13].

TRP channels are a group of ion channels that serve as sensors for a wide range of physical and chemical stimuli. In free nerve endings, an increase in heat activates a specific group of nociceptors that are characterized by the expression of heat-and capsaicin-activated TRP channel TRPV1. However, since the ablation of TRPV1 in mice does not completely take away their ability for heat detection, some other ion channels might also be involved in noxious pain perception[14].

1.2.1.1 The TRPV1 channel

The transient receptor potential channel of the vanilloid receptor type, subtype 1 (TRPV1) is a non-selective cation channel widely expressed in the central and peripheral nervous system that contributes to normal and pathological pain[15]. The TRPV1 channel is formed as a tetrameric quaternary structure and their subunits possess 6 transmembrane domains and a pore domain between the fifth and sixth transmembrane domain [16]. In each subunit, the N- and C-terminal domains (both intracellular) have available phosphorylation/dephosphorylation sites as well as interaction sites with other proteins[17]. In the peripheral nervous system, the receptor is preferentially expressed in the C-fiber nociceptors in the TG[18, 19] and DRG[20, 21], and it is also expressed, in a lesser extent, in Aδ-fiber nociceptors [22].
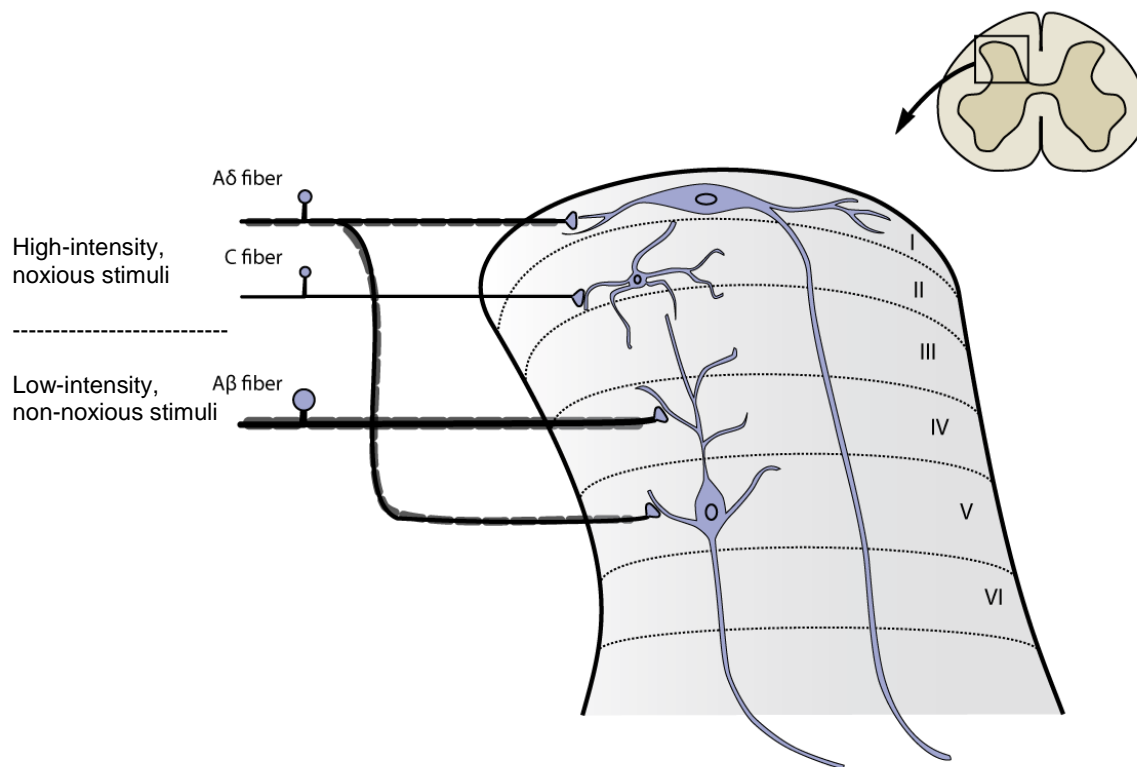
Figure 2: Nociceptive afferent fibers terminate on projection neurons in the dorsal horn of the spinal cord. Projection neurons in Lamina I receive direct input from myelinated (Aδ) nociceptive afferent fibers and indirect input from unmyelinated (C) nociceptive afferent fibers via *stalk cell interneurons* in lamina II. Lamina V neurons are predominantly of the wide dynamic-range type. They receive low-threshold input from the large-diameter myelinated fibers (Aβ) of mechano-receptors as well as both direct and indirect input from nociceptive afferent fibers (Aδ and C). In this figure the lamina V neuron sends a dendrite up through lamina IV, where it is contacted by the terminal of an Aβ primary afferent. A dendrite in lamina III arising from a cell in lamina V is contacted by the axon terminal of a lamina II interneuron. Modified from [1]. Laminar boundaries are shown by dashed lines.

The TRPV1 channel can be activated by capsaicin, resiniferatoxin (RTX), noxious heat (> 43 $^{\circ}$ C), extracellular acidification and various lipid molecules[15, 23, 24]. The activation of the channel temperature induces the firing of action potentials which propagates towards the dorsal horn or sensory nucleus in the brain, where sensory information is relayed to second-order neurons and which subsequently results in pain sensation and lowering of body temperature[14].

The involvement of the TRPV1 channel in pain processing has been widely studied over the last decades[25]. The ability to integrate multiple concomitant stimuli and to possess channel activity coupling to downstream signal amplification processes through calcium permeation and membrane depolarization allows TRPV1 channels in nociceptive neurons to function as a sensor in both normal and pathological conditions[26]. The TRPV1 receptor is upregulated in DRG neurons after inflammation[27, 28], and mice lacking the TRPV1 receptor show deficits in thermal hyperalgesia[22, 29], showing a direct role in contribution to pain perception under inflammatory conditions. Moreover, an increase in TRPV1 expression and function was observed in DRG of rodents in colorectal cancer pain, inflammatory nociception, and others[30, 31]. Consequently, pharmacological studies in animals treated with drugs that

block TRPV1[32, 33], or small-interference RNA (siRNA) that reduce its expression [34] have also shown a reduction in inflammatory pain and in chronic neuropathic pain. Several up-to-date TRPV1 antagonists have been developed, and they have shown a reduction in neuropathic and inflammatory pain in animal models[33, 35-40]; nonetheless, at clinical level these antagonists have shown partial or modest efficacy on healthy volunteers[41-43] and unwanted side-effects such as increase in core body temperature (>40 °C) [44, 45], a compromised noxious heat response, which increases the risk of accidental burns [41, 46, 47].

Mutant null mice TRPV1^{-/-} respond poorly to chemical stimulations, present impaired acute pain detection and show deficits in their thermoregulation ability[22, 48-50]. Additionally, these animals under inflammatory conditions display reduced secondary hyperalgesia[51]. However, it has also been shown normal acute heat detection in TRPV1^{-/-} mice[52]. In humans, using a functional blockade of TRPV1^{+} nerve fibers and psychophysical experiments, it was observed that laser-induced heat nociception was completely abolished[53]. These apparent contradictory effects might be explained by the following facts: by one side, it is known that capsaicin-insensitive A-fiber nociceptors may also mediate hyperalgesia in neuropathic pain conditions[53]. By the other side, the test stimuli used influences the readout observed: since rapid near-infrared laser-heat stimulation is the standard way to measure heat pain testing in humans[54, 55] able to reach temperature steps of several Celsius degrees in factions of seconds[2, 56], much slower heating is used in most animal experiments. Since heat activated channels act fast upon stimulation, rapid heat ramps through laser stimulation are more suitable for its study.

1.2.1.2 The TRPM3 channel

Heat-induced nociception involves the activation and interaction of more than only one type of TRP receptor activation[13]. Intensive research has been done to elucidate which other ion channels are implicated in this process, and if so, what is their distribution, and what are their specific roles in sensory neurons and possible cooperation mechanisms. The TRPM3 receptor (Transient Receptor Potential Melastatin-3), together with TRPV1 and other members of the TRPV family, is a divalent-permeable cation channel present in sensory neurons[57-61], as well as kidney, brain, testis and spinal cord[62]; and has been shown to be essentially thermosensitive[57], as well as to have other biological functions in mechanoregulation and vasorelaxation[62]. Moreover, since the mutant mice lacking TRPM3 channel have severe deficits in the development of inflammatory hyperalgesia[57], and inhibitors of TRPM3 such as liquiritigenin, diclofenac, or flavanones like isosakuranetin show strong antinociceptive properties[59, 60, 63, 64], the TRPM3 channel has emerged as a candidate to act in response to noxious heat[13, 14, 57, 61]. Therefore, understanding the molecular mechanisms that control TRPM3 channel activation by noxious heat in sensory neurons would provide valuable information for development of new strategies to treat acute pain.

The TRPM3 channel can be selectively activated by the neurosteroid Pregnenolone Sulphate (PS) and the dihydropyridine Nifedipine [65]. Sill it is unclear whether endogenous PS concentrations in the sensory system can reach levels that activate TRPM3 in vivo[65]. Therefore, it was proposed that other physiologically relevant stimuli might cause nociception mediated by activation of the TRPM3 channel, and found that the channel can be activated by noxious heat at 40 °C and that trpm3^{-/-} mice ex-

hibit reduced sensitivity to noxious heat, demonstrating that the channel is specifically required for heat sensation[57].

1.2.2 The μ-opioid receptor as a potential pharmacological target for treatments against acute pain

Opioid receptors belong to the superfamily of G protein–coupled receptor (GPCR) and the subfamily of rhodopsin receptor[66]. Opioid receptors are expressed by central and peripheral neurons, among other cell types [67]. The signaling pathways of opioid receptors are well characterized[67]. Once the ligand binds to the receptor, conformational changes allow coupling of mainly $G_{i/o}$-proteins to the intracellular C-terminus of opioid receptors. At the G_α subunit, GDP is replaced by GTP and a dissociation of the trimeric G-protein complex into G_α and $G_{\beta\gamma}$ subunits occurs. Afterwards these subunits can inhibit adenylyl cyclase and thereby cyclic adenosine monophosphate (cAMP) production, and/or directly interact with diverse ion channels in the membrane. Ion-channels are mainly regulated via $G_{\beta\gamma}$ -subunits [68]. Opioid receptors modulate various Ca^{2+} channels; suppress Ca^{2+} influx and the excitation and/or neurotransmitter release.

Opioids produce their analgesic effect primarily by interacting with the G-protein coupled μ-opioid receptor (MOR)[69], which is present in small-diameter DRG neurons and the superficial layer of the dorsal horn. Once activated, MOR receptors are able to prevent presynaptically the excitatory release of glutamate and/or neuropeptides on those peripheral neurons upon noxious stimuli, and therefore provide an antinociceptive effect[67, 70]. Some of the downstream targets of MOR in peripheral nerves known up to date are voltage-gated Na^+ channels, HCN channels, K^+ channels and TRPV1 channels, among others[71-76], mostly by interrupting their regulation by the cAMP/PKA pathway. It has also been reported that sustained interactions with the TRPV1 channel might be associated in the development of morphine tolerance[69].

Agonists of the μ-opioid receptor (MOR) are nowadays the most powerful analgesic drugs clinically available, being especially prescribed for acute pain conditions, like postoperative pain management, or in terminal conditions[77]. However, these drugs when misused, may cause several side effects like antinociceptive tolerance[78] and addiction[69, 77, 79].

1.3 Dorsal horn neurons

Dorsal horn neurons from the spinal cord are neurons belonging to the central nervous system that receive and integrate sensory input from primary afferent neurons, and that respond to specific types of noxious and non-noxious stimuli[7]. On these neurons, connections from primary neurons are converged and processed by complex circuits involving *excitatory and inhibitory interneurons* which integrate multiple inputs in a single coordinated action. As a consequence of this processing, the resulting signal is transmitted either to *projection neurons* for relay in several brain areas, or to the ventral horn, in which case they contribute to spinally-mediated nocifensive reflexes[7]. At the dorsal horn, the balance between excitation and inhibition is crucial for maintaining normal sensory function, and therefore understanding the neuronal circuits between primary afferents and projection neurons has key conse-

quences in the development of therapies against the onset and maintenance of inflammatory and neuropathic pain[7].

Interneurons correspond to the dorsal horn neurons whose axons remain in the spinal cord and arborize locally. They comprise the vast majority of neurons in laminae I-III. They can be inhibitory, using GABA and/or glycine as their main neurotransmitter, or excitatory, using glutamate as their main neurotransmitter. Projection neurons, in contrast, possess cell bodies which are located in lamina I and between lamina III-VI and their axons extend to several brain regions, like some thalamic nuclei, the caudal ventrolateral medulla (CVLM), the nucleus of the solitary tract (NTS), the parabrachial area (LPb), and the periaqueductal grey matter (PAG)[7].

Depending on their synaptic input, three different classes of dorsal horn neurons can be found. If a neuron possesses only Aβ fiber input, then this neuron is only the recipient of primary afferent activity in response to non-noxious mechanical stimulation at its receptive field, and conversely it is not able to respond to noxious stimulation. This group of neurons is called low threshold mechanosensitive (LTM). If a neuron possesses only nociceptive input (nociceptive Aδ and C fibers), then this neuron is only the recipient of primary afferent activity in response to noxious stimulation and conversely it is unable to respond to non-noxious stimulation. This second group of neurons is called nociceptive specific (NS) or high threshold mechanosensitive (HTM). There is a third group of neurons that possess both Aβ- as well as Aδ- and C- fiber input and are able to respond to both non-noxious and noxious stimulation in a graded manner. Those neurons are called wide dynamic range (WDR)[12].

NS and WDR neurons are located in both superficial (lamina I) and deep (lamina IV to VI) layers of the dorsal horn, and they function in both exteroceptor-initiated (that is activated by objects in the external environment) and interoceptor-initiated (that is activated by bodily changes in the internal environment) pain[80]. The differences in fiber input in those neurons give them different response properties. WDR neurons show different activity patterns (frequency of action potentials discharge) upon non-noxious vs. noxious stimulation: its activity increases as the strength of the stimulation increases, encoding the distinction between non-noxious and noxious stimulation. On the other hand, as the majority of NS neurons receive input from multiple types of nociceptive afferent neurons, they are not able to distinguish between different kinds of noxious stimulation[80]. It is important to keep in mind that within the dorsal horn both excitatory and inhibitory interneurons, as well as astrocytes and microglia under pathological conditions, can modify the response of NS and WDR cells, and thereby the output of the dorsal horn[12].

The signal transmissions occur through neurons in the dorsal horn of the spinal cord to neurons of the spinothalamic tract. In this level, dorsal horn high threshold (HT) neurons and wide dynamic range (WDR) neurons are involved. These nociceptive dorsal horn neurons are located at the laminae I, II and IV-VI, where high threshold A-delta mechanoreceptors (lamina I and IV-VI) and polymodal high threshold C-nociceptors (lamina II) terminate[81, 82]. Both neuron types respond by increasing discharge rate when heating increases to skin temperatures in the noxious range [83]. However, some differences in properties exist in those neurons: while responses of WDR neurons can encode small differences in nociceptive temperatures, for HT neurons this does not occur[84]. Moreover, the mechanosensitive receptive fields of those neurons have been reported to be large for WDR neurons, encompassing the whole foot and part of the leg, and in HT neurons the receptive fields are substantially

smaller[84]. Likewise, it has been indicated that nociceptive-specific HT neurons function as providers of information about the quality and spatial localization of noxious stimuli, while WDR neurons are responsible for the speed of detection and encode the intensity of noxious stimuli[83-86].

1.4   Laser stimulation as a method for nociception studies

Heat-induced nociception involves activation of high-threshold thermosensitive free nerve endings of sensory neurons (transduction), mediated by opening of receptor proteins located in their plasmatic membrane. Heat stimuli above the temperature threshold of the receptor leads to depolarization of the neuron. Depolarization, in turn, lead to opening of voltage gated sodium channels, which give rise to action potential (AP) discharges[87, 88]. These action potentials code for stimulus intensity by their firing frequency, and are transmitted via Aδ- and C- fibers to dorsal horn neurons in the spinal cord and consecutively to the brain, where the pain is sensed[5, 89-92].

The reasons to use laser stimulation rather than other means of heat stimulation are fourfold in nature: it is a natural stimulus (heat), it is reliable in means of stimulus parameters and response characteristics, its stimulation modes (intensity, duration or area stimulated) are adjustable, and it does not produce tissue damage on subjects at intensities normally used, so it can be used in different skin areas[89, 93]. Therefore, it has been used as a tool to study neural mechanisms of thermal pain sensation without concurrent activation of mechanoreceptive afferents[94 95 2, 96]. Moreover, laser stimulation elicit clear potentials in human brain [55] as well as in other mammals [97-99], activating in a synchronized way the anterior cingulate cortex and suprasylvian region (parietal operculum, SII), among other brain areas [89, 93, 100].

Laser-induced heat has been used as noxious thermal stimulation to observe cortical activity (EEGs) [97, 101-119]; and since lesions causing neuropathic pain mostly concern the pain-temperature pathways, it has been considered the easiest and most reliable neurophysiological method of assessing nociceptive function in health and disease [120, 121].

Depending on the wavelength of emission, skin transmission properties and blood flow, different penetration depths on the skin after laser stimulation can be reached: while for CO_2 infrared lasers (10600 nm) emission is absorbed already in the first 100 μm of superficial skin layer[122], Argon and Copper laser emissions (488-515 nm and 510-577 nm) are able to reach in average 250 and 400 μm skin depth, crossing the dermal/epidermal border. Nd:YAG (neodymium-doped yttrium aluminium garnet) laser emissions (1064-2000 nm) are able to penetrate deeper into the skin, being in average 700 μm and reaching up to 3.7 mm skin depth[89]. Depth penetration in the skin for near-infrared emissions (1475 nm) is on average 1.25 mm[123], were 72% absorbed in epidermis (up to 120 μm depth), 20% in dermis (0.120 – 4 mm depth) and 8% in subcutaneous tissue[124]. Considering that receptor depth for cutaneous C-fiber nociceptors are estimated to be located between 150-200 μm depth[125], as well as Aδ nociceptors, both in hairy and glabrous skin[126], near infrared emissions are able to heat homogeneously their free nerve endings throughout the skin layers.

Since a wide range of laser stimulators have been developed so far (most common ones described above: 1.4 *Laser stimulation as a method to activate heat-gated*

ion channels), the results obtained from them have shown different aspects of the nociceptive pathway. Studies using laser stimulation to investigate single neuron properties in primary afferents have been performed extensively during recent decades[10, 50, 56, 94, 95, 113, 114, 118, 127-130]. Bromm and colleagues measured microneurographic recordings of primary afferents in the radial nerve in response to laser-heat stimulation on the receptive fields of identified units and observed that the largest receptor class which was activated by CO_2 laser stimuli were polymodal C-nociceptors[114]. Then, Treede and coworkers found that the sizes of mechanosensitive and heat-sensitive receptive fields of polymodal C-nociceptors in monkeys are virtually equal[10]. Five years later; the same working team identified two different types of mechano- and heat- sensitive A-fiber nociceptors (AMH) innervating the hairy skin of the monkey, having AMHs type I a temperature threshold of 53 °C and type II of 46 °C[9]. A comparative study using infrared diode laser stimulation (980 nm wavelength, 200-400 ms duration time) of DRG primary neurons and psychophysical measures in healthy volunteers has shown that the use of infrared laser stimulation in both rats and humans is a reliable method for the study of laser-heat activated nociception in the periphery, having the thresholds for heat-evoked currents similar (41 °C) between cultured neurons or pain sensation in human volunteers[131]. Using a skin-nerve preparation of mouse and infrared laser stimulation Pribisko and Pearl recorded a high proportion of nociceptors with C-afferent fiber response latencies, and only a few of them with A-afferent fiber response latencies to laser stimulation[132].

Studies using laser-heat as a model to investigate the nociceptive system at the dorsal horn of the spinal cord[133-135], and at the brain[91, 99, 110, 114, 115, 127, 136-143], used laser with beam diameters down to 1 mm. While Devor and coworkers observed mainly that dorsal horn neurons responding to laser-heat stimuli were located in superficial and deep zones from the dorsal horn, and were able to evoke potentials through signals mediated by C- polymodal nociceptors[133]; Sikandar and collaborators extended those observations by recordings in dorsal horn neurons in the spinal segment L4-L5 in rodents and detected response latencies to different laser intensities mediated by both C- (in all power intensities) and Aδ- fiber afferents (only at higher power intensities)[134]. By ablating TRPV1^{+} afferents in mice, Zhang and collaborators observed impairment in the responsiveness to noxious heat of nociceptive dorsal horn neurons[135].

All those studies have demonstrated that laser stimulation is a type of noxious heat stimulation and its transmission occurs exclusively on nociceptive neurons; however, regarding the properties of the mechanosensitive receptive fields of those neurons very little information is available. Specific information about heat-sensitive receptive fields has only been documented in polymodal cutaneous C-fiber nociceptors in monkeys, where the mechanosensitive receptive fields coincided in size to the laser-heat sensitive receptive fields[10], but no information has been given regarding laser-heat sensitive receptive fields in dorsal horn neurons[133].

1.5   Question and Aims

The nociceptive system protects mammals against -even putative- tissue damaging so- called noxious stimuli. Noxious heat is such a natural stimulus, cold, mechanical and chemical stimuli are other potentially harmful stimuli making proper protection in essential daily life. Furthermore, mechanisms underlying acute pain do contribute to longer lasting pain states such as inflammatory or neuropathic pain. Studies on heat transduction mechanisms have been using laser stimulation as a mean of heat delivery, mainly because of the following advantages: it is contactless, rapidly increasing and short lasting, provides responses with high temporal and spatial resolution and enables the possibility to observe LEPs in humans.

Until now, extensive research characterized the capsaicin-receptor TRPV1 (transient receptor potential channel of the vanilloid receptor subfamily, subtype 1), which is present in nociceptors and is activated beyond several other stimuli by noxious temperatures above 42 °C. Whereas TRPV1 alone is not sufficient to induce heat pain alone, other heat-sensitive transduction channels co-expressed in the same fiber with TRPV1 are essential for the detection of heat pain. Furthermore, knowledge regarding processing of those stimuli when entering the central nervous system is limited further offering putative targets for the pharmacological treatment of those pain states.

Thus, this study intends to expand the knowledge on mechanisms of heat-induced nociception using near-infrared laser stimulation as a rapid, accurate and appropriate way to deliver noxious heat pulses. Responses to laser-heat will be analyzed at functionally different levels: either at single molecule level (*in vitro* on heterologous expression systems measuring excitability via microfluorimetric live-cell calcium imaging), at single nociceptor level using primary sensory neurons of rats as well as using a more physiological model in vivo, i.e. electrophysiological recordings within the dorsal horn of the spinal cord upon peripheral noxious and non-noxious sensory stimulation of the hind paw in living Sprague-Dawley rats. The following main questions will be addressed specifically:

-Do brief laser-heat stimuli activate the membrane channel TRPM3, if so, which are its activation characteristics compared to TRPV1?

-Does laser-heat activation of TRPM3 also play a role for noxious heat detection in native primary sensory neurons?

-Is there a direct affection of the TRPM3 activation by heat and chemical via activation of peripherally co-expressed MORs?

-Which are the characteristics of the dorsal horn neurons responding to laser-heat stimulation regarding frequencies and location of responding cells?

-Which are the response and functional characteristics of the laser sensitive neurons?

-What type of afferents encode the laser-induced responses?

Hypothesis:

In primary neurons, laser-heat stimuli are sensed by TRPV1$^+$ and/or TRPM3$^+$ neurons. In the dorsal horn, only neurons that possess nociceptive afferent input (composed of fibers containing those ion channels) respond to noxious laser stimulation. In the same way as in the periphery, the laser-sensitive neurons show receptive fields for mechanical stimulation and for laser stimulation with same location and size.

2   MATERIALS AND METHODS

2.1   Materials

2.1.1   Chemicals

2.1.1.1   Commercial Chemicals

Name	Manufacturer
Accutase	PAA (Austria)
Agar-agar	Carl Roth (Germany)
Albumin standard (BSA)	Thermo Scientific™ (USA)
Ampicillin	Bioline GmbH (Germany)
B-27	PAA (Austria)
BSA Fraction V pH 7.0	PAA (Austria)
Calcium Chloride	Carl Roth (Germany)
Capsaicin	Sigma Aldrich (Germany)
Collagen 0.1%	Sigma Aldrich (Germany)
Collagenase (from *Clostridium histolyticum*) Type V	Sigma Aldrich (Germany)
Collagenase CLS II	Biochrom (Germany)
DAMGO	Sigma Aldrich (Germany)
DMEM/F-12	Sigma Aldrich (Germany)
DMSO	Carl Roth (Germany)
D-PBS 1 x Gibco®	Invitrogen™ (USA)
DTT 0.1 M	Invitrogen™ (USA)
Ethanol 100%	Sigma Aldrich (Germany)

F12–Dulbecco's modified Eagle's medium	Sigma (Germany)
FBS Gibco®	Invitrogen™ (USA)
FCS	PAA Laboratories (Austria)
Fetal Bovine Serum	GIBCO
FURA-2AM	Merk KGaA (Germany)
Geneticin	Sigma Aldrich (Germany)
Glucose	Carl Roth (Germany)
Glycerol (99%)	Sigma Aldrich (Germany)
HEPES	Carl Roth (Germany)
Horse serum	PAA (Austria)
Isoflurane	AbbVie (Germany)
Isopropanol	Merck (Germany)
Kanamycin	Bioline (Germany)
Ketamin	Intervet (Germany)
Laminin	Sigma Aldrich (Germany)
L-Glutamine	PAA (Austria)
Liquemin 5000	Ratiopharm (Germany)
Magnesium Chloride	Carl Roth (Germany)
MEM	Invitrogen™ (USA)
Methanol	Carl Roth (Germany)
NaCl 0.9%	Fresenius Kabi (Germany)
NaHCO3	Carl Roth (Germany)

Nerve Growth Factor	Invitrogen™ (USA)
Neurobasal medium	Invitrogen™ (USA)
OptiMEM	Invitrogen™ (USA)
Pancuronium bromide	Inresa (Germany)
PBS 10x	Invitrogen™ (USA)
Penicillin/streptomycin	Sigma Aldrich (Germany)
Phosphatase Inhibitor	Sigma Aldrich (Germany)
Phosphatase Inhibitor Cocktail 2	Sigma Aldrich (Germany)
Pluronic F-127	Merk KGaA (Germany)
Poly-L-Lysine	Carl Roth (Germany)
Potassium Chloride	Carl Roth (Germany)
Pregnenolone sulphate	Sigma Aldrich (Germany)
SDS	Carl Roth (Germany)
Silicon oil M100Roth	Carl Roth (Germany)
Silicone Gel Dow Corning 111	Dow Corning Corporation (USA)
Sodium Chloride	Carl Roth (Germany)
Sodium Hydroxide	Carl Roth (Germany)
Trapanal®	Inresa (Germany)
Trypsin	Sigma –Aldrich (USA)
Verapamil	Santa Cruz Biotechnology (USA)

2.1.1.2 In house created chemical solutions and buffers

Buffer/Solutions	Components
Tyrode	137.6 mM NaCl
	5.4 mM KCl
	0.5 mM MgCl
	1.8 mM $CaCl_2$
	5 mM D-glucose
	10 mM HEPES
High Potassium Solution 1 (K 140 mM)	140 mM KCl
	3 mM NaCl
	0.5 mM $MgCl_2$
	1.8 mM $CaCl_2$
	10.0 mM Hepes
	5.0 mM D-glucose
E001 solution (Ringer's solution modified)	145 mM NaCl
	10 mM CsCl
	3 mM KCl
	2 mM $CaCl_2$
	2 mM $MgCl_2$
	10 mM HEPES
	10 mM D-glucose
High Potassium Solution 2 (K 75 mM)	70 mM NaCl

	10 mM CsCl
	75 mM KCl
	2 mM $CaCl_2$
	2 mM $MgCl_2$
	10 mM HEPES
	10 mM D-glucose
BSA solution	25 mL DMEM
	3 g BSA

2.1.2 Kits

Name	Manufacturer
Wizard® Plus Maxipreps Kit	Promega (USA)
Wizard® Plus SV Minipreps-Kit	Promega (USA)
PureYield™ Plasmid Miniprep System	Promega (USA)
PureYield™ Plasmid Maxiprep System	Promega (USA)
RotiFect	Carl Roth (Germany)

2.1.3 Plasmids

Name	Manufacturer
pcDNA3.1rTRPV1_VL8	*Gifted by Dr. rer. nat. U. Binzen, Mannheim, Germany*
pcDNA 3 hMOR_YFP	*Gifted by Prof. Dr. J. Oberwinkler, Marburg, Germany*

2.1.4 Consumables

Consumables	Source
Borosilicate glass capillaries GB150F-10	Science Products (Germany)
Brown-Flaming Micropipette Puller, Model P-80	Sutter Instrument (USA)
Cell culture flasks Falcon™ 25 cm^2	BD Biosciences (Germany)
Disposable pipette Falcon™ 1 mL / 2 mL / 5 mL / 10 mL / 25 mL	BD Biosciences (Germany)
Eppendorf Safe-lock Tubes 0.5 mL / 1.5 mL / 2 mL	Eppendorf (Germany)
Falcon™ Polypropilene Tubes 15 mL / 50 mL	BD Biosciences (Germany)
Flat bottom plates Falcon™ 6 / 12 / 24 well	BD Biosciences (Germany)
Magnetic closed chamber for continuous perfusion RC-21BR	Warner Instruments (USA)
Parafilm® M, Bemis	Bemis Company (USA)
Plattform for magnetic closed chamber PM-2	Warner Instruments (USA)
Polyethylene tubes	Smiths Medical International (UK)
Polyethylene tubes 1/16" OD	Warner Instruments (USA)
Quartz glass plate dimensions 200*200*3 mm	GVB (Germany)
Round cover slips 25 mm round	Warner Instruments (USA)
Sterile filter (0.22 μm), Fisherbrand®	Fisher Scientific (Germany)
Surgery materials: scissors, forceps	F.S.T Fine Science Tools (Germany)
BD Perfusion50 mL Syringes Luer-Lok™ Tip	BD Biosciences (Germany)

2.1.5 Equipment and Software

Equipment	Manufacturer
AC-DC amplifier Neurolog 106, DigitimerNeurolog System	Digitimer (UK)
Autoclave Type ELVC 5075	Systec GmbH (Germany)
Blood pressure display unit	Stoelting (USA)
Centrifuge type 1406	Hettich GmbH (Germany)
CED-1410 interface	Cambridge Electronic Design (UK)
Digital CCD camera ORCA-R2	Hamamatsu (USA)
Diode laser stimulator SK9-2001 1475/635 nm (skin)	Schäfter & Kirchhoff (Germany)
Incubator for Cell culture HERAcell 150i	Thermo Fisher Scientific (USA)
Infra-red camera Optris PI160	Optris GmbH (Germany)
Infusion Pump AL-1000	World Precision Instruments (USA)
Inverted microscope IX81	Olympus Europa (Germany)
Laser power sensor 30(150)A-LP1-18	Ophir Photonics (USA)
Laser stimulator DL1470 (single cells)	Rapp Optoelectronics (Germany)
Light microscope	Hellmut Hund (Germany)
Oscilloscope Classic 6000 DSO	Gould Instrument Systems (USA)
pH-meter	Hanna Instruments (USA)
Micropipettes Eppendorf research for 1000/200/100/10/1 μL volume	Eppendorf (Germany)
Preamplifier EXT-10C	npi electronic (Germany)

Refrigerator -20 °C	Liebherr-International Deutschland GmbH (Germany)
Refrigerator 4 °C	Liebherr-International Deutschland GmbH (Germany)
Refrigerator -80 °C	Liebherr-International Deutschland GmbH (Germany)
Respiratory Pump Rodent Ventilator Model 683	Harvard Apparatus (USA)
Shaker	Heidolph (Germany)
Spectrophotometer	Eppendorf AG (Germany)
Spinal frame	David Kopf Instruments (USA)
Safety cabinet type II model EN 12469	Heraeus (Germany)
Tele-thermometer	Yellow Springs Instrument (USA)
Thermocouple model BAT-12	Physitemp (USA)
Point scanning device model UGA-42-Firefly	Rapp Optoelectronics (Germany)
Vortex machine 7-2020	Neolab (Germany)
Water bath	Grant Instruments (UK)
Weight balance model TE214S	Sartorius AG (Germany)

Software package	Tool company
Adobe Creative Cloud	Adobe 21
Microsoft Office	Microsoft (USA)
Origin	OriginLab Corporation (USA)
Clampfit 9.2	Axon Instruments (USA)
Prism 5	GraphPad Software (USA)
Spike 2	Cambridge Electronic Design (UK)
Xcellence software	Olympus Europa (Germany)
MATLAB 7.10	MathWorks (USA)

2.2 Methods

2.2.1 Primary culture and cell lines

-Primary culture of DRG neurons

Adult Sprague-Dawley rats were sacrificed by decapitation under deep anesthesia, which was delivered by inhalation of isoflurane (5%, AbbVie, Germany). The skin of the back was opened by a single longitudinal midline incision and then spinal cord was excised by two longitudinal incisions along the entire length of the rat back, cutting ribs, muscles and connective tissue as much as possible. In order to expose the DRGs, the vertebral bodies of the spinal column were removed by two longitudinal incisions in rostrocaudal direction, keeping a 45° angle from the ventral side. The tissue was immediately transferred to ice-cold and gassed DMEM medium (gas mixture of 95% O_2 and 5% CO_2), and DRGs from all cervical, thoracic and lumbar segments were harvested, carefully removing extra nerve tissue.

Isolated DRGs were washed 3 times on fresh DMEM media and then enzymatically partially digested for 1 h by addition of 1 mL accutase and 1 mL collagenase at 37 ºC. Then, DRGs were once again washed with fresh culture media and transferred to a 15 mL falcon tube in 1 mL of DMEM medium, and tissue was homogenized by pipetting them through fire-polished glass pipettes, starting from the glass pipettes with bigger aperture to smaller aperture, and taking care that the cells are kept under constant CO_2 flux. The homogenized cells were carefully added on top of 10 mL BSA solution and centrifuged 10 min at 800 g, the supernatant was discarded and the cell pellet was suspended in 1 mL DMEM and carefully added on a 15 mL falcon tube containing 10 mL of DMEM, followed by 5 min centrifugation at 400 g.

The pellet was then resuspended in 120 µL of DMEM and distributed on 12 cell plates containing laminin-precoated cover glasses (10 µg/mL, Sigma-Aldrich, Germany). Laminin coating was done by applying 50µL of laminin diluted 1:30 from stock 1g/L at the center of each cover glass. The cover glasses with the laminin mixture were incubated at 34 ºC in a humidified atmosphere with 5% CO_2 during at least 2 h. Shortly before seeding of the cells, the laminin mixture was carefully aspirated from the cover glasses and let dry at 34 ºC in a humidified atmosphere with 5% CO_2.

Dissociated DRG cells were incubated for 2 h at 34 °C in a humidified atmosphere with 5% CO_2 in order to let them adhere to the base of the cover glass. Finally, 1 mL of neurobasal medium supplemented with NGF was added to each cell plate and stored at 34 ºC in a humidified atmosphere with 5% CO_2. All experiments were performed on the following 24-36 h after seeding the cells.

-HEK 293 cell line

Cells were cultured on flasks (Falcon® BD Biosciences, Germany) in 6 mL DMEM media supplemented with 10% FBS (GIBCO) and 1% penicillin-streptomycin (GIBCO) and maintained at 37 °C in a humidified atmosphere with 5% CO_2. Cells were passaged one to two times per week. For experiments, cells were seeded on coverslips coated with poly-L-lysine (Sigma-Aldrich).

-HEK_TRPM3 α2 variant (2Xα2B7) stable cell line

Cells were cultured on cell culture flasks (Corning) containing 6 mL MEM media supplemented with 10% fetal bovine serum (Invitrogen) and 1% geneticin (Sigma-Aldrich, Germany) and maintained at 37 °C in a humidified atmosphere with 5% CO_2. Cells were passaged one to two times per week.

For experiments, cells were seeded on coverslips previously coated with poly-L-lysine (Sigma-Aldrich). Coating was done one day before by covering them with poly-L-lysine diluted 1:10 in distillated water for 20 min, then removed and washed two times with water and let dry at RT.

2.2.2 Transient Transfection of the μ-opioid receptor

The stable cell line HEK_TRPM3 was transiently transfected with the plasmid containing the μ-opioid receptor. To achieve this we used a vector containing the human MOR cDNA tagged with GFP (hMOR_GFP), construct that was developed and kindly provided by the Institute for Physiology and Pathophysiology of the University of Marburg, Germany, led by Professor Dr. Johannes Oberwinkler. The protocol used is as follows.

HEK_TRPM3 cells at a confluency of 70% were subjected to a transfection protocol using the kit RotiFect (Carl Roth). For each plate, 100 μL of OptiMEM + 3 μg DNA + 9 μL RotiFect were mixed in a 1.5 mL- Eppendorf tube and incubated during 20 minutes at RT. Then, 600 μL from the cell media were added to the DNA mixture and then the content was distributed drop by drop into the cell plate. After a slow cross-style shaking of the plate, the cells were incubated at 37 °C in a humidified atmosphere with 5% CO_2 for 24-48 h.

Twenty-four hours after transfection, cells were subjected to a passage 1:3 (one diluted to three, from one plate three plates are seeded) and again stored at 37 °C in a humidified atmosphere with 5% CO_2 until 48 h post transfection, to continue with the functional analyses.

2.2.3 Functional assays

In all cellular experiments, functional assays were done using the calcium imaging technique in either HEK_TRPM3 cells or DRG primary cultures. The experimental paradigm consisted of three repeated stimulations in order to activate the TRPM3 channel, with concomitant activation of MOR before- and during- second TRPM3 activation. The stimuli applied to activate TRPM3 channel were either chemical (chemical agonist) or thermal (laser heat), and the activation of the MOR was achieved through stimulation with the synthetic analog of morphine, DAMGO.

Cells (either HEK_TRPM3_hMOR 48 h post transfection, or DRG primary culture 12-36 h after seeding) were transferred into extracellular solution E001, pH 7.2, osmolarity $\cong$ 325 mOsm containing NaCl 145 mM, CsCl 10 mM, KCl 3 mM, $MgCl_2$ 2 mM, $CaCl_2$ 2 mM, D-glucose 10 mM and HEPES 10 mM, and loaded with the fluorescent dye FURA-2AM (3 μM for HEK_TRPM3 cells and 3 μL Pluronic F-127, 1 μM for DRG cells; Merk, Germany) for 45 min at RT in dark. Cells were placed in a closed magnetic chamber (Warner Instruments, USA) for gravity driven-continuous perfusion experiments. The gravity driven perfusion system included an inlet through

a manifold that connected eight 50 mL syringe lines; and an outlet with a negative pressure loop and reservoir connected to a vacuum system. Cells were initially perfused for 10 min (flow rate of ~3 mL/min) with extracellular solution (E001) before the start of the experiment.

-Solutions used on the perfusion system

Line	Solution
S1	Extracellular solution (E001) (see p. 15)
S2	PS 50 µM
S3	DAMGO 1 µM
S4	Vehicle (DMSO) 7.04 mM
S5	PS 50 µM + DAMGO 1 µM
S6	PS 50 µM + Vehicle
S7	Capsaicin 10 µM
S8	Ionomycin 10 µM / High potassium solution 70 mM (see p. 15)

-Protocol for HEK_TRPM3_hMOR cells activation by agonist application and modulation by MOR activation

Time (min)	Substance perfused + stimulation	Code
0-2.5	Baseline (E001)	[S1]
2.5-5	PS 50 µM	[S2]
5-7.5	Washout (E001)	[S1]
7.5-10	DAMGO 1µM / Vehicle 7.04 mM	[S3] / [S4]
10-12.5	PS 50 µM + DAMGO 1 µM / PS 50 µM + Vehicle	[S5] / [S6]
12.5-15	Washout (E001)	[S1]
15-17.5	PS 50 µM	[S2]
17.5-20	Washout (E001)	[S1]
20-22.5	Ionomycin	[S8]
22.5-25	Washout (E001) + Stop at min 25	[S1]

-Protocol for DRG cells activation by agonist application and modulation by MOR activation

Time (min)	Substance perfused + stimulation	Code
0-2.5	Baseline (E001)	[S1]
2.5-5	PS 50 µM	[S2]
5-7.5	Washout (E001)	[S1]
7.5-10	DAMGO 1µM / Vehicle 7.04 mM	[S3] / [S4]
10-12.5	PS 50 µM + DAMGO 1 µM / PS 50 µM + Vehicle	[S5] / [S6]
12.5-15	Washout (E001)	[S1]
15-17.5	PS 50 µM	[S2]
17.5-20	Washout (E001)	[S1]
20-20.5	High potassium solution 70 mM	[S8]
20.5-22.5	Washout (E001)	[S1]
22.5-25	Capsaicin 10 µM	[S7]
25-27.5	Washout (E001) + Stop at min 27.5	[S1]

Fluorescence was measured using an inverted microscope (IX-81 with Xcellance Software, Olympus, Germany) and an ORCA-R2 CCD camera (Hamamatsu Corp., USA). After alternating excitation with light of 340 nm and 380 nm wavelength, the ratio of the fluorescence emission intensities at 510 nm (340 nm/380 nm) was calculated and digitized at 0.5 Hertz.

In experiments with DRG primary cell cultures, a cell was considered an excitable neuron and later evaluated only when showing depolarization by high potassium solution (70 mM). For imaging DRG neurons Verapamil 20 µM was added to all extracellular solutions to block endogenous voltage-gated calcium channels. However, in order to distinguish neuronal from non-neuronal cells in these cultures the high-K^+ solution (70mM) was normally used without Verapamil to depolarize the cells at the end of the experiment.

2.2.3.1 Laser stimulation

Laser stimulation on single cells was performed with a DL1470 infrared laser stimulator (1470 nm wavelength, maximal 10W power output, Rapp Optoelectronic, Germany) coupled to a point scanning device model UGA-42-Firefly (Rapp Optoelectronic, Germany). The laser stimulator and the point scanning device were configured

under control of the software from manufacturer. In order to identify the cells that were positively transfected with the MOR vector, pictures of imaged cells were taken under white light illumination and under blue fluorescence at 20X magnification.

The selection criteria for laser stimulation was performed in the following order: first, cells were imaged in DIC (transmitted light) in order to observe them and focus a plane where cells are homogeneously distributed and avoid those areas where cells might be stacked (a cell on top of another cell). Then, transmitted light was turned off and cells were imaged under blue fluorescent light, in which cells that carry the GFP shine in green. A picture was taken and was overlaid with the DIC picture (Figure 3). Then, cells were imaged at 340 and 380 nm and pictures were taken for each one of them. A new overlay was done between these two pictures, where cells that initially were high in calcium could be distinguished as they show a higher 340/380 nm ratio as the others. Usually these cells have shown a very high green fluorescence as well. In all cases, these cells were less than 5% of the total cells for each experiment.

From the cells that showed a regular 340/380 nm ratio and green fluorescence levels, 9 cells were selected for laser stimulation and 3 non-green fluorescent cells were selected as well and stimulated with laser as controls. By selecting cells for laser stimulation, it was considered to keep at least 50 µm radius around each cell was kept without laser-heat stimulation (Figure 3). Three laser stimulations, namely L1, L2 and L3 were given with an energy magnitude of 696.85 µJ.

-Protocol for HEK_TRPM3_hMOR cells activation by laser heat and modulation by MOR activation.

Time (min)	Substance perfused + stimulation	Code
0-2.5	Baseline (E001)	[S1]
2.5-5	E001 + L1 at min 2.5	[S1] + L1
5-7.5	DAMGO 1µM / Vehicle 7.04 mM	[S3] / [S4]
7.5-10	DAMGO 1 µM / Vehicle 7.04 mM + L2 at min 7.5	[S3] / [S4] + L2
10-12.5	Washout (E001)	[S1]
12.5-15	E001 + L3 at min 12.5	[S1] + L3
15-17.5	PS 50 µM	[S2]
17.5-20	Washout (E001)	[S1]
20-22.5	Ionomycin	[S8]
22.5-25	Washout (E001) + Stop at min 25	[S1]

-Protocol for DRG cells activation by laser-heat and modulation by MOR activation

Time (min)	Substance perfused + stimulation	Code
0-2.5	Baseline (E001)	[S1]
2.5-5	E001 + L1 at min 2.5	[S1] + L1
5-7.5	DAMGO 1µM / Vehicle 7.04 mM	[S3] / [S4]
7.5-10	DAMGO 1 µM / Vehicle 7.04 mM + L2 at min 7.5	[S3] / [S4] + L2
10-12.5	Washout (E001)	[S1]
12.5-15	E001 + L3 at min 12.5	[S1] + L3
15-17.5	PS 50 µM	[S2]
17.5-20	Washout (E001)	[S1]
20-20.5	High potassium solution 2 (70 mM)	[S8]
20.5-22.5	Washout (E001)	[S1]
22.5-25	Capsaicin 10 µM	[S7]
25-27.5	Washout (E001) + Stop at min 27.5	[S1]

2.2.3.2 Data analysis of functional assays

The overall readout was a time course of the increase in fluorescence ratio of 340/380 nm as a measure of increase in intracellular calcium concentration[144]. The changes in fluorescence ratio were stored as pictures taken from fluorescence at 340 nm and 380 nm at a rate of 0.5 Hz. After each experiment, videos were re-analyzed and the cells that responded to the treatment were selected with the software as ROIs. Data was imported into the software "Origin" and data points of ratio of fluorescence 340/380 nm along time were plotted. Cells that presented an unusual high ratio 340/380 nm from the beginning of the experiment (over 0.6 in ratio) were not included in the analysis (approximately 5% of cells from each experiment). Individual cell traces were collected and the mean values ± SEM for each group were plotted.

In some cases the percentage of inhibition (PI) was calculated as well. This was calculated using the following formula:

$$PI = [(\Delta PS \ \Delta(PS+DAMGO))/\Delta PS] \times 100\%,$$

where the values of a time series before and after the application of the inhibitory compound were averaged and from this average (ΔPS), the value during the application of the pharmacological inhibitor was subtracted ($\Delta(PS+DAMGO)$). The result was divided by the average of the values obtained before and after drug application (ΔPS) and multiplied by 100. The PI for HEK_TRPM3 transfected and non-transfected cells,

as well as for DRG primary cultured cells was calculated, plotted and tested through the t-test or the Mann-Whitney test, according to data distribution.

When differences in baseline values between groups were detectable, another way of analyzing data was performed as follows: the individual percentage of increase in ratio 340/380 nm was subtracted to its initial baseline value for S1, S2, and S3 responses (baseline calculated as mean value of frames between times 0 – 2.5 min), and those response values were then normalized to S1. The normalized responses from HEK_TRPM3 transfected and non-transfected cells, as well as for DRG primary cultured cells was calculated, plotted and tested through the t-test or the Mann-Whitney test, according to data distribution. Each single dish investigated was regarded as an independent experiment where mean responses of the capsaicin-sensitive and –insensitive subpopulations of neurons were determined.
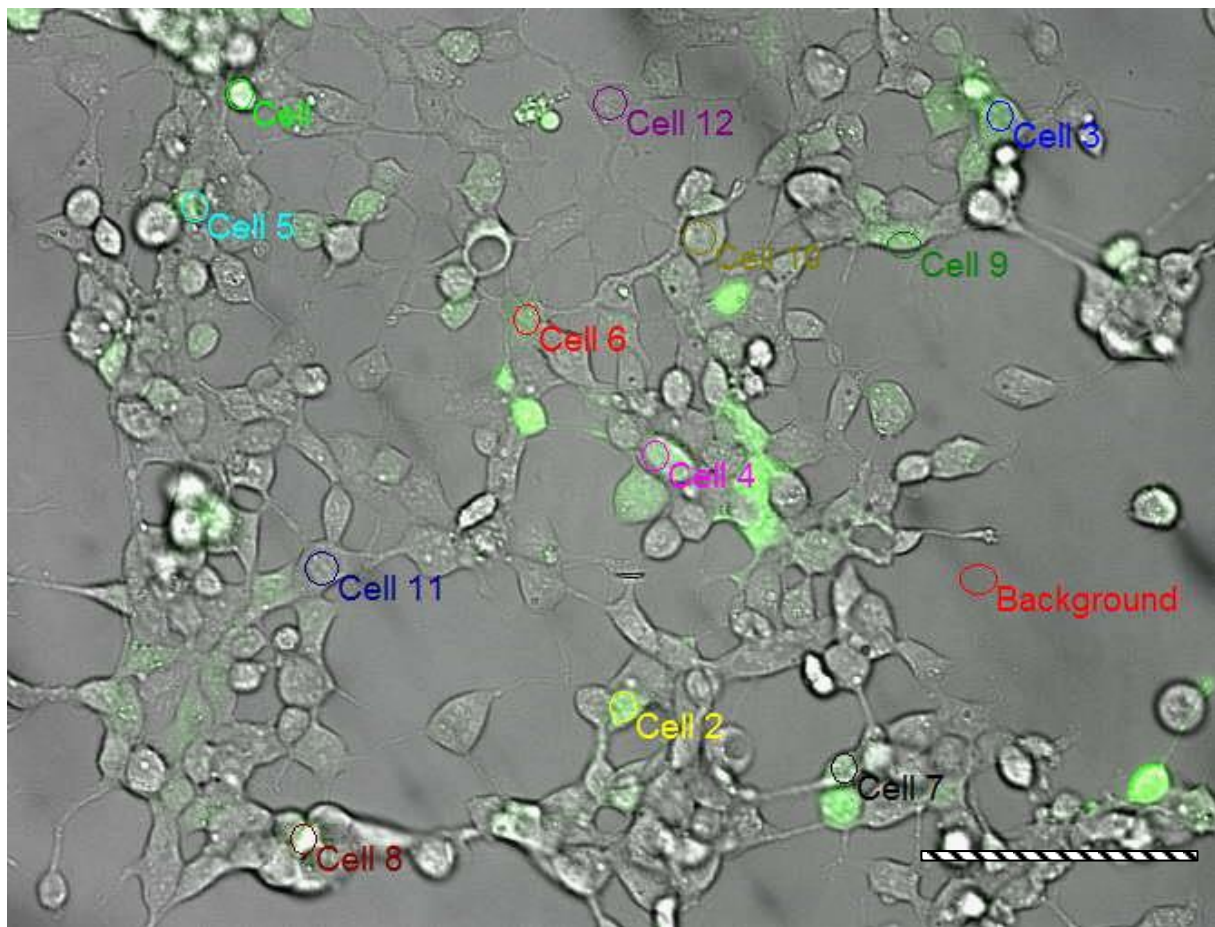

Figure 3: Example of an overlay picture of DIC and GFP fluorescence showing transiently transfected HEK_TRPM3_µOR cells 48 h after transfection. Images taken at 20X magnification. ROIs indicate the fluorescent cells selected for laser stimulation. Cells were selected by green fluorescence, ratio 340/380 nm levels at baseline and plane distribution on the field of view (ideally cells are on the dish as a monolayer). Laser stimulation was performed in cells 1 to 12. Cells 1 to 9 were selected positively to GFP, while cells 10 to 12 (not fluorescent) were used as controls (scale bar: 100 µm).
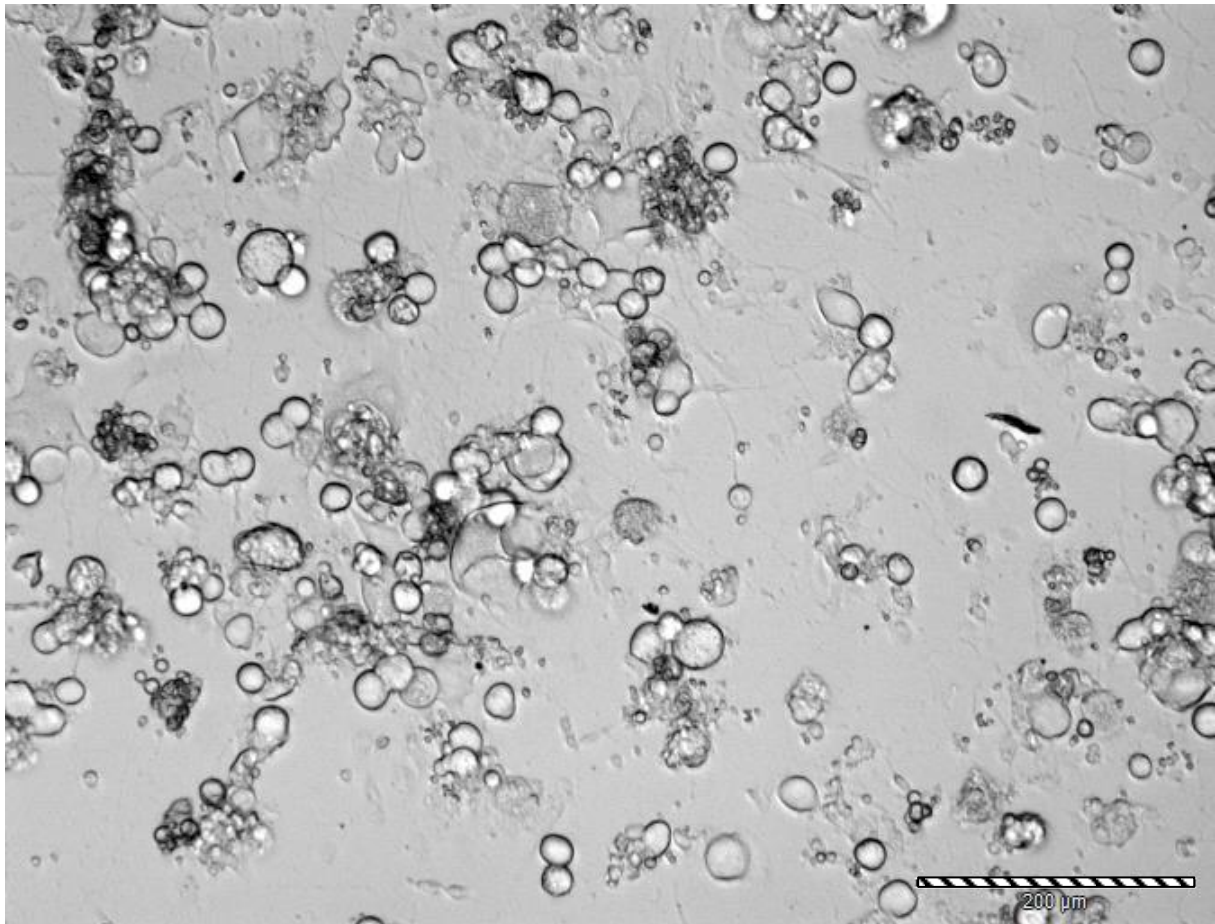
Figure 4: Example of a DIC picture of showing primary culture of DRG cells from rat 48 h after transfection. Image taken at 10X magnification. In these experiments, the modulation of endogenous TRPM3 channels by MOR was assayed upon agonist- induced responses, therefore, a broader field of recording view allow simultaneous analyses of a higher number of cells (scale bar: 200 µm).

2.2.4 *in vivo* electrophysiology experiments

Animals

Experiments were performed in a total of 9 adult male wild-type Sprague-Dawley rats (body weight 350-450 g). From them, 4 animals dropped out after intraperitoneal injection of anesthetic, therefore data was obtained from 5 animals.

The rats were housed in individual cages and had free access to food and water. The experimental procedure and the number of animals used was approved by the local authority responsible for animal experimentation and carried out in accordance with the German law on the protection of animals (AZ: 35-9185.81/G-174/15) and followed the guidelines outlined in the European Council Directive and the ethical proposals of the IASP[145].

Laser-beam size determination

In order to determine the diameter of the local increase in temperature on the

skin elicited by laser stimulation, experiments were performed recording a rat hind paw explant with an infrared camera (Optris PI160, Optris GmbH, Berlin, Germany) upon repeated laser stimulations using different laser power intensities starting from 10 mW and up to 100 mW in steps of 10 mW. An extra recording was done at 45 mW as well, because the heat-withdrawal threshold of the animals was at about this magnitude. The surface temperature of the paw explant among time was obtained at an acquisition rate of 120 Hz. Laser pulses were delivered at a rate of 0.1 Hz.

From the recordings obtained at 45 mW and 100 mW power intensities, the skin spot where the temperature increased because of laser stimulation was ana-lyzed as follows: using the analyzing software (USB IR CAM) the central spot was determined (minimal area measureable where the maximal increase in temperature occurred) and from this spot (called position 0), 16 different spots at certain positions were selected: 4 upper, 4 lower, 4 to the right, and 4 to the left, with an interspace distance between them of 320 μm. From all these points, the changes in surface skin temperature were measured among 5 different laser stimulations. The magnitudes of maximal increase in temperature were averaged for each of the positions tested and plotted in the software GraphPad Prism. Data was normalized to the maximum tem-perature value (at position 0) and the 1/e value of the bell shaped distribution for both power intensities was determined and regarded as beam size.

Laser-induced heat pain threshold determination

One day before the electrophysiological recordings, the laser-induced heat withdrawal thresholds were determined at the left hind paw from each animal used subsequently for recordings. Laser pulses were generated by a diode laser stimulator (Schäfter & Kirchhoff; 150 μm beam diameter, 1475 nm wavelength). The stimulus duration was 200 ms in all experiments. A set up for animal behavioral testing origi-nally consisting of a base, columns, a perforated platform and animal enclosures (Ugo Basile SRL, Italy) was used, with one modification. The usual perforated plat-form was replaced with quartz glass plates (2 mm thick, GVB GmbH, Herzogenrath, Germany). Animals were placed on the glass plate inside an animal enclosure (one per testing). Habituation time before behavioral measurements was 15 minutes. Cau-tion was taken to clean any contamination that might have occurred during that time. The pilot laser was fixed to a micromanipulator located directly under the glass floor, focusing on the left hind paw of the animal. Laser-heat stimuli were applied at differ-ent power intensities, starting from 10 mW and increasing at a rate of 10 mW per step. Thresholding was achieved using the method of limits: the laser power was in-creased until the animal showed responses to the laser stimuli, registered and then decreased until no response occurred, registered and increased again until 3 upper and 3 lower limits were defined. The mean of those values was calculated.

2.2.5 Electrophysiological recordings of spinal dorsal horn neurons

Anesthesia of the animals

The animals were deeply anesthetized with thiopental sodium (Trapanal®, Inresa GmbH, Germany), 100 mg kg^{-1} i.p. initially, followed by i.v. infusion (external jugular vein) of 10–20 mg kg^{-1}h^{-1} thiopental sodium using an infusion pump (AL-1000, World Precision Instruments Inc., USA) to maintain a deep and constant level of an-esthesia (no flexor reflexes or blood pressure reactions exceeding 10 mm Hg oc-curred to noxious stimuli). Muscular relaxation was induced with pancuronium bro-

mide (Inresa GmbH, Germany, 0.5 mg kg^{-1}h^{-1} i.v.). Mean arterial blood pressure measured in the right common carotid artery and body core temperature were continuously monitored and kept at physiological levels (>80 mm Hg, 37-38 ^{o}C). The animals were artificially ventilated with a gas mixture of 47.5% O_2, 2.5% CO_2, and 50% N_2.

General surgical preparation

-Catheter implantation

A medial skin incision was made from the chest to the chin. Salivary glands and muscles were separated bluntly to expose the trachea, the right common carotid artery and the right external jugular vein. Polyethylene tubes (Smiths Medical International Ltd., UK) with 1 mm inner diameter (i.d.) and 2 mm outer diameter (o.d.) were pulled out until reaching the required diameter for the insertion into the right carotid artery for blood pressure registration and the right jugular vein for drug administration. The tube of the right common carotid artery and the attached syringe were filled with Liquemin (Liquemin 5000, active ingredient: Heparin-Sodium, Ratiopharm GmbH, Germany) in tyrode to prevent blood clotting in the artery catheter (0.5 mL Liquemin in 50 mL Tyrode). Tyrode is an artificial interstitial fluid solution whose osmotic pressure and ion concentration are similar to those of interstitial fluid. The artery catheter was connected to the device (blood pressure display unit, Stoelting, USA) measuring mean arterial blood pressure. The vein catheter was used for continuous administration of the anesthetic via the infusion pump. In all experiments mean arterial blood pressure was above 80 mm Hg.

-Artificial ventilation

Animals were connected to a respiratory pump via a trachea cannula. The ventilation pump (Rodent Ventilator Model 683, Harvard Apparatus, Inc., USA) was adjusted to a breathing frequency of 90-100 breaths per minute and a breath volume of 2.0 mL/breath. According to literature, the breath volume of a rat is around 1.3 to 2.0 mL per breath at 60 to 114 breaths per minute[146]. A gas mixture of 47.5% O2, 2.5% CO2, and 50% N2 was used for artificial ventilation. The mixture caused a pO2 above 100 mm Hg, a pCO_2 between 30 and 40 mm Hg and a pH close to 7.4 in blood[147].

-Body temperature

The body core temperature of the animals was measured by a thermal sensor inserted 3-4 cm into the rectum and monitored via an analog temperature display (tele-thermometer, Yellow Springs Instrument Co., Inc., USA), because the animals tended to cool down quickly during anesthesia; warming lamps were used to keep the body temperature between 37 - 38 °C.

-Laminectomy

The animals were mounted in a spinal frame (David Kopf Instruments, USA) and the skin of the back was cut in the midline and a pool was formed by the skin flaps. The lumbar spinal segments L1 to L5 were surgically exposed through laminectomy. After that, the dura mater was incised longitudinally in order to make the microelectrode penetrations into the dorsal horn possible. The vertebral column was

fixed by metal clamps. To minimize breath-related movements of the spinal cord, a unilateral pneumothorax was performed by inserting a small tube (i.d. 3 mm, o.d. 4.5 mm) in the 8th intercostal space. The exposed spinal segments L1 to L5 and the corresponding dorsal roots were covered with a tyrode-moistened cotton ball and the wound filled with hand-warm agar solution (0.5 g agar in 20 mL Tyrode) to stabilize the spinal cord. After the agar-gel had hardened, the cotton was cut out and the exposed spinal cord was covered with warm silicon oil (M100Roth, Carl Roth GmbH, Germany).

-Recording neuronal activity

Extracellular recordings of dorsal horn neurons were made ipsilateral to the laser irradiated hindpaw (see below: *Laser stimulation*) in the left spinal segment L4, because this segment receives most of the input from the hind paw glabrous skin. Glass microelectrodes were fabricated from borosilicate glass capillaries (o.d. 1.5 mm, i.d. 0.86 mm, GB150F-10, Science Products GmbH, Germany) using a horizontal pipette puller (Brown-Flaming Micropipette Puller, Model P-80, Sutter Instrument Co., USA). The microelectrodes filled with 5% sodium chloride were used to record action potentials of single dorsal horn neurons extracellularly. The static resistance of the glass microelectrodes ranged from 8 to 25 MΩ. Vertical microelectrode penetrations into the dorsal horn were made to a depth of maximal 1000 µm from the dorsal surface of the spinal cord. Recorded action potentials were amplified 10 times by a preamplifier (EXT-10C, npi electronic GmbH, Germany) and 10 times by an AC-DC amplifier (Neurolog 106, DigitimerNeurolog System, Digitimer Ltd., UK). The potentials were filtered (low frequency: 5-500 Hz, high frequency: 50 kHz; Neurolog 125, Digitimer Neurolog System, Digitimer Ltd., UK). All data was monitored on an oscilloscope (Classic 6000 DSO, Gould Instrument Systems, USA) and digitized online via a CED-1410 interface (Cambridge Electronic Design Limited, UK) at a sampling rate of 20 kHz. This data was then stored in a personal computer using Spike 2 software (Cambridge Electronic Design Limited, UK).

In the process of the electrophysiological recording of dorsal horn neurons, the general parameters (threshold of action potential, latency of action potential and depth of the recording) of the neuron were determined. The background activity (resting activity) of the neuron was recorded for 60 s in the absence of any stimulation to determine the rate of the spontaneous activity. A neuron was considered having resting activity if it produced ≥ 1 impulse per minute[148]. Afterwards, mechanical stimulation was applied on glabrous skin of the left hind paw of the animals to determine the type of the neurons (see below: *Classification of the neurons*). In addition, locations and sizes of the receptive fields were also determined (see below: *Identification of receptive fields*). Recordings of dorsal horn neurons were made for up to 4 h. During this period, 5 to 10 neurons were recorded in the single animals. At the end of the experiments the animals were euthanized under deep anesthesia with an overdose of the anesthetic.

-Electrical stimulation

As a search stimulus during microelectrode tracking, the left sciatic nerve was placed on a bipolar, hooked ball platinum electrode and electrically stimulated with square pulses (intensity 5 V, width 0.3 ms, repetition rate 0.33 Hz). All dorsal horn neurons stably responding to this search stimulus with action potentials were tested

for mechanosensitive receptive fields in the plantar skin (see below: *Mechanical stimulation*).

The latency of the action potential was measured at a current corresponding 1.2 times the electrical threshold of the neuron. If action potentials showed a clear jitter and/or did not follow 333 Hz stimulation, the dorsal horn neurons were differentiated from primary afferent axons and considered second order neurons[147, 149, 150].

Mechanical stimulation

After the general parameters and the resting activity of the recorded neuron were determined, mechanical stimuli were applied to determine the receptive field and the response type of the neuron (see below: *Classification of the neurons*). All stimuli were applied at the glabrous skin of the hind paw. As innocuous stimuli, light touch with an artist's brush and moderate (innocuous deformation) pressure with a blunt probe were used; as noxious ones, pinching with a sharpened watchmaker's forceps and noxious (strong squeezing) pressure with a blunt probe were applied. The moderate pressure was about 1 N/cm^2, and the noxious pressure was about 10 N/cm^2. In contrast to pinch, touch and moderate pressure did not elicit pain-related behavior in awake rats.

Classification of the neurons

All neurons were classified according to their response behavior to mechanical stimulation:

1) Low threshold mechanosensitive (LTM) neurons which responded primarily to touch or moderate pressure.

2) Wide dynamic range (WDR) neurons which responded to touch, moderate pressure and pinch in a graded manner.

3) High threshold mechanosensitive (HTM) neurons which responded to pinch but not to touch and moderate pressure.

Laser stimulation

In all cases, the left hind paw of the animals was used for laser irradiation. Single laser pulses were applied to the plantar skin inside and outside the mechanosensitive receptive field of the neuron. Laser pulses were generated by a diode laser stimulator (Schäfter & Kirchhoff; 150 µm beam diameter, 1475 nm wavelength). The laser power applied during the recording of dorsal horn neurons was 100 mW, the stimulus duration 200 ms. The power intensity applied was above the individual heat pain threshold of the animal, which was determined one day before the recording with the same laser (see above: *Laser-induced heat pain threshold determination*) A neuron was considered responsive to the laser heat stimulus when at least 1 action potential was elicited within 1000 ms after onset of the stimulus.

Identification of receptive fields

The excitatory receptive field of a sensory neuron is defined as the body region in which the presence of a stimulus leads to firing action potentials in a neuron. The receptive fields of dorsal horn neurons were identified with graded mechanical

stimuli applied to the glabrous skin of the hind paw and registered manually in a standard outline of the rat plantar paw on an A4 paper. Once the mechanosensitive receptive field of a neuron was determined, laser-heat stimuli were applied inside and outside this area, and for each neuron that showed responses to laser-heat, the laser-heat receptive fields were determined as well and registered manually in a standard outline of the rat plantar paw on an A4 paper.

2.2.6 Quantitative evaluation of the size and the location of receptive fields

A computer-assisted method to quantify the size and the location of receptive fields on the hind limb was developed. It was based on an existing program designed with MATLAB software, version 7.10 (MathWorks, Inc, Natick, MA, USA). In this method, the relative area and the location of receptive fields of every neuron were calculated from the manually recorded receptive fields on a A4 paper. The standard outlines of the receptive fields were scanned and digitized by a computer. The resolution of the picture was 300 dpi. The computer program analyzed the number of the pixels of the plantar paw and calculated the relative area of the receptive field (absolute area of the receptive field / absolute area of the plantar paw, expressed in percentage). The relative area of the receptive field was used for evaluation.

2.2.7 Data Analysis

Unless otherwise stated, all data is expressed as mean ± SEM. The U-test of Mann and Whitney was used to determine significant differences between relative areas of the receptive fields. $P < 0.05$ was considered as significant (two-tailed).

Action potentials were detected and analyzed with the software Spike 2. Briefly, events were detected through the tool "New wavemark", which was set up to find action potentials in the whole recording channel through in time-developed templates. The newly created event channel was then duplicated and drawn as instantaneous frequency of the action potential firing. Then, from this channel a frequency histogram was calculated, selecting the time frame where laser stimulation took place. Bins were set for 100 ms width.

3 RESULTS

3.1 Modulation of responses from TRPM3 channels by activation of the μ-opioid receptor MOR.

3.1.1 Laser stimulation on cell cultures

Laser-heat activation threshold on single cells for heterologous expression systems

To determine parameters of laser-induced heat activation, functional assays in response to three repeated laser-heat stimulations (L1, L2 and L3) at energy intensities from 368.85 µJ to 696.85 µJ were made on non-transfected HEK293 (n = 833 cells belonging to 6 independent experiments), HEK_TRPV1_VL8 (n = 703 cells belonging to 5 independent experiments) and HEK_TRPM3 cells (n = 514 cells belonging to 6 independent experiments), followed by specific agonist stimulation and ionomycin (Figure 5). The paradigm is that laser-heat stimulation on single cells generates a local increase in temperature on them. In cells containing heat sensitive ion channels, heat responses should be at threshold intensities reproducible and not compromise viability of the cells. On the other hand, cells without heat sensitive ion channels the lased-induced heat will increase the temperature of the cell and lead to cell death.

In all cases increases in laser energy leads to increases in L1 responses (red bars). In non-transfected HEK293 cells (Figure 5A) the first L1 response over threshold (123% baseline, in figure marked as horizontal dotted lines) occurred starting at 409.85 µJ and onwards. Non-transfected HEK293 cells responded only to the first laser response with an irreversible increase in calcium, being unable to follow repeated laser stimulations. High laser energy intensities over 573.85 µJ in non-transfected HEK 293 cells compromise its viability and may have led to cell death.

In HEK_TRPV1_VL8 cells (Figure 5B), responses to L1 over threshold were observable starting from 491.85 mJ, and responses to repeated laser stimulations occurred starting from 573.85 µJ of energy and onwards. At this energy intensity the response amplitudes to repeated laser stimulation increased among repetitions (L1 = 186.3 ± 11.6, L2 = 196.7 ± 12.4, L3 = 224.9 ± 15.3% over baseline, n.s, 2 way ANOVA) demonstrating that HEK_TRPV1_VL8 cells are able to follow repeated laser-heat stimulation with specific responses and increasing the magnitude of response among repetitions.

Moreover, responses of HEK_TRPV1_VL8 cells to capsaicin were high and sustained in all experiments (range: 271.6 ± 25.7- 663.3 ± 75.5% of baseline calcium concentration). Such increases in calcium concentration were, however, unable to completely come back to baseline before PS stimulation was performed and therefore, some unspecific amplitudes over baseline were present upon PS application on those cells (Figure 5B, brown bars; please note that the amplitude was always lesser than for capsaicin). Interestingly, the response amplitude of capsaicin responses decreased substantially in the experiments with laser-heat stimulation at energies of 532.85 and 573.85 µJ (amplitude: 271.6 ± 25.7 and 330.5 ± 23.1% over baseline) and came back to higher levels for higher energy laser-heat stimulation experiments. This decrease was significant for these datasets in comparison with most of the capsaicin amplitudes tested (p < 0.001, 2-way ANOVA with multiple comparisons)

HEK_TRPM3 cells responded to the first laser stimulation increasing its amplitudes exceeding threshold when the energy applied equaled or exceeded 614.85 µJ. Responses exceeding threshold to three repeated laser stimulations occurred starting from 696.85 µJ. Moreover, at this energy intensity the response amplitudes to repeated laser stimulation slightly increased among repetitions (L1= 162.2 ± 27.4, L2= 162.6 ± 21.9, L3= 215.7 ± 30.7, n.s., two way ANOVA with multiple comparisons) demonstrating that HEK_TRPM3 cells are able to follow repeated laser-heat stimulation with specific responses and increasing the magnitude of response among repetitions. Moreover, responses of HEK_TRPM3 cells to PS were high and sustained in all experiments (range: 534.7 ± 35.3 − 742.2 ± 22.9% baseline calcium concentration). Interestingly, the response amplitude of PS responses also decreased substantially in the experiments with laser-heat stimulation at energies of 655.85 and 696.85 µJ (amplitude: 535.3 ± 27.7 and 534.7 ± 35.3% over baseline). This decrease was significant for those datasets in comparison with the rest of the PS amplitudes (p < 0.001, 2-way ANOVA with multiple comparisons).

Based on these observations, the estimated threshold in terms of laser intensity for HEK_TRPV1_VL8 and HEK_TRPM3 cells corresponded to 491.85 µJ and 614.85 µJ.

The increase in amplitude responses after ionomycin stimulation was tested in order to show the maximal increase in intracellular calcium possible (gray bar). For all experiments tested, those values were between 5-8 times baseline calcium concentrations.

3.1.2 Modulation of TRPM3 in heterologous expression systems

Functional experiments on HEK_TRPM3 cells transfected with the MOR were investigated in response to either noxious laser-heat stimulations or by adding the agonist pregnenolone sulphate (PS), with or without the concomitant application of the selective MOR agonist DAMGO. Results were sorted by chemical or laser responses.

MOR-mediated modulation of agonist-induced TRPM3 cell responses

First we performed experiments in HEK_TRPM3 cells in response to repeated PS stimulation (Figure 6, protocol of the time course in 2.2.3 *Functional assays*). The paradigm was that activation of the TRPM3 channel by its specific agonist, PS would rise the intracellular calcium levels by opening of the channel in both transfected and non-transfected cells, however, when the specific MOR agonist DAMGO is co-administered with PS, HEK_TRPM3 cells transfected with the MOR will have a decreased amplitude of the PS response, due to a modulation of the TRPM3 channel exerted by the binding of DAMGO to the MOR. On the other hand, PS responses in non-transfected cells should not be affected by co-administration of DAMGO.

In non-transfected HEK_TRPM3 cells, increases in intracellular calcium concentration occurred rapidly and were reversible for every time PS 50 µM was added into the system (Figure 6A black trace, times 2.5 to 5 min: max amplitude 1.5 ± 0.003 ratio 340/380, n = 30 cells belonging to 3 independent experiments). This result demonstrates that the TRPM3 channel opens in response to the addition of its specific agonist and therefore is functional on those cells.
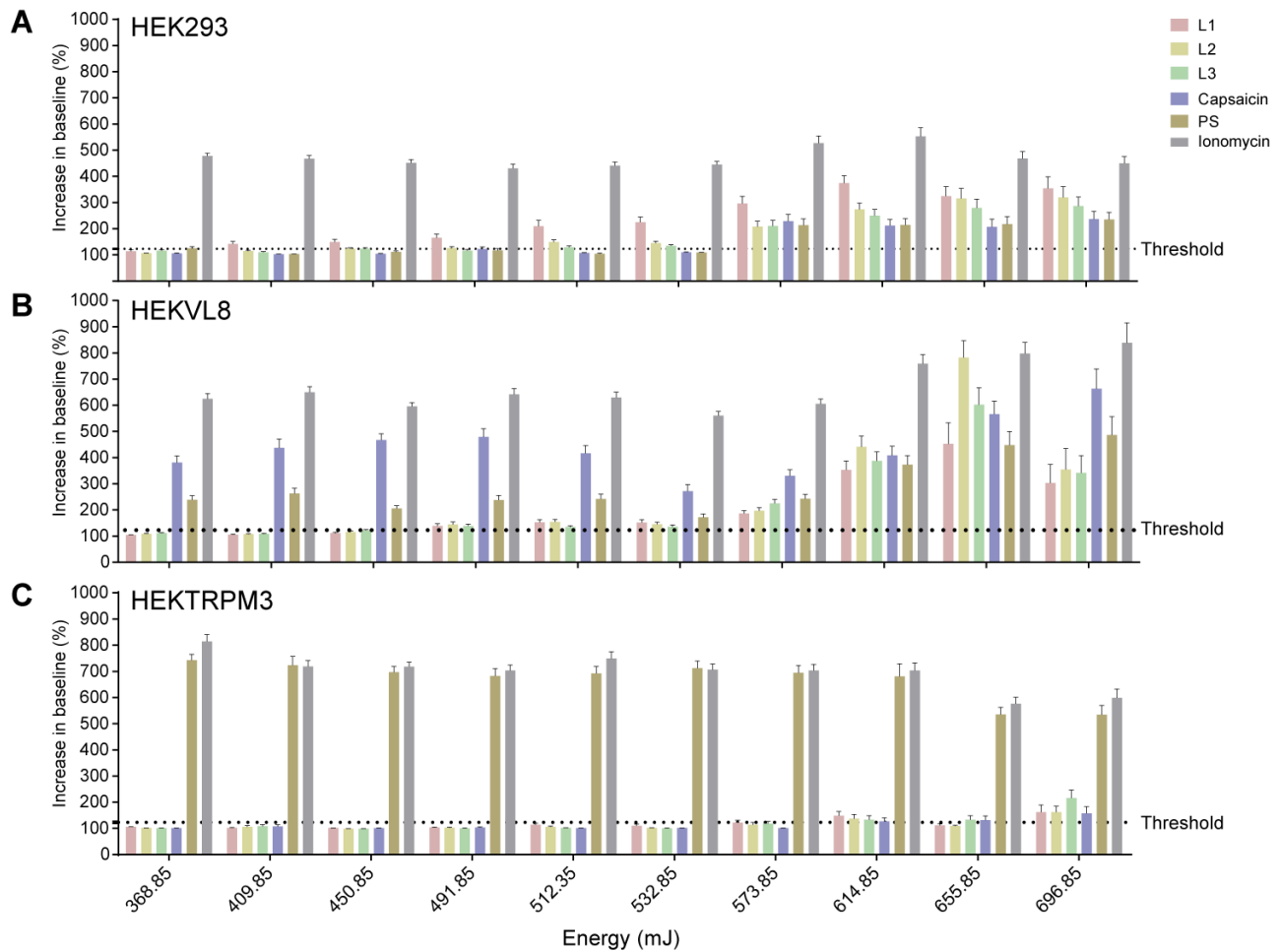
Figure 5: Functional analyses of HEK 293 cells, HEK_TRPV1_VL8 and HEK_TRPM3 cells to three repeated laser stimulations. Summary of the maximal increase in amplitude over baseline for A) HEK293, B) HEK_TRPV1_VL8 and C) HEK_TRPM3 cells upon repeated laser stimulations at different energies. For each energy magnitude tested, three laser stimulations were performed (red, yellow and green bars) with an ISI of 5 minutes between stimulations. Subsequently, application of capsaicin 10 µM (blue bar), pregnenolone sulphate 50 µM (brown bar) and ionomycin 10 µM (gray bar) proceeded, each of them applied in a total volume of 1 mL to the cells and during 1 min, followed by a washout with tyrode solution for 1 min. Specific responses to capsaicin and PS were only observable in HEK_TRPV1_VL8 and HEK_TRMP3 cells. Responses to three laser stimulations over threshold (123% baseline amplitude, horizontal dotted lines) occurred for HEK_TRPV1_VL8 and HEK_TRPM3 at 573.85 and 696.85 µJ. Laser responses on HEK293 cells over baseline (energy of 573.85 µJ onwards) were irreversible and therefore, unspecific.

In the same way, during the second PS stimulation which was performed simultaneous to the addition of DAMGO 1 µM, the response amplitudes on those cells did not differ significantly from the first one (Figure 6A black trace, times 10-12.5 min: 1.2 ± 0.005 ratio 340/380, Mann-Whitney Test, n.s.) which indicates that since the MOR is not present on non-transfected HEK_TRPM3 cells, then DAMGO is not exerting any effect on the response amplitudes of PS of them. Finally, PS was perfused a third time, again responses are sustained and high (Figure 6A black trace, times 15-17.5 min: 1.4 ± 0.003 ratio 340/380), lasting as much as the agonist is present in the system.

In MOR transfected cells (HEK_TRPM3_MOR) after the first perfusion of PS it was also possible to observe a high increase in ratio 340/380 occurring during the time the agonist was added into the system (Figure 6A red trace, times 2.5 to 5 min: 1.2 ± 0.004 ratio 340/380, n = 28, cells belonging to 3 independent experiments); however when PS was simultaneously added with DAMGO 1 µM, a markedly decrease in response amplitudes occurred (Figure 6A red trace, times 10-12.5 min: 0.6 ± 0.002 ratio 340/380). When DAMGO was out of the system and PS was added a third time, response amplitudes increased again in a similar degree as the first PS stimulation (Figure 6A red trace, times 15-17.5: 1.1 ± 0.006 ratio 340/380).

When comparing both traces during first, second and third PS stimulation, response amplitudes from transfected HEK_TRPM3_MOR and non-transfected HEK_TRPM3_NT cells during 2nd PS application were significantly different (concomitant to DAMGO application, Figure 6A red and black traces during times 10-12.5 min, 0.6 ± 0.002 vs 1.2 ± 0.005, p<0.001, Mann-Whitney Test). During third PS stimulation the response amplitudes for both groups were similar; interestingly, in both cases this amplitude was slightly smaller than for the first PS stimulation (Figure 6A HEK_TRPM3_MOR: 1.1 ± 0.006 vs 1.2 ± 0.004, n.s; HEK_TRPM3: 1.4 ± 0.003 vs 1.5 ± 0.003, n.s, Mann-Whitney Test). These slight and non-significant differences might indicate some tachyphylaxis effect on the TRPM3 receptor after repeated activation by the agonist. Tachyphylaxis is a natural phenomenon consisting of a consecutive decrease in response amplitudes upon repeated stimulations.

The percentage of inhibition of agonist-induced responses mediated by MOR was 63.35 ± 0.13% in transfected cells, while for non-transfected cells this value corresponded to only 3.35±0.28%. Those differences in PI between groups are significant (Mann-Whitney Test: p<0.001, Figure 6B) and show a strong inhibitory effect on agonist-induced TRPM3 activity when MOR is activated.

MOR-mediated modulation of laser heat-induced TRPM3 cell responses

Since the threshold for HEK_TRPM3 cells for laser-heat stimulation was determined in *3.1.1 Laser stimulation on cell cultures* to be 614.85 mJ, energies over that threshold were used to stimulate those cells. In the following experiments, we intended to investigate if the modulation mediated by MOR in TRPM3 response amplitudes induced by agonist application occurs as well when we activate the TRPM3 channel by heat stimulation. The paradigm was that activation of the TRPM3 channel by laser-heat will rise the intracellular calcium levels by opening of the channel in both transfected and non-transfected cells, however, when the specific MOR agonist DAMGO is added to the system, HEK_TRPM3 cells transfected with the MOR will have a decreased response amplitudes to heat, due to a modulation of the TRPM3 channel exerted by the binding of DAMGO to the MOR. On the other hand, laser-heat responses in non-transfected cells should not be affected by DAMGO.

Activation of the TRPM3 channel by laser-heat stimulations (696.85 mJ, calibration curve in *Appendix 1*) was rapidly achieved and was reversible on HEK_TRPM3 cells (Figure 7, protocol of the time course in 2.2.3 *Functional assays*). In non-transfected HEK_TRPM3_NT cells, following three repeated laser-heat stimulations, responses occurred rapidly and were reversible (Figure 7A, black trace during times 2.5, 7.5 and 12.5 min, maximum increase in fluorescence ratio 340/380 of 0.66 ± 0.04, 0.54 ± 0.02 and 0.49 ± 0.02 times for the first, second and third laser
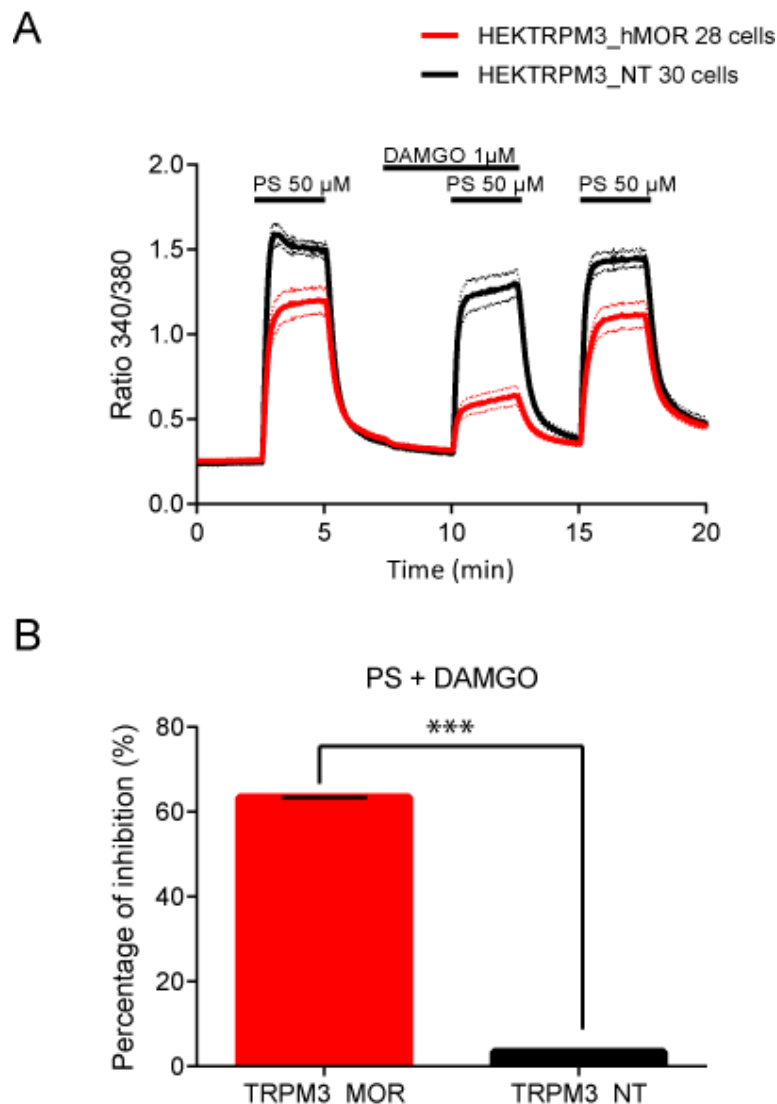
Figure 6: MOR activation modulates chemical-induced TRPM3 responses on transiently transfected HEK_TRPM3_MOR cells. A. Time course of the increase in ratio 340/380 nm in non-transfected HEK cells stably expressing the TRPM3 ion channel (HEK_TRPM3_NT, black trace) and HEK_TRPM3 cells transiently transfected with the µ-opioid receptor (HEK_TRPM3_hMOR, red trace) in response to chemical stimulation. Three chemical-induced stimulations of the TRPM3 channel with the specific agonist of TRPM3, Pregnenolone Sulphate (PS) were applied at times 2.5, 10, and 15 min, and during 2.5 min each (lower black bars); while the specific MOR agonist, DAMGO was applied at time 7.5 min and during 5 min (upper black bar). Traces are shown as mean value (solid lines) ± SEM (dotted lines) for each time point. B. Percentage of inhibition on HEK_TRPM3_NT and HEK_TRPM3_hMOR cells mediated by addition of DAMGO during the second agonist-induced response.

stimulation, n= 17, cells belonging to 6 independent experiments). However, it was possible to observe already in them a clear tachyphylaxis effect on those heat-activated responses: When normalizing response amplitudes to the first laser stimulation they were 100%, 81.81% and 74.24% of the first laser stimulation for the 1st, 2nd and 3rd laser stimulations.

Using the amplitude values obtained for HEK_TRPM3_NT cells upon laser stimulation, tachyphylaxis effects on amplitude could be estimated for HEK_TRPM3_MOR cells. Therefore, if no effect of MOR was present on transfected cells, the expected amplitude values should have been: 0.48, 0.39 and 0.36 times in increase in ratio for first, second and third laser stimulations (these values were obtained by calculating the 100%, 81.81% and 74.24% of S1 for HEK_TRPM3_MOR cells). However, for transfected cells the measured maximum response amplitudes reached 0.48 ± 0.005, 0.37 ± 0.001 and 0.38 ± 0.001 times in increase in ratio (Figure 7A, red trace during times 2.5, 7.5 and 12.5 min, n= 49, cells belonging to 6 independent experiments). This decrease in S2 from 0.38 in HEK_TRPM3_NT to 0.36 in HEK_TRPM3_MOR indicates an action of MOR on heat-induced TRPM3 responses.

When comparing both traces during first, second and third laser-heat stimulation, response amplitudes from transfected HEK_TRPM3_MOR and non-transfected HEK_TRPM3_NT are statistically different at all time points (red and black traces during times 2.5, 7.5 and 12.5 min, first laser stimulation $p<0.05$, second and third laser stimulation $p<0.001$, Mann-Whitney Test).

The percentage of inhibition for HEK_TRPM3_MOR reached up to $44.46 \pm 0.42\%$, while for HEK_TRPM3_NT this value corresponded to $9.03 \pm 1.40\%$. These differences are significant between cell types (Figure 7B, Mann-Whitney Test: $p<0.001$) and confirm that MOR was able to inhibit heat-induced TRPM3 responses as well; however, the degree of inhibition was smaller than in the case of chemical-mediated TRPM3 responses (presented above).

The response amplitudes of the TRPM3 cells upon chemical activation (1.5 ± 0.003 of the ratio 340/380, n= 30) was larger than upon laser-heat stimulation (0.66 ± 0.011; n= 49, $p<0.001$, Mann-Whitney Test).

3.1.3 Modulation in primary culture of sensory neurons

MOR-mediated modulation of agonist-induced TRPM3 responses in DRG neurons

Once proved that in heterologous expression systems MOR activation can exert a modulatory effect on both agonist- and laser heat- TRPM3 responses, it was decided to explore whether those effects occur in nature by testing primary cultured sensory neurons obtained from DRG tissue from adult Sprague-Dawley rats (See 2.2.1 *Primary culture and cell lines*).

In the same way as in 3.1.2 *Modulation of TRPM3 in heterologous expression systems*, functional experiments on DRG cells were investigated in response to the agonist PS with or without the concomitant application of DAMGO, with some modifications (protocol on 2.2.3 *Functional assays*): after three repeated PS stimulations (second concomitant to DAMGO), neurons were additionally shortly stimulated with a high potassium solution, which depolarizes neurons and subsequently with capsaicin

10 µM, in order to select and analyze neurons that co-express both TRPM3 and TRPV1 channels separately.
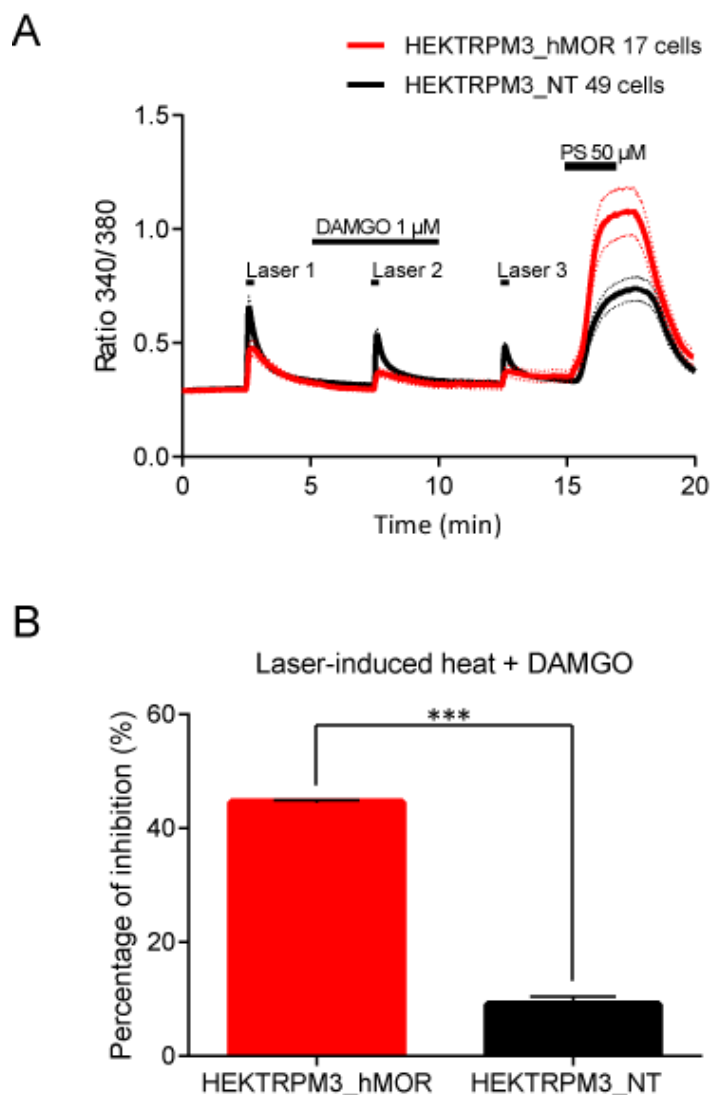
Laser-heat induced TRPM3 responses

Figure 7: MOR activation modulates laser-heat-induced TRPM3 responses on transiently transfected HEK_TRPM3_MOR cells. A. Time course of the increase in ratio 340/380 nm in non-transfected HEK cells stably expressing the TRPM3 ion channel (HEK_TRPM3_NT, black trace) and HEK_TRPM3 cells transiently transfected with the µ-opioid receptor (HEK_TRPM3_hMOR, red trace) in response to laser-induced heat stimulation. Three laser-induced heat stimulations of the TRPM3 channel were applied at times 2.5, 10, and 15 min (lower black bars Laser 1, Laser 2 and Laser 3); while the specific MOR agonist, DAMGO was applied at time 5 min and during 5 min (upper black bar). Traces are shown as mean value (solid lines) ± SEM (dotted lines) for each time point. B. Percentage of inhibition on HEK_TRPM3_NT and HEK_TRPM3_hMOR cells mediated by addition of DAMGO during the second laser-heat induced response

The experimental paradigm is that in DRG neurons, the neurons expressing the TRPM3 channel are target of inhibition of their activity when the MOR is activated by binding to its specific agonist, DAMGO. Neurons that do not express the TRPM3 channel are not affected by MOR modulation. In this case, since amplitude responses of the TRPM3 channel to PS stimulations in heterologous expression systems gave strong and reliable responses, and because by chemical stimulation the activity of the TRPM3 channel can be simultaneously tested in many more cells than with laser stimulations, this method was used in DRGs.

Stimulation with PS evoked a high and reliable response in TRPM3-expressing neurons (Figure 8A, red and black traces, PS1 mean 1.2 ± 0.017 and 1.3 ± 0.019 ratio 340/380). During the 2nd PS stimulation (which is concomitant to DAMGO) the response amplitudes were significantly different between DAMGO treated DRGs and Vehicle-treated DRGs (red trace: 1.0 ± 0.008, n= 72 cells from 7 independent experiments and black trace: 1.3 ± 0.014, n= 68 cells from 6 independent experiments, $p<0.001$, Mann-Whitney Test). When those cells are a 3rd time stimulated with PS after washout of DAMGO, the response amplitudes are still significantly different (1.0 ± 0.008 and 1.3 ± 0.014, $p<0.001$, Mann-Whitney Test), however, the baseline amplitude values between those traces were different, even from the beginning of the experiment (mean amplitudes at baseline: 0.75 ± 0.0003 and 0.86 ± 0.0003, $p<0.001$, Mann-Whitney Test).

When the data was analyzed in subgroups of responding cells sorted by co-expression of the TRPV1 channel (namely $TRMP3^{+}\_TRPV1^{+}$ and $TRMP3^{+}\_TRPV1^{-}$, Figure 8 B and C), the MOR mediated inhibition could be seen in both subgroups (in B: 2nd PS stimulation 1.1 ± 0.009 and 1.3 ± 0.012, and in C: 2nd PS stimulation 0.85 ± 0.007 and 1.3 ± 0.018 for DAMGO and vehicle- treated cells), however, a marked difference in baseline values can be observed in the subgroup of $TRPM3^{+}/TRPV1^{-}$ neurons. This marked difference in baseline argues for analyses including normalization of the data to 1st PS stimulation, as depicted in 2.2.3.2 *Data analysis of functional assays*.

The normalized response amplitudes are shown in Figure 9. Responses to 1st PS stimulation were set to 100% in all cases. For 2nd PS stimulation, a significant decrease in response amplitude was only observable on the DAMGO treated cells, for both $TRPM3^{+}\_TRPV1^{+}$ (Figure 9A, upper and lower left panel: 77 ± 3 and 97 ± 4% of 1st PS response, $p<0.001$, Mann-Whitney Test) and $TRPM3^{+}\_TRPV1^{-}$ cells (Figure 9A, upper and lower right panel: 82 ± 4 and 101 ± 3% of 1st PS response, $p<0.001$, Mann-Whitney Test). This result indicates that there are no differences in the MOR inhibition extent between $TRPM3^{+}/TRPV1^{+}$ and $TRPM3^{+}/TRPV1^{-}$ subpopulations since no differences in the response amplitudes during co-application of DAMGO were detected.

DRG, chemical stimulation

A DRG_TRPM3⁺

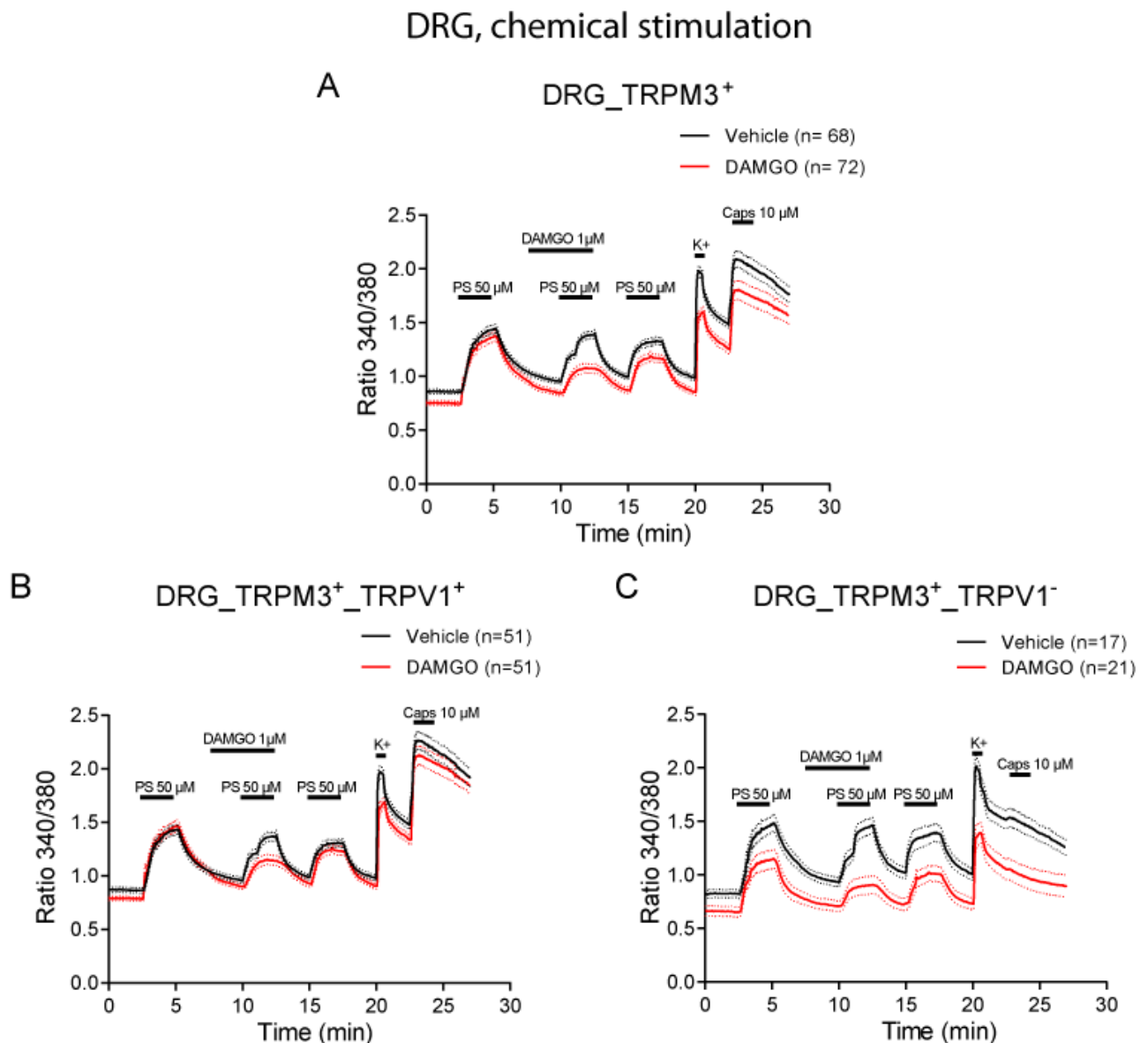B DRG_TRPM3⁺_TRPV1⁺

C DRG_TRPM3⁺_TRPV1⁻

Figure 8: Functional analyses of the effect of MOR activation on primary cultured sensory neurons in response to chemical stimulation. Time course of the increase in ratio 340/380 nm in primary cultured DRG neurons during chemical stimulation of the TRPM3 receptor with the agonist PS. In A: DRG neurons that responded to PS. In B and C: DRG neurons that responded to PS sorted by co-sensitivity to the selective TRPV1 agonist, capsaicin (in B, neurons that responded to both PS and Caps; in C, neurons that responded to PS and not to Caps). Black trace, vehicle-treated neurons, red trace, DAMGO-treated neurons. Traces are shown as mean (solid lines) ± SEM (dotted lines) for each time point.

When comparing amplitude changes between DAMGO and vehicle treatments in those cells, no differences were found between them (Figure 9B: 2nd PS response for DAMGO treated cells 77 ±3 and 82 ± 4% of 1st PS response, n.s. p= 0.55; and for Vehicle treated cells: 97 ± 4 and 101 ± 3% of 1st PS response, n.s. p= 0.07, Mann-Whitney Test). The normalized responses to the 3rd PS stimulation did not vary among subgroups (Fig 9A upper left and right panels: 85 ± 3 and 93 ± 3% of 1st PS response in TRPM3$^+$/TRPV1$^+$ subgroup, n.s., Mann-Whitney Test; and 94 ± 6 and 98 ± 6% of 1st PS response in TRPM3$^+$/TRPV1$^-$ subgroup, n.s., Mann-Whitney Test).

The proportion of responding neurons sorted by sensitivity to PS, Caps, both or none between treatment with DAMGO or vehicle are shown in Figure 10. All in all, about 33% and 22% of the total analyzed DRG cells responded to repeated PS stimulation in vehicle and DAMGO conditions (Figure 10, sum of blue and green proportions). From the DRG neurons that responded to PS, a small fraction of them (between a third and a fourth, in Figure 10 blue fractions, corresponding to the 7.87% and 6.29% of the total vehicle and DAMGO treated neurons) did not respond to capsaicin application (Figure 9C, time 22.5 min). On the other hand, the proportions of neurons only responding to capsaicin did not change among treatments (Figure 10, yellow fractions: 37.50 and 37.72% in vehicle and DAMGO treated neurons, n.s. Chi-square Test).

A significant decrease could be observed when comparing the proportions of TRPM3$^+$/TRPV1$^+$-responding neurons in the DAMGO-treated cells in comparison to the vehicle-treated cells (Figure 10, green fractions, 15.27% and 25%, p<0.001 Chi-square test, Chi-square= 27.58), while the proportion of TRPM3$^-$/TRPV1$^-$ increase (29.63% vs. 40.72%). These differences might account for an unexpected effect of DAMGO on TRPV1-mediated responses.
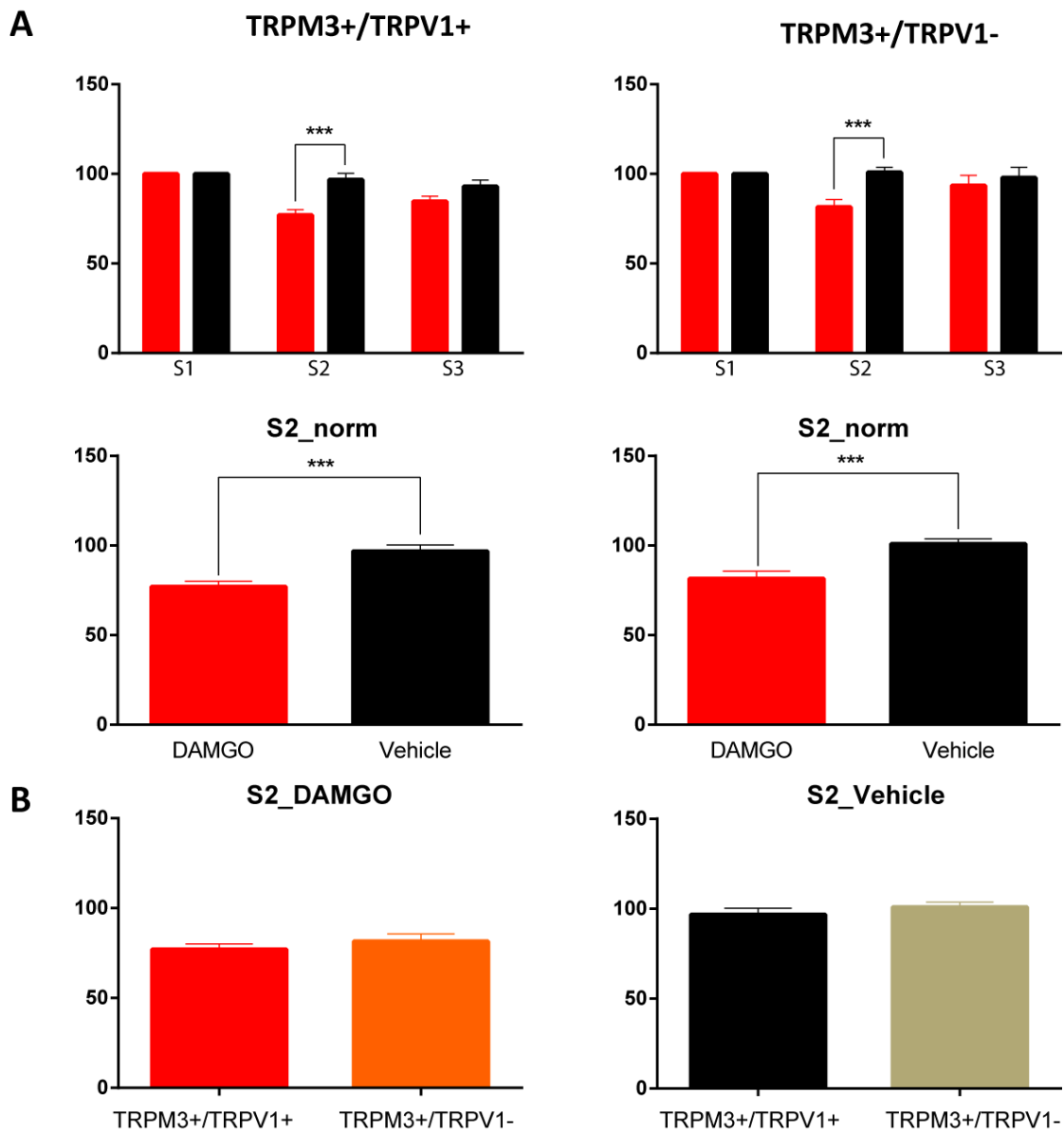
Figure 9: Functional analyses of the effect of MOR activation on primary cultured sensory neurons in response to chemical stimulation. A. Amplitude values normalized to first PS stimulation (S1), sorted by co-sensitivity to capsaicin, a specific TRPV1 agonist. Upper panel, values for S1, S2 and S3. Lower panel, values for S2 only. Black bars, vehicle-treated neurons, red bars, DAMGO-treated neurons. B. Normalized amplitude of response for S2, sorted by treatment (DAMGO- or Vehicle-treated cells). Almost no differences can be observed between neuron subpopulations. Red bar and black bar: normalized S2 responses from TRPM3$^+$/TRPV1$^+$ neurons under treatment with DAMGO and vehicle. Orange and grey bar: normalized S2 responses from TRPM3$^+$/TRPV1$^-$ neurons under treatment with DAMGO and vehicle. Data is shown as mean ± SEM for each time frame.
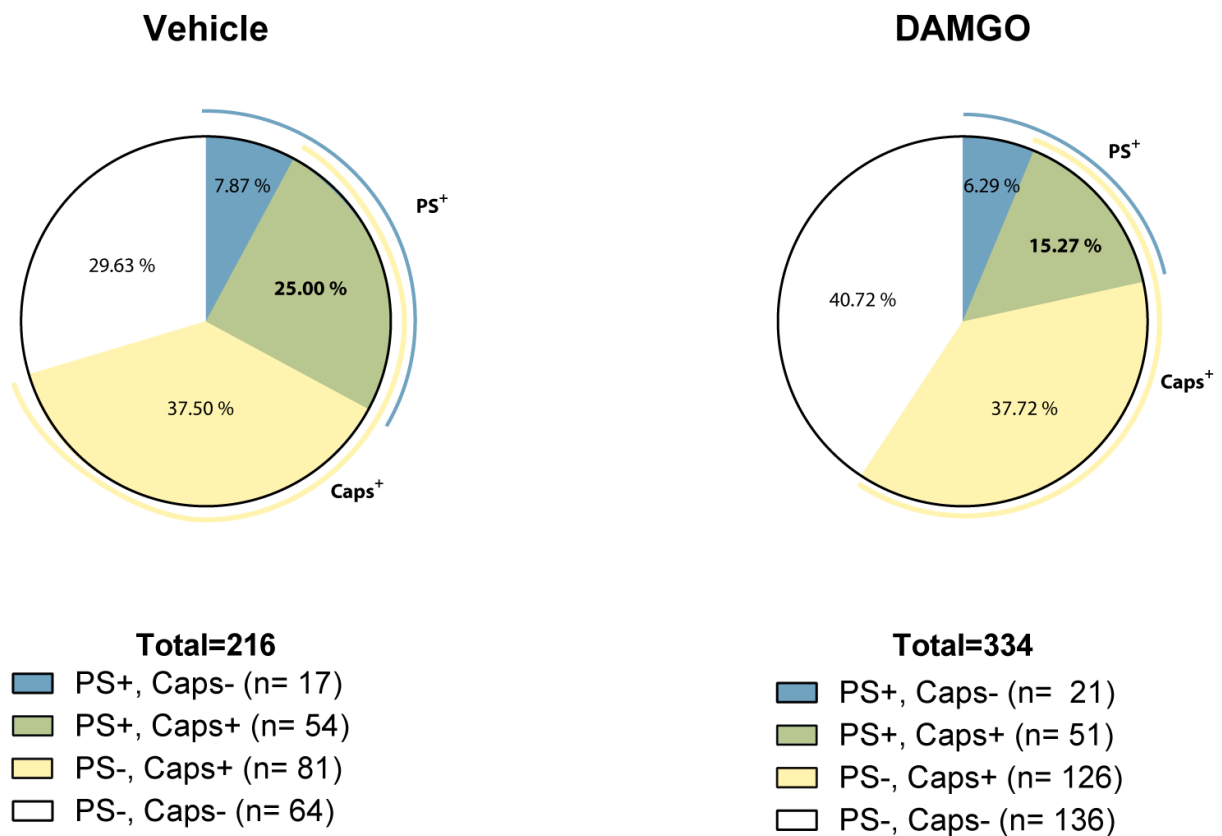
Figure 10: Distribution of the proportions of PS and/or Caps+ sensory neurons upon DAMGO treatment. Pie charts showing the distribution of the analyzed neurons. Blue: neurons that responded to PS. Yellow: neurons that responded to capsaicin. Green: neurons that responded to both chemicals. White: neurons that did not respond to either chemical. In parenthesis the number of cells analyzed per group is indicated.

3.2 Dorsal horn neurons activation in response to laser induced noxious heat in rats.

3.2.1 Laser-heat stimulation elicits a fast and reversible local increase in skin surface temperature

In the foot explant, laser irradiation (200 ms duration time, 100 mW) produced a localized (spot size 1.36 ± 0.32 mm in diameter, Figure 11A-B) increase in surface temperature of 14.46 ± 0.06 °C (Figure 11C - D) above basal temperature of the explant (14.64 °C). This increase in temperature of 14.46 ± 0.06 °C corresponded to a heat ramp of 70°C/s.

The increase in skin temperature was independent of the initial basal temperature of the paw explant: in two different experiments (basal temperature of 14.64 ±0.07 and basal temperature of 28.5 ± 0.2 °C) the change in temperature was tested at 100 mW and corresponded to increases in temperature of 14.46 ± 0.06 °C and 13.96 ± 0.16 °C. Those values did not differ significantly (n.s., Mann-Whitney test).

No heat accumulation occurred on the paw explant with an interstimulus interval (ISI) of 10 s (Figure 11D). By measuring the local increase in temperature in the foot explant at different laser power intensities, the relationship between power and increase in skin surface temperature was determined (Figure 11C). With this, a conversion of individual heat withdrawal thresholds from power to temperature values was possible: the heat withdrawal threshold in rats was in average 45 mW, a value that corresponds to an increase in temperature of 8.13 ± 0.07 °C (Figure 11E, calculated from Figure 11C). Considering a normal basal temperature of 33 °C at the skin of a rats hindpaw, then the withdrawal threshold for rats tested corresponded to an increase in temperature up to 41 °C.

From the increases in skin temperature at different laser power magnitudes along time we intended to estimate the time required to reach threshold for noxious temperatures (Figure 11F). At increasing laser intensities, the rise in surface temperature increased and the noxious temperature was reached faster. Using 100 mW power and 200 ms laser pulses, the time required to reach the withdrawal threshold increase in temperature of 8.13 °C corresponded to 110 ms (yellow dotted line, Figure 11F).

3.2.2 Laser-heat withdrawal thresholds in awake animals

One day prior to recordings, the animals were tested for laser-heat withdrawal thresholds (see Methods, Figure 11E). The mean threshold value among individual thresholds was 44.48 ± 4.43 mW (Figure 11E, left bar). This power magnitude produced a localized increase in surface temperature of 8.13 ± 0.07 °C (measured in foot explant, Figure 11E, right bar and Figure 11F, purple line). Therefore, during recordings the power of the laser was set to 100 mW, assuring that this power was at suprathreshold intensity for all animals.
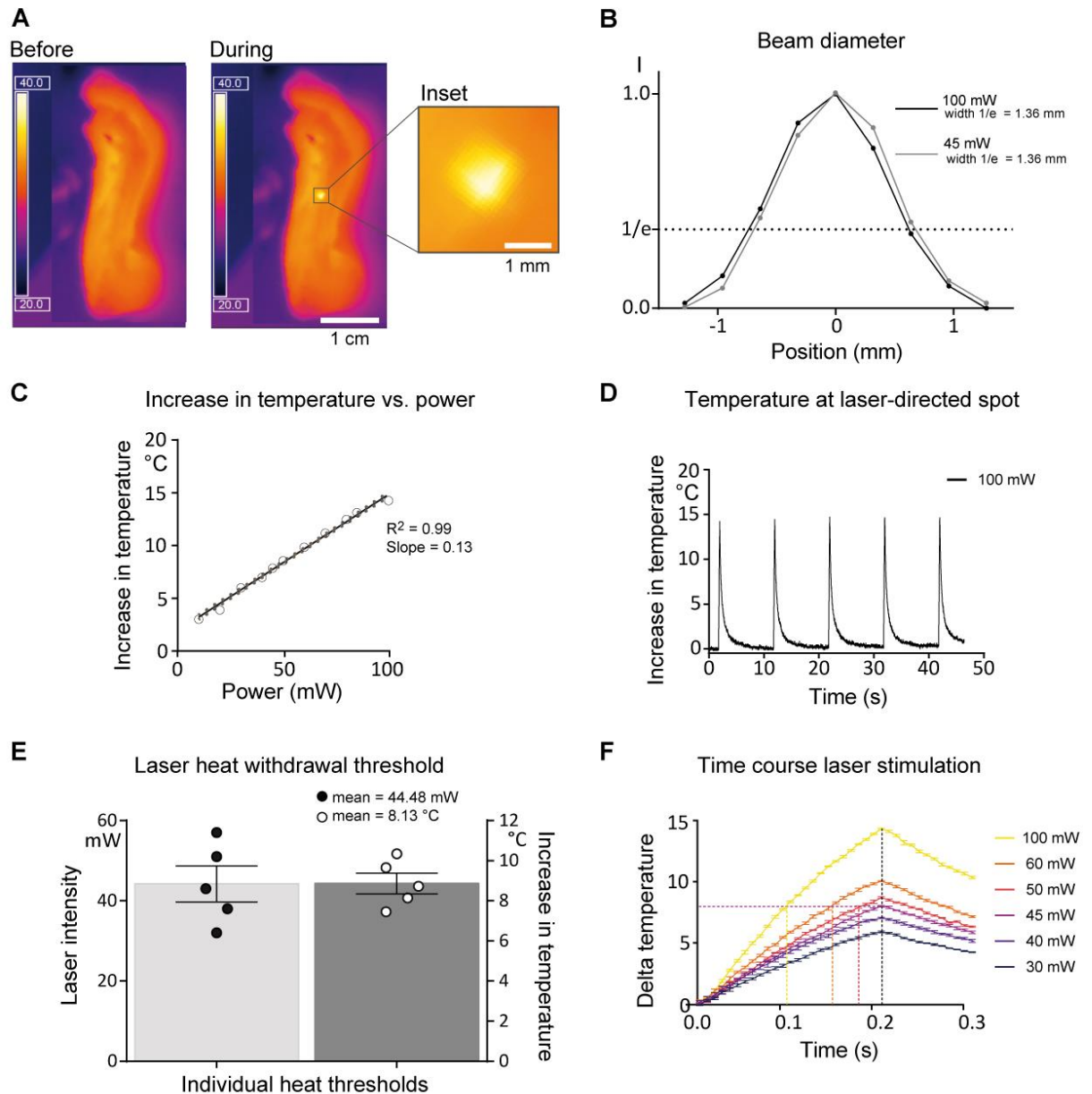
Figure 11: Laser-heat application to the skin produced a small, brief and contactless heat stimulation. A) Infra-red pictures showing the surface temperature of a rat paw before and during laser stimulation. B) Beam diameter of the skin area where surface temperature increased, determined by 1/e. Size of the laser-directed spot: 1.36 ± 0.32 mm in diameter. C) Correlation between the power and the increase in temperature elicited on the skin of a paw explant. Data points represent the mean value of 5 stimulations for a given power. A regression line with 95% confidence interval is shown (solid and dotted lines). D) Temperature time diagram showing the increase in temperature evoked by 5 consecutive laser stimulations. E) Individual values and group mean value of laser-heat withdrawal threshold in means of power (left bar) or increase in surface temperature (right bar, calculated from panel C and measured in foot explant. For each animal tested, the withdrawal thresholds for evoked laser-heat were less under 100 mW. F) Time course during the first 300 ms after laser stimulation showing the increase in temperature elicited on the skin for six different laser-power magnitudes: 100 mW (yellow), 60 mW (orange), 50 mW (red), 45 mW (purple), 40 mW (violet) and 30 mW (blue). Data is shown as mean ± SEM for each time frame. The maximal temperature reached at heat-withdrawal threshold power (45 mW) is 8.13 °C (purple dotted line). The time required at 100 mW to reach that temperature is 110 ms (yellow dotted line).

3.2.3 Dorsal horn neurons responding to laser-heat are nociceptive

All in all, 41 neurons were recorded in 6 animals (Table 1). Of these, 14 were LTM neurons (34.1%), 20 WDR neurons (48.8%), and 7 HTM neurons (17.1%, Figure 13A). Eleven of the 41 neurons responded to the laser-heat stimulus (26.8%). The neurons were recorded in a depth between 110 to 880 μm in the dorsal horn (Figure 13B). While for LTM neurons the recording depth ranged from 280 to 660 μm, the recording depths for WDR and HTM neurons were widely distributed (110 to 810 μm and 120 to 700 μm, Figure 13B). Examples of each type of recorded neuron in response to mechanical and laser-heat stimulation are shown in Figure 12.

3.2.3.1 Response properties to mechanical stimulation

After five consecutive innocuous mechanical stimulations (touch, 1/s, total time 5 s), LTM neurons responded by firing action potentials when their receptive field was stimulated (Figure 12A1, 3-5 APs/stroke, rapidly adapting input). When mechanical noxious stimuli were applied (pinch, 5 s), the neurons mainly responded during onset and offset of stimulation, corresponding to the "touch" part of the pinching process. Moreover, after electrical stimulation of the sciatic nerve, LTM neurons show A-fiber input only at a short mean latency of 3.3 ± 0.2 ms (not shown).

In WDR neurons during touch and pinch stimulation, responses were elicited in a graded manner (Figure 12B1, 8.5 ± 2.2 APs/stroke for touch and 124 ± 21.5 APs/pinch, slowly adapting input). In HTM laser-heat sensitive neurons a clear firing of action potential upon pinch stimulation was observed (Figure 12C1, 133 ± 61.6 APs/pinch, slowly adapting input), while no responses to touch nor moderate pressure (5 s) were detectable, confirming their intrinsic property as noxious-carriers only. In WDR and HTM neurons electrical stimulation of the sciatic nerve elicited action potentials with short response latency (mean A-fiber input latency 3.4 ± 0.6 ms) followed by action potentials with long response latencies (mean C-Fiber input latency 101.5 ± 12.5 ms, single unit values in Table 2).

3.2.3.2 Response properties to laser-heat stimulation

Not a single LTM neuron responded to laser-heat stimulation (max. power 100 mW) neither inside their mechanosensitive receptive field nor outside of it (Figure 12A2 and Figure 13A). Reversely, dorsal horn neurons processing nociceptive input from the plantar glabrous skin (WDR, HTM) responded to the laser-heat stimulus, however not all of them were laser-sensitive (black area in open bars for WDR and HTM neurons, Figure 13A). In WDR laser-heat sensitive neurons, responses to laser–heat occurred within 236 - 292 ms after stimulus onset (Figure 12B2); while for HTM laser-heat sensitive neurons those responses occurred during the first 239 – 418 ms after stimulus onset (Figure 12C2). Together, these results indicate that only dorsal horn neurons processing nociceptive input respond to noxious heat stimuli and that the peripheral input is transmitted by both A- and C-fibers.
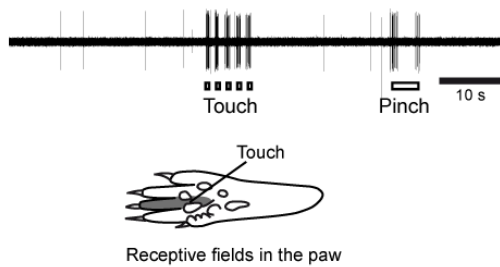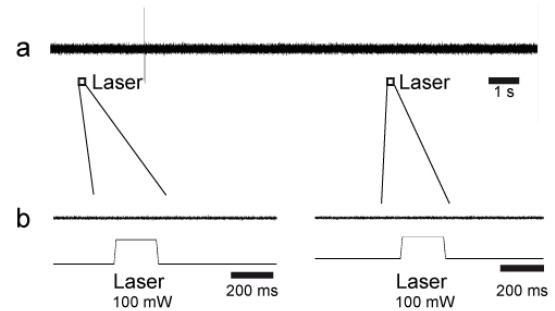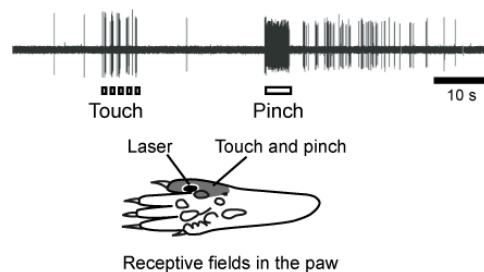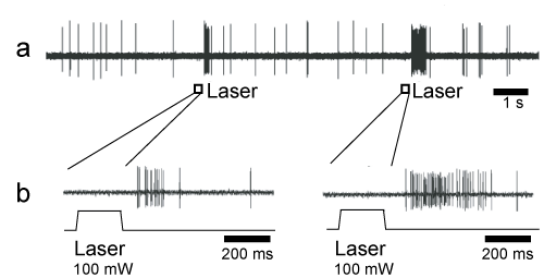
Figure 12. Types of dorsal horn neurons classified by mechanical stimulation of the skin. Responses of A) a LTM neuron, B) a WDR neuron and C) a HTM neuron evoked by 1. mechanical stimulation or 2. laser-heat stimulation of the plantar glabrous skin. Touch: touching the skin with an artist's brush repeatedly; Mod. Pressure: moderate innocuous pressure to the skin applied with a blunt probe. Pinch: pinching the skin with a sharpened watchmaker's forceps. Open bars underneath the registrations in 1 indicate time and duration of stimulation. a) Responses to laser-heat stimulation (100 mW, 200 ms). b) Responses shown in a) at a higher resolution. Only the two nociceptive HTM and WDR neurons responded to laser-heat application. In B) and C), schemes showing receptive field's size and distribution are repetitions from data shown in Figure 14, added here for comparison purposes.
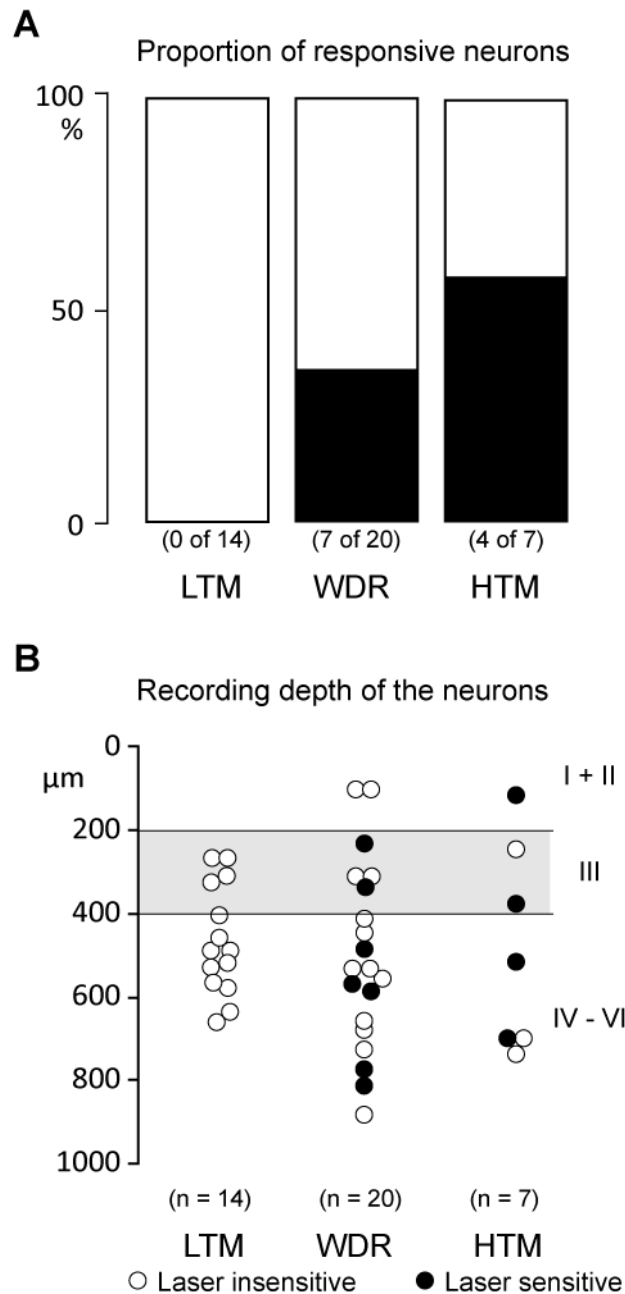
Figure 13. Only subpopulations of nociceptive neurons within all dorsal horn laminae are laser-heat sensitive. A) Proportion of laser-heat sensitive dorsal horn neurons (black area in the open bars). No differences between the number of laser responsive WDR and HTM neurons were found (Fisher exact test, P= 0.39) B) Recording depth of the neurons in the dorsal horn. Lines indicate the approximate borderlines between Lamina I +II (superficial dorsal horn), Lamina III and Laminae IV-VI (deep dorsal horn). LTM: Low threshold mechanosensitive neurons; WDR: wide dynamic range neurons; HTM: high threshold mechanosensitive neurons. The numbers in parentheses represents the number of neurons.

3.2.4 Receptive fields sensitive to heat were small and located inside the mechanosensitive receptive fields

In laser-sensitive dorsal horn neurons, the heat-sensitive receptive field was always located inside the mechanosensitive one. Heat sensitive areas apart from the mechanosensitive field were not found (Figure 14A). In all cases the heat-sensitive receptive field was distinctly smaller than the mechanosensitive one (mean: $2.73 \pm 0.38\%$ vs. $12.93 \pm 1.18\%$ of the total plantar surface; $P < 0.01$), while the mechanosensitive receptive field area between laser-heat insensitive neurons (mean: $17.11 \pm 1.26\%$, $P = 0.19$; Figure 14B) did not significantly differ from that of laser-heat sensitive neurons.

Heat-sensitive receptive field sizes were 26% of mechanosensitive receptive fields in WDR and 37% in HTM laser-sensitive neurons ($P = 0.46$, Figure 14C).The sizes of the heat receptive fields ranged between 10% and 60% of the mechanical receptive field.

3.2.5 Properties of laser-heat induced action potential discharges

The number of action potential discharges in response to the first positive laser stimulation (Figure 15A and Table 3) was higher in HTM neurons than in WDR neurons (14 ± 0.7 vs 9 ± 4.3) however those differences did not reach significance ($p = 0.8$, Mann-Whitney Test, Figure 15A).

After stimulus onset, laser sensitive WDR neurons elicited the first action potential within 266 ± 16 ms, while for HTM neurons the mean latency was 308.3 ± 55 ms. No significant differences were found between both types ($p = 0.9$, Mann-Whitney Test, Figure 15B). Moreover, when we consider that the time needed to reach noxious temperature was 110 ms (as shown in 3.2.1 *Laser-heat stimulation elicits a fast and reversible local increase in skin surface temperature*), and subtract this time from the measured latency values: then action potential firing in laser-heat sensitive dorsal horn neurons occurred in average 155.7 ± 28 ms for WDR neurons and 198.4 ± 55 ms for HTM neurons. These values are comparable with the C-fiber latencies measured with electrical stimulation of the sciatic nerve (159 ± 3.9 ms for WDR and 190 ± 5.6 ms for HTM neurons, Figure 16, panel F).
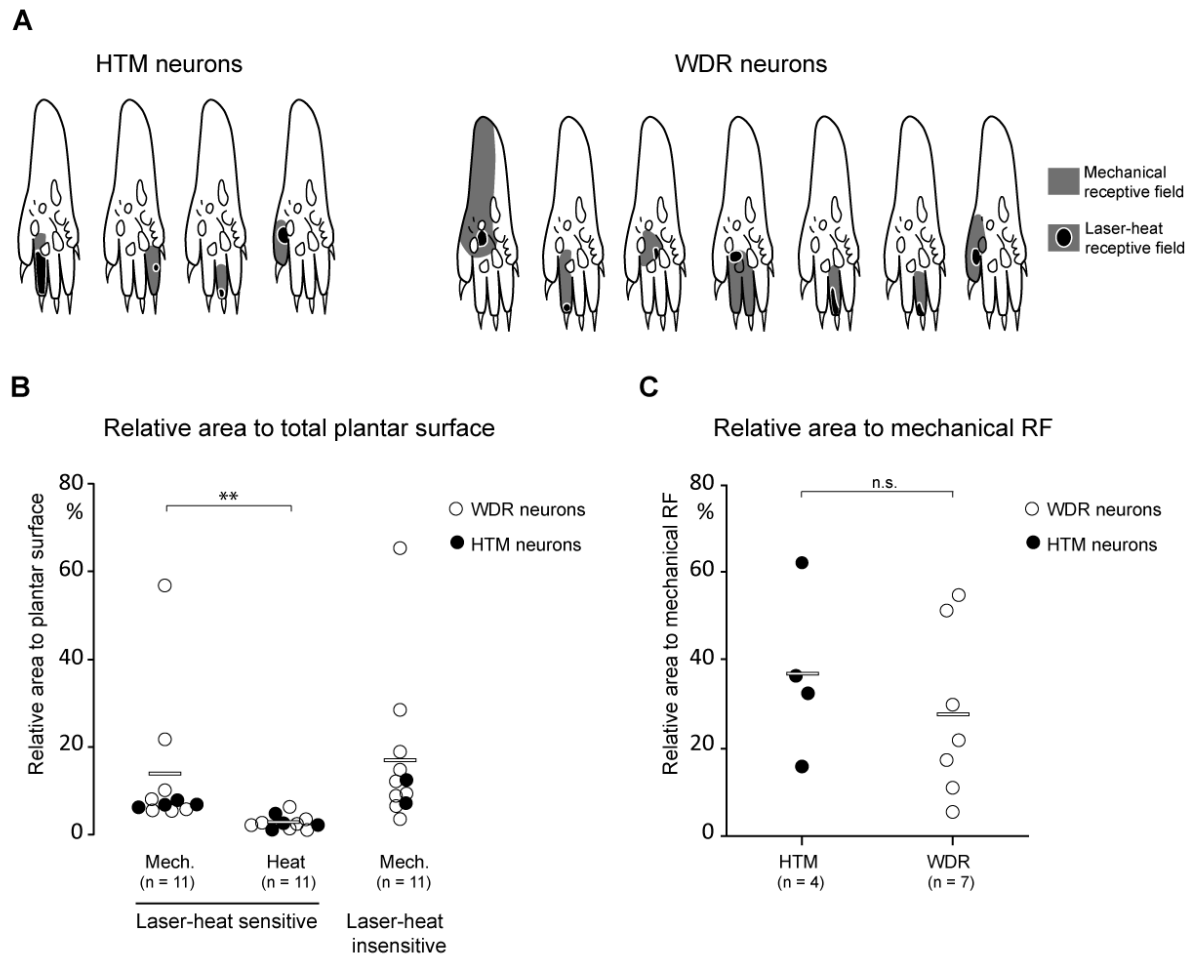
Figure 14. Receptive field areas for mechanical stimulation are much larger than for laser-heat stimulation. A) Schemes of receptive field's size and distribution from laser-heat sensitive nociceptive neurons for mechanical and laser-heat stimulation. B) Receptive field area for mechanical and laser-heat stimulation in laser-heat -sensitive and -insensitive WDR and HTM neurons, relative to the total area of the plantar surface. Heat RFs are significantly smaller than mechanosensitive RFs (Mann-Whitney Test, $p<0.01$), while in the sizes of mechanical receptive fields between laser-heat sensitive and laser insensitive neurons no significant differences were found (Mann-Whitney Test). C) Receptive field area for laser-heat stimulation relative to the size of the respective mechanosensitive RF for each of the heat-sensitive WDR and HTM neurons. The sizes of heat RF did not significantly differ between nociceptive neuron types (Mann-Whitney Test). Open bars indicate the mean value for each group. mech.: mechanosensitive receptive fields; heat: receptive fields responsive to laser-heat stimulation. The numbers in parentheses show the number of neurons for each group.
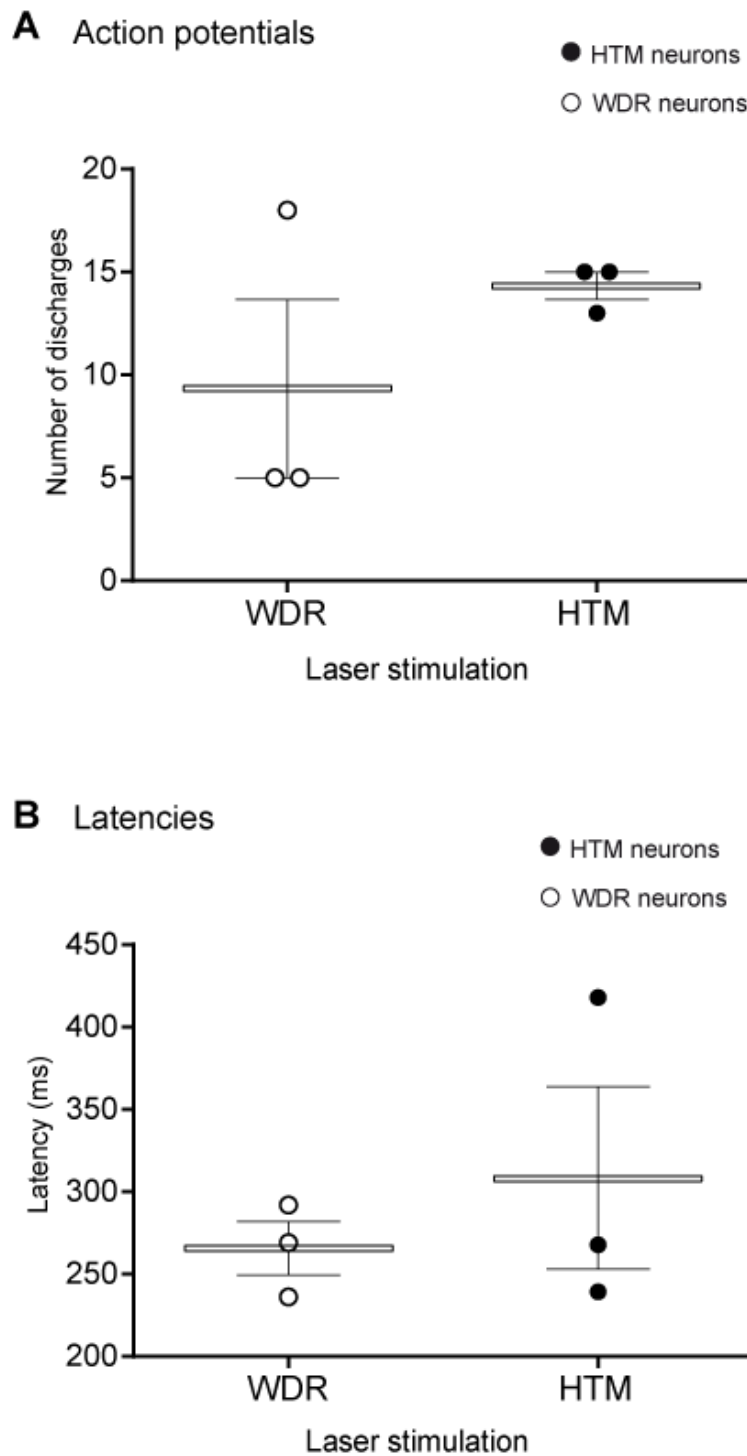
Figure 15. Response properties of laser-heat sensitive neurons upon laser stimulation. A) Discharge frequencies and B) response latencies evoked by the first positive laser stimulation (total n = 6, HTM marked as black dots n = 3, and WDR marked as open dots, n = 3). Horizontal bars indicate mean values. In all comparisons no significant differences were found (Mann-Whitney Test).
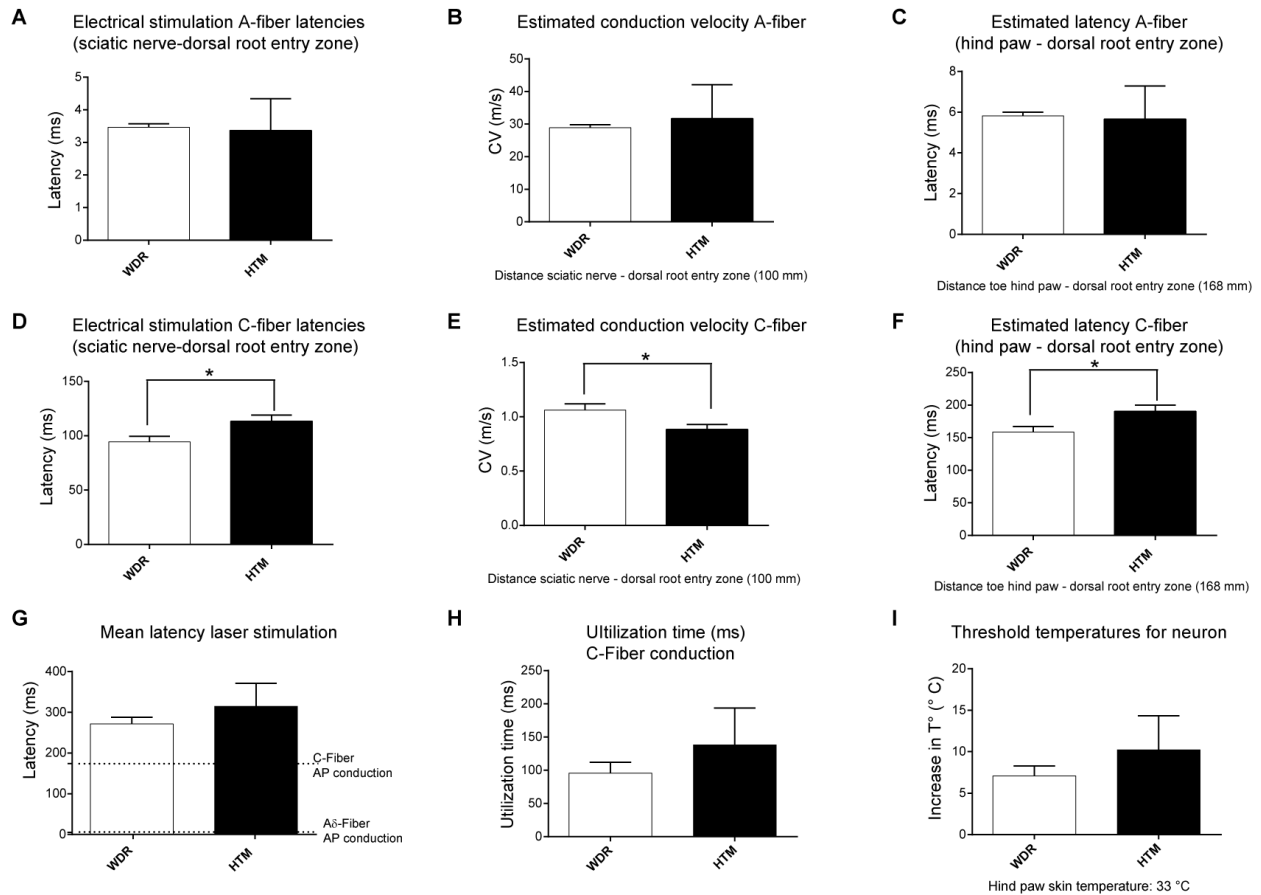
Figure 16 Conduction properties and threshold temperatures of laser-sensitive dorsal horn neurons. A) A-Fiber latencies and D) C-Fiber latencies of the laser-sensitive WDR and HTM dorsal horn neurons recorded following electrical stimulation in the sciatic nerve. From these latencies, and considering a distance between sciatic nerve and dorsal root entry zone of 100 mm, the conduction velocities from A- and C- fibers were calculated and shown in B) and E). From the conduction velocities calculated and considering a distance between hind paw to dorsal root entry zone of 168 mm, the latencies were estimated for C) A-Fiber input and F) C-Fiber input. G) Mean response latencies evoked by the first positive laser stimulation. Dotted lines indicate the time required for C- fiber AP conduction (170 ms) and A-Fiber AP conduction (5.6 ms). H) Mean utilization times for laser stimulation calculated as the difference between the latencies obtained in G) minus the C-Fiber AP conduction time (170 ms). I) Estimation of the increase in temperature required to elicit laser-induced responses, calculated from Figure 11C. Data presented as mean ± SEM (total n = 6, HTM marked as black dots n = 3, and WDR marked as open dots, n = 3). Comparisons between neuron types were evaluated using the Mann-Whitney Test.

Table 1. Input source of dorsal horn neurons. The table lists the number of neurons for each animal studied. LTM: Low threshold mechanosensitive neurons; WDR: wide dynamic range neurons; HTM: high threshold mechanosensitive neurons. LS: Laser-heat sensitive neurons for each category

Table 1: Input source of dorsal horn neurons

	Type of neuron recorded							
	All neurons		LTM		WDR		HTM	
Animal	Total	LS	Total	LS	Total	LS	Total	LS
1	10	2	3	0	6	1	1	1
2	6	0	1	0	3	0	2	0
3	8	3	3	0	5	3	0	0
4	6	2	2	0	3	1	1	1
5	6	2	3	0	2	1	1	1
6	5	2	2	0	1	1	2	1
Total	41	11	14	0	20	7	7	4

Table 2: General aspects of the laser sensitive dorsal horn neurons

Laser-heat withdrawal threshold (mW)	Recording depth (µm)	Type of neuron, Unit	TTL	Electrical stimulation (sciatic nerve) A-Fiber input Threshold (mV)	A-Fiber input Latency (ms)	C-Fiber input Threshold (mV)	C-Fiber input Latency (ms)	C.V. (m/s) [a] electrical A-Fiber input	C-Fiber input	Latency (ms) [b] A-Fiber input	C-Fiber input	Receptive field mechanical Size (%) [c]	Location	Receptive field laser Size (%) [c]	Location	Mechanical stimulation (n° APs) Touch	Moderate Pressure	Pinch
n.t.	120	HTM 1/1	no	n.t.	n.t	n.t.	n.t.	n.t.	n.t.	n.t.	n.t.	7.74	digit 4	4.84	Inside MRF (base of digit)	0	0	127
57	380	HTM 3/4	yes	n.t.	3.6	n.t.	110	27.78	0.91	6.05	184.80	7.22	digit 2	2.65	Inside MRF (base of digit)	0	0	252
37	700	HTM 4/6	yes	920	4.2	8.9	110	23.81	0.91	7.06	184.80	6.72	digit 3	1.07	Inside MRF (internal right side of digit)	0	0	101
30	520	HTM 5/5	yes	620	2.3	n.t.	120	43.48	0.83	3.86	201.60	6.54	digit 5	2.14	Inside MRF (base of digit)	0	n.t.	46
n.t.	590	WDR 1/9	no	n.t.	n.t.	n.t.	n.t.	n.t.	n.t.	n.t.	n.t.	56.79	heel and base of digit 5	6.31	Inside MRF (center of plantar paw)	6	n.t.	166
50	340	WDR 2/3	no	810	3.35	26	92	29.85	1.09	5.63	154.56	7.93	digit 4	2.38	Inside MRF (tip of digit)	4	n.t.	175
50	240	WDR 2/4	no	910	3.6	17	90	27.78	1.11	6.05	151.20	5.38	base of digit 4	2.78	Inside MRF	11	n.t.	55
50	780	WDR 2/8	no	n.t.	3.4	n.t.	100	29.41	1.00	5.71	168.00	21.64	digit 3 and 4	1.2	Inside MRF (base of digit 3)	13	n.t.	105
57	n.t.	WDR 3/7	yes	n.t.	n.t.	n.t.	90	n.t.	1.11	n.t.	151.20	6.21	digit 3	3.43	Inside MRF (internal right side of digit)	15	n.t.	77
37	570	WDR 4/5	yes	520	3.5	11	100	28.57	1.00	5.88	168.00	5.92	digit 3	1.03	Inside MRF (tip of digit)	1	29	155
30	490	WDR 5/4	yes	n.t.	n.t.	n.t.	n.t.	n.t.	n.t.	n.t.	n.t.	10.1	digit 5	2.22	Inside MRF (base of digit)	7	n.t.	178

a: C.V.= Conduction velocity, calculated considering a distance of 100 mm between sciatic nerve and dorsal root entry site.
b: Latency, estimated from conduction velocities, considering a distance of 168 mm between toe and dorsal root entry site.
c: Sizes of receptive fields are shown as percentages of total plantar paw.
n.t.: not tested

Table 3: Response properties of the laser sensitive neurons recorded with TTL pulses

Unit	Laser stimulation			
	number of APs	Latency (ms)	Utilization times (ms) [a]	Threshold for neuron (° C) [b]
HTM 3/4	15	267.8	97.8	7.24
HTM 4/6	13	239.3	69.3	5.14
HTM 5/5	15	418	248	18.36
WDR 3/7	5	292	122	9.04
WDR 4/5	5	236.1	66.1	4.90
WDR 5/4	18	269.1	99.1	7.34

a: Utilization times were calculated as the difference between laser latency and C-Fiber AP conduction time.

b:Temperature threshold for neuron (above skin temperature) calculated using the function obtained for skin temperature changes during laser-heat stimulation at maximal power (100 mW: y=74X+0.0078, Figure 11F)

4   DISCUSSION

4.1   Laser-heat induces TRPM3 activity, and activation of the MOR reduces the activity of endogenously expressed TRPM3 in sensory neurons

Noxious laser-heat rapidly and transiently activated the ion TRPM3 channel in heterologous expression systems with an activation threshold of 614.85 µJ. When co-expressing the MOR in those systems, a reduction of both agonist- and more importantly noxious heat- induced activity of the TRPM3 channel could be observed upon concomitant TRPM3 and MOR activation. This modulation also occurs in endogenously expressed TRPM3 channels from sensory neurons in the rat and mouse, in which the mechanism of action is through direct binding of the $G_{\beta\gamma}$ subunit to the TRPM3 receptor (mechanism described in a collaborative work with the department of Molecular Physiology from the University of Marburg, leaded by Professor Johannes Oberwinkler)[151]. Since this mechanism occurs specifically in the peripheral nervous system, these results would allow new targets for pharmaceutical treatments of acute pain without developing the unwanted side effects of current systemic opioid therapy.

4.1.1   Transduction of noxious laser-heat stimulation by TRPM3 channels

Noxious heat sensing is a fundamental biological process required for survival. Studying the channels that are activated in response to heat is not only important for a better understanding of their mechanisms but could also lead to the development of new therapies against pathological conditions of persistent pain.

Calcium imaging allows an accurate spatial and temporal visualization of the activity of ion channels upon specific activation, and using heterologous expression systems expressing only one type of ion channel allows the determination of its specific properties, like activation threshold. In these experiments, the responses of two different heterologous expression systems (HEK_TRPV1_VL8 and HEK_TRPM3) was compared to different energy levels of repeated laser-heat stimulation. Normal HEK cells not expressing heat-sensitive ion channels (HEK293) were used as negative controls.

For the TRPM3 channel, the laser-heat threshold was 614.85 µJ. Vriens and colleagues observed activation of the TRPM3 channel by increasing the temperature of the cell plate up to 43°C [57]. Interestingly, experiments in artificial planar lipid bilayers have shown that only by addition of phosphatidylinositol-4,5-biphosphate (PIP_2) concomitant to heat stimulation an incomplete opening of the TRPM3 channel occurs, indicating that other endogenous factors –existent in living cells- are required to reach the full open conformation of the channel in response to heat (up to 43 °C)[152, 153].

The fact that the threshold for laser-heat in TRPV1 channels was lower than in TRPM3 channels could be explained by the evidence from TRPV1$^{-/-}$ mice, which do not change their acute pain thresholds[22, 29]. Another explanation can be the differences in their Q_{10} values, which can be understood as a thermal sensitivity scale. The Q_{10} corresponds to the increase in current upon a 10 °C temperature increment. While the Q_{10} for TRPV1 corresponds to 14.8[23], for TRPM3 channels this value is only 7.2. Still, both values are high compared to heat-insensitive ion channels, which show a Q_{10} value of < 2, as shown in [61]. However, Q_{10} values obtained from different

experiment should not be directly compared since its determination strongly depends on experimental conditions.

A third line of evidence that supports the observations presented here might rely on the findings of Greffrath and colleagues; they observed in DRG neuron primary cultures, specifically in small diameter sensory neurons, two types of heat-evoked inwards currents: low-threshold (≤ 45 °C) rapidly activating and high threshold (47-49 °C) slowly activating inward currents[154]. In this report, they proposed that these inward currents would belong to the heat sensitive TRPV2 channel. Years later however it was concluded that the TRPV2 channel is not playing a key role in noxious heat sensing, since mice lacking TRPV2 have not shown differences in response to noxious heat [13]. Now that the TRMP3 channel is better characterized, it seems logical to think that the high-threshold inward currents observed by Greffrath and colleagues would belong to TRPM3 channels, which are known to be expressed in low diameter DRG neurons as well[57]. Nowadays it is acknowledged that in mice, three TRP channels are part of the system to detect noxious heat[13, 155].

The increases in calcium concentration in HEK293 cells were irreversible; indicating that in those cells laser-heat stimulation compromises its viability. This is noticeable by observing an initial increase in amplitude after the first laser stimulation, and then response amplitudes equal or slightly smaller than the previous stimulation response, denoting that the increase in calcium in those cells did never come back to baseline after the first laser stimulation, and a only slight but constant decrease in intracellular calcium concentration occurred among time. This clearly indicates that those response amplitudes are unspecific. This became evident when the specific agonists for TRPV1 and TRMP3 were added (capsaicin and PS, blue and brown bars). At energy intensities of 573.85 μJ and onwards, apparent positive responses to both PS and capsaicin are observable. However those channels are not present on these cells and responses to PS and caps were not existent at smaller laser energy intensities, therefore, it is reasonable to argue that the responses observed correspond to the initial high increase in calcium upon 1st laser stimulation.

The unspecific response to laser-heat using energy pulses equal or higher than 573.85 μJ is comparable to the unspecific increase in ratio observed at temperatures starting from 40 °C by Vriens and colleagues[57]. Since these unspecific increases do not come back to baseline values, they indicate the unviability of those cells. This observation rises up the importance of those heat-transducer ion channels for cell survival. In fact, no studies on non-transfected HEK cells and heat sensation have been performed until now. Some evidence of endogenous expression of ion channels in HEK293 cells exist up to date[156, 157], however this evidence in scarce, one of them only shows evidence at mRNA level, and the channels found are not related with heat perception.

The responses of HEK_TRPM3 cells to its agonist, the endogenous neurosteroid Pregnenolone Sulphate (PS), were high in amplitude and reproducible among repetitions. This result is in accordance with observations by others: Vriens and colleagues observed responses on both HEK_TRPM3 cells and DRG neurons from mice in response to PS at concentrations starting from 0.1 μM [57]. Indeed, the EC_{50} of PS for TRPM3 is ~23μM [65], however it is not yet clear whether PS can reach *in vivo* a concentration high enough to act as a genuine endogenous ligand[13]. Consequently, agonist-induced responses observed here, which were applied at a concentration of 50 μM, were higher in amplitude when compared to laser-heat induced responses.

Remarkably, the response amplitudes to PS were higher in non-transfected HEK_TRPM3 cells than in HEK_TRPM3_MOR cells (Figure 6A). This phenomenon might be related to some effect in the transfection procedure. It would have been of interest to compare the responses presented here to vehicle-treated cells. These differences in response amplitudes in HEK cells transiently transfected with the MOR have been observed by others as well[151].

Activation of the TRPM3 channel by laser heat also showed differences in the response amplitudes between non-transfected HEK_TRPM3 cells and HEK_TRPM3_MOR cells (Figure 7A); however, after repeated laser stimulations at 614.85 µJ of energy, two observations need to be remarked. First, the response amplitudes for the second and third laser stimulation are virtually equal in transfected cells. This might be due to the effect of DAMGO on the second laser stimulation, which would have been higher if DAMGO were not present on those cells.

Second, the amplitude for the PS stimulation (time 15-17.5 min) was much higher in MOR transfected cells than in the stably expressing HEK_TRPM3 cells (red vs black trace in times 15-17.5 min, maximum 1.1 and 0.74 of ratio 340/380). This observation might reflect some compromised viability of the channel in NT cells due to repeated laser-heat stimulation, which is not occurring in HEK_TRPM3_MOR since the modulation of the second response might prevent receptor fatigue,), arguing for a protective effect of the opioid system on cell viability upon repeated laser-heat stimulations. Additionally, since in these cells the response to PS afterwards was even larger on the transfected HEK_TRPM3_MOR cells, the effect seem to be very specific for noxious laser-heat stimulations. This result argues for a direct pharmacological action of DAMGO on MOR modulating the TRPM3 channel.

4.1.2 Peripheral modulation of the TRPM3 channel by MOR activation

It is well known and established that systemic opioid receptors inhibit pain in the CNS, however, the peripheral way of action in peripheral neurons have been observed only recently by a new mechanism involving dissociation of the G complex and direct interaction of the Gβγ subunit with the TRPM3 channel[151].

The results shown here demonstrate that the MOR mediated inhibition observed in heterologous expression systems also occurred in cultured primary sensory neurons of rats indicating that the mechanism is functional in living organisms. Indeed the mechanism has been observed as well in DRG from mice[151 158, 159]. In a complementary way, the data of this thesis shows that this mechanism also modulates laser-heat induced TRPM3 channel activation.

The reduction of the TRPM3 channel activity was in the reported data over 75% of its normal activity when activated with agonist and treated with vehicle stimulations[151 158, 159]. In contrast, the results presented here have shown a more modest reduction; the normalized response percentages between $TRPM3^+/TRPV1^+$ and $TRPM3^+/TRPV1^-$ subgroups was 77 ± 3% and 82 ± 4.1% (which means 23 ± 3% and 18 ± 4.1% inhibition of the 1st PS response).

Two reasons might explain these differences between the recent papers and the data presented here. First, the method for quantifying the response amplitudes

was different. Due to marked differences in baseline values existent in the results presented here, data was normalized to first PS response (Figure 8). If the differences in baseline values are not taken into account and the percentage of inhibition is calculated as for heterologous expression systems, then the percentage of inhibition accounts up to 30-35% (Appendix 2). This however demonstrates that this reason does not completely explain the differences in inhibition degree. A more plausible reason is that some differences in the expression levels of the MOR between rat and mouse account for this different results. While MOR receptors account for a 20.9% of the total DRG population in the rat [160], in mouse this counts up to 36.2% [161]. Moreover, the question how much of this MOR positive fibers are co-expressed with TRPM3$^+$ fibers between different species would answer the question more certainly.

In the same way, while TRPV1 expression in rat has been accounted to be about 35.7% of all DRG neurons [154]. In the results presented here, the proportion of neurons responding to capsaicin was 53%-62.5%. On the other hand, the proportion of neurons expressing TRPM3 channel in mice and rats has been estimated to be about 60% of DRG and TG neurons[57, 162], while in the results presented here it was only 21.5%-33% in DRG. These differences might be explained by the method used for quantification.

While functional experiments can show the proportions of channel-carrying neurons that are indeed functional might be more accurate to detect protein, some cells are lost in the process to get them in culture dishes. Immunohistochemical methods in DRG frozen sections require careful counting of the neurons of each section avoiding data over- or underestimation. An ideal method would show activity of the channel in complete DRG sections, where neurons possessing the TRPM3 channel can be observed not only by activity upon stimulation but also its distribution among the DRG.

Since the normalized response percentages between TRPM3$^+$/TRPV1$^+$ and TRPM3$^+$/TRPV1$^-$ subgroups were similar (77 ± 3% and 82 ± 4%), it is possible to conclude that the inhibition mediated by MOR on TRPM3 channel activity occurs independent of TRPV1 co-expression, which supports the specificity of this mechanism. These results are in accordance to previous reports[151, 158, 159]. But how does this mechanism works? The MOR is a G protein-coupled receptor. The binding of DAMGO to the MOR, activates the receptor, and the heterotrimeric complex interacts with the cytosolic surface of the GPCR. After binding to GTP, the complex is dissociated into G_α-GTP and a $G_{\beta\gamma}$ subunit. TRPM3 activity is inhibited by direct binding to $G_{\beta\gamma}$ [13, 151, 158, 159].

Following functional quantification, heat responding neurons that do not express the TRPM3 channel account for 15% of $trpm3^{-/-}$ sensory neurons[57], which means, the subgroup of neurons responding to PS but not to capsaicin was ablated. In the experiments performed here, this fraction corresponded to a 6.3-7.9% of the total number of cells analyzed (blue fractions in Figure 10). This could be due to different co-expression patterns between rat and mouse. In any case, both results indicate that the TRPM3 channel in sensory neurons is mostly co-expressed with other heat sensitive channels. As is it in humans [163]

One intriguing observation coming from the results of this research are the differences in the proportions of TRPM3$^+$/TRPV1$^+$ and TRPM3$^+$/TRPV1$^-$ responding DRG neurons. While with vehicle treatment the proportion of co-expressing neurons

is 25%, in DAMGO treated cells this proportion is only 15% (Figure 10). This is a very challenging observation to explain, since before the second PS stimulation (concomitant to DAMGO) cells are treated exactly equally. One possible reason is that even after washout of DAMGO, some of these agonists remain in the system and affect the responses of TRPV1 channels on neurons that co-express TRPM3 and TRPV1, however, this is unlikely because of *(laser response on hek cells)*. This goes in line with the results from Dembla and collaborators, where they observed as well that capsaicin-induced Ca^{2+} signals did not recover after DAMGO washout[151]. Direct effects of the MOR in TRPV1 have been reported previously as well[69, 73, 164].

Another point to consider is that the cellular function might be different between neuron subgroups with different expression patterns of TRPV1 and TRPM3. Indeed, by analyzing electrophysiological and ion flux measurements in primary sensory neurons of rats, Nagy and Rang observed that distinct ion channels responded either to heat or capsaicin, concluding that different molecular entities account for membrane responses to heat and capsaicin[165, 166]. Now it is known that at least one of these other molecular entities is the TRPM3 channel.

4.1.3 Implications in human heat pain signaling and treatment of acute pain

The TRPM3 channel is involved in acute pain and inflammatory hyperalgesia, and therefore many pharmacological approaches targeting it as a potential pain therapy have been attempted. Preclinical studies have shown that many of the TRPM3 inhibitors like isosakuranetin[167], flavanones[59] and primidone[162] inhibit pain responses to intraplantar injection of PS, increase latency to noxious heat stimuli and reduce heat hyperalgesia in inflammatory or neuropathic pain conditions. Moreover, and in contrast to the TRPV1, inhibition of the TRPM3 channel in sensory neurons with different classes of antagonists does not affect body core temperature[59, 162, 167]. Targeting MOR may have therapeutic potential as an intervention to prevent potentiation of TRPV1 responses through the PKA pathway in inflammation [73] and to prevent TRPM3-induced noxious activity [151]

Nowadays, the prescription against acute pain conditions like for example post-operative pain is often systemic opioid agonists, like morphine. More controversial, these drugs are also prescribed in chronic pain conditions like cancer-induced pain. While they are effective in ameliorating the pain, its continuous administration leads to severe side effects like tolerance, respiratory depression, addiction, constipation and others that decrement the life quality of the patients. The recent discovery of the direct modulation mediated by peripheral opioid receptors on the TRPM3 channel activity induced by the neurosteroid PS would open a new path in the development of new therapies against acute pain conditions.

The results presented in this thesis confirm these observations and moreover demonstrate that peripheral opioid receptors are able to reduce the TRPM3 channel activity induced by noxious laser-heat stimulation, directly linking the role of the peripheral MOR mechanism as antinociceptive. Since the concentrations required activating the TRPM3 channel by PS are not yet described to occur in peripheral neurons, noxious heat, rather than PS, noxious heat is more likely the stimulus type that indeed activates the TRPM3 channel in peripheral neurons. Together these results open up the opportunity to develop new therapies to treat pain addressing peripheral

activation of MOR and consequently inhibiting TRPM3-mediated nociception. The great advantage of these potential therapies would be the lack of the unwanted secondary effects of systemic opioids.

4.1.4 Technical considerations

Since our results strongly depend on the fluorescence values given by the cells, we should not discard the possibility that fluctuations in lamp intensity might have affected our measures in some extent. However it is unlikely that these effects count up to a high degree of error, because as mentioned before, the observations presented in this research are similar to the ones observed recently.

It was always intended to perform a balanced number of control and experimental data in the same day, in order to keep conditions as equal as possible between measurements. However it was not always the case and the experiments shown here account for trials performed among several weeks. However, variation in between experiments for example, differences in the transfection efficiencies between sets of experiments did not affect the overall mean values of the readouts more than 5%. In most cases responses were stable among repetitions. Still and as in all experiments, results are always affected by randomness.

It remains to be determined up to which temperatures exactly do cells increase their temperatures when laser pulses at the thresholds energies used in this study are applied.

4.1.5 Summary and conclusions

Laser-heat transiently activates the ion TRPM3 channel in heterologous expression systems with a threshold of activation of 614.85 µJ. The activity of the TRPM3 channel can be modulated by activation of the MOR. This modulation also occurs in endogenously expressed TRPM3 channels from sensory neurons in the rat, in which the mechanism of action is through direct binding of the $G_{\beta\gamma}$ subunit to the TRPM3 receptor after dissociation of the complex originally located at the cytosolic side of the MOR. Since MOR receptors are only expressed at the peripheral nervous system, these results would allow new targets for pharmaceutical treatments of acute pain without developing the unwanted side effects of current systemic opioid therapy.

4.2 Laser-heat sensitive receptive fields are smaller than mechanosensitive receptive fields in dorsal horn neurons sensitive to laser-heat stimulation

The results presented here show that in the dorsal horn of the spinal cord, encoding of suprathreshold laser-heat stimulation applied in the periphery is mainly mediated by a subgroup of nociceptive WDR and HTM neurons that are found in all layers of the dorsal horn. The mean withdrawal threshold of the animals, measured one day before recordings is consistent with the threshold for the dorsal horn nociceptive neurons. This threshold was estimated considering input was transmitted by C-fibers. For all laser sensitive neurons, the laser-heat sensitive receptive fields were smaller and located inside the mechanosensitive receptive fields.

4.2.1 Spinal processing of laser-induced nociceptive signals

In a first instance laser-heat stimulation activates afferent inputs that then transmit the signal to the dorsal horn of the spinal cord. In monkeys, the afferent inputs activated by laser-heat in the glabrous skin have been described as C-mechano heat (CMH) nociceptors, whose threshold for laser-heat was 41°C and conduction velocity 0.8 m/s, and A-fiber mechano-heat (AMH) nociceptors type I, whose threshold was 53°C and conduction velocity 40 m/s[9]. In humans, laser-heat stimulation of the skin activates polymodal CMH fibers as well, with a mean threshold of 102 mJ[141], or 39.8 °C for C-fibers and 46.9 °C for Aδ-fibers[90], and the nerve conduction velocities of C-nociceptors is about 1.3 m/s[142]. In primary sensory neurons, laser-heat stimulation of small DRG neurons evokes inward currents concomitant with the stimulation[168], and in a subpopulation (about 37%) of primary neurons those laser-heat induced inward currents transform into action potential discharges[54].

Recordings of dorsal horn neurons in response to laser-heat stimulation on the skin have also shown a primarily C-fiber mediated input [133-135], while it has been proposed that TRPV1^{+} Aδ fibers do contribute to this input as well [135]. The results showed here demonstrate that in the dorsal horn, encoding of suprathreshold laser-heat stimulation is mainly mediated by C-fiber input, with a mean neuron threshold of 40.1 °C for WDR neurons and 43.3 °C for HTM neurons.

4.2.2 Spinal encoding of noxious heat

The proportions of nociceptive neurons that responded to laser stimulation were a third of the total recorded WDR neurons and one half of the total recorded HTM neurons, which are known to receive input from nociceptive primary afferents. In the case of HTM neurons, the afferent input was only nociceptive, while WDR neurons processed both non-nociceptive and nociceptive input [80]. The fact that none of LTM neurons responded to laser stimuli corroborates the noxious quality of the laser simulator used, since LTM neurons only possess input from non-nociceptive Aβ fibers and thus are not activated by laser-heat stimuli [134]. It remains to be investigated if the percentage of responding neurons would increase by increasing laser intensities; however, that might compromise tissue damage and seems to be unlikely, since suprathreshold intensities (100 mW) much higher than the heat withdrawal threshold of the animals (44.48 ± 4.43 mW) were applied.

In the present study the recording depth of laser-heat sensitive neurons were distributed homogeneously among all laminae from the spinal dorsal horn. These observations are in contrast with what has been published before [133-135]. In rats using CO_2 laser stimulation[133] it has been shown that laser responsive neurons are located in mainly two depths of the dorsal horn: a superficial zone between 100-400 μm depth, and then a deeper zone below 600 μm. Sikandar and collaborators recorded only WDR neurons in the deep dorsal horn (lamina V - IV) and NS neurons in the superficial dorsal horn (lamina I), though they mention the existence of WDR neurons in the superficial dorsal horn, they excluded them from their study [134]; and Zhang and collaborators recorded laser sensitive neurons in the dorsal horn only from lamina I [135].

The mean heat withdrawal threshold for laser-heat stimuli in awake animals was 44.48 ± 4.43 mW. Laser stimuli of this power elicited a local increase in skin surface temperature of 8.13 ± 0.07 °C. Considering skin hind paw temperature of about 33 °C, in the experiments presented here noxious temperatures occurred starting at 41 °C. This threshold is similar to the activation threshold for the TRPV1 receptor in DRG primary culture, which has its peak activity at 42 °C [131], and is very similar to the mean threshold estimated in this research for WDR neurons (40.1 °C), and HTM neurons (43.3 °C). In fact, this might indicate that laser-heat stimuli would reach threshold for WDR neurons before HTM neurons in the dorsal horn.

Interestingly, the firing rates to laser-heat stimulation tended to be higher for HTM neurons than for WDR neurons. Upon noxious mechanical stimulation, dorsal horn WDR neurons usually show higher firing of action potentials than HTM neurons [169], and the same observation was made before in the case of laser-heat stimulation [134]. These discrepancies might be related to the nature of laser-heat stimuli. Causes of this higher firing rate in HTM neurons in response to laser stimulation might be: (a) afferent input differences between HTM and WDR neurons; input of HTM neurons might include more CMH fibers than the input of WDR neurons, or (b) differences in the synaptic properties in which transmission of laser-heat induced signals from primary afferents to WDR neurons occurred at intensities that did not reach the threshold for those neurons.

The most striking observation from this study are the markedly smaller heat-sensitive receptive fields in comparison with the mechanical receptive fields of the laser-sensitive neurons. In cutaneous C-fiber nociceptors in monkey, the mechano-sensitive receptive fields coincided in size with the laser-heat sensitive receptive fields [10]. Until now, the differences in size between mechanosensitive and heat-sensitive receptive fields have not been described by electrophysiology, because studies on dorsal horn neurons properties to heat stimulation either used contact heat, which unavoidably activates concomitant mechanical afferents, or CO_2 laser stimulation, which possesses much larger stimulation diameters than diode laser, and does not penetrate the skin homogeneously therefore elicits asynchronous afferent activation. There are only two studies on infrared diode laser and spinal dorsal horn recordings (1340 nm and 920 nm)[134, 135]. However, neither information about size of mechanical nor heat receptive fields of the recorded neurons were reported.

The type of afferents that encode the differences in receptive field size upon mechanical vs heat stimulation modalities in dorsal horn neurons might vary between WDR and HTM neuron types. So far, afferent fiber input types determined with mechanical stimulation of their receptive fields has been described. The input of WDR neurons with receptive fields in glabrous skin include rapidly adapting (RA) and slowly adapting (SA) mechanoreceptive input, namely RAI-LTMR, SAII-LTMR, SAI-LTMR and SA-HTMR, which are associated with Aβ, Aδ-HTMR and C-HTMR afferent fibers [170]. From them, only the latter two are nociceptive. Since the responses of WDR neurons increase gradually to graded increases of noxious stimulations, it is thought that Aδ- and C-fiber nociceptors are converging on those neurons as well as large diameter Aβ sensitive mechanoreceptive afferents [171]. In contrast, input of HTM neurons with receptive fields in glabrous skin only include Aδ-HTMRs and C-HTMRs. There might be differences in the peripheral branching patterns between fibers that are sensitive to thermal or mechanical modalities, where in the laser sensitive HTM neurons a higher proportion of C-HTMRs might converge than in the laser sensitive WDR neurons.

4.2.3   Implications in human heat pain signaling

In humans there is some evidence that supports the observations obtained here. In a case of nerve root lesion, Lorenz and co-workers observed that dermatomes were smaller for laser-heat than for touch stimulation [140]. In this case, only by assessing LEPs it was possible to detect a clear impairment in spatial acuity as a consequence of the root lesion. LEPs were completely absent for laser-heat stimulations at the affected dermatomes while showing normal signals in the unaffected control dermatomes. They conclude that due to unmyelinated C-fibers, pain dermatomes are narrower than tactile dermatomes[140].

It has been described that a distinct activation of C- or Aδ-fibers is possible using different methods of laser stimulation[172]. One of these methods consists of using laser-heat pulses to reach specifically the threshold temperature for C- fibers (40 °C), which is lower than for Aδ-fibers (46 °C). This can be done by 1) exposing the skin to two repeated heat ramps, the first intended to activate C-Fibers reaching 40 °C (50 °C/s, 150 ms) and after 5 s a second heat ramp is applied reaching 48 °C, intended to activate Aδ-fibers; or 2) by using a low intensity laser beam and interpose a thin aluminum plate with perforations of 0.125 mm^2 as a spatial filter.

Another method is to use small diameter laser stimulators. Laser stimulators with diameter under 0.5 mm have a probability of 0.9 to activate C-fibers in humans, mainly because of the distribution density of C-fiber terminals in the skin[172]. In this study, a laser stimulator with a beam diameter of 0.15 mm was used, which is three times smaller than the estimate proposed. Then, the chances to activate C-fiber with our laser stimulator are much higher than before.

4.2.4   Technical considerations

The characteristics of the laser stimulation on the skin in humans are often described as punctate, which is a quality associated with C-fiber nociceptive processing.

In the results shown here, laser stimulation pulses delivered in the skin provided a very rapid rise of skin temperature in a small delimited area, demonstrating a high spatial resolution. Moreover, the increase in temperature was transient, coming back to baseline levels in a couple of seconds and did not show any heat accumulation among repetitions (Figure 11D). Temporal resolution was therefore appropriate for nociception studies.

4.2.5   Summary and conclusions

Despite the vast knowledge about transduction mechanisms of noxious laser-heat stimulation in primary afferents, very little is known at the level of spinal dorsal horn neurons. In this study we show that the processing of peripheral contactless noxious heat stimulation is carried out by a subset of WDR and HTM neurons. Their main characteristics are: 1) neurons that respond to suprathreshold laser-heat stimulation are only nociceptive, 2) laser sensitive neurons are found at all depths of the dorsal horn, 3) the heat-receptive fields are smaller than their mechanosensitive re-

ceptive field and always located inside mechanosensitive receptive fields, 4) the estimated heat threshold for these neurons is comparable to the heat withdrawal threshold in awake rats.

4.3 A role of TRPM3 in transduction of laser-heat stimuli to the dorsal horn of the spinal cord

From the electrophysiology experiments it was concluded that the transmission of noxious laser-heat stimulation to the dorsal horn of the spinal cord was carried mostly, if not all, by polymodal C-Fibers. Reasons to argue that the TRPM3 channel, together with TRPV1 and potentially other heat sensing ion channels are expressed primarily in unmyelinated C-fibers and serve as detectors of noxious heat stimuli are mainly two.

First the threshold activation for TRPM3 channels in heterologous expression systems was 614.85 µJ. While TRPV1 channels are expressed in small diameter fibers and in some small subset of Aδ-fibers, TRPM3 channels have been so far only found in small diameter sensory neurons[57]. Therefore, the idea that TRPM3$^+$ sensory neurons are responsible for laser-heat detection and transmission to the dorsal horn of the spinal cord is plausible, without discarding that TRPV1$^+$ neurons also play an important role in the process.

It is expected then, that TRPM3$^+$ afferent fibers terminate in the same laminae in the dorsal horn of the spinal cord as polymodal CMH fibers. No reports have been found so far regarding the question if those fibers expressing the TRPM3 channel terminate in some specific areas of the dorsal horn. This is however unlikely since we observed laser-heat sensitive neurons among all layers of the dorsal horn.

In a more integrative way, heat-gated ion channels in primary sensory neurons act in a collaborative way giving the input to WDR and HTM laser sensitive neurons. It is plausible that the differences in input proposed by the electrophysiology results explaining the differences in laser-heat sensitive and mechanosensitive receptive field sizes are reflected by different proportions of neurons co-expressing TRPM3 and TRPV1, and maybe even other heat sensitive ion channels. Indeed, recently a report has recently demonstrated that three ion channels are involved in the detection of noxious heat in mice. In this study they developed triple knockout mice for TRPV1, TRPM3 and TRPA1 which show completely abolished noxious heat detection [155] Since the threshold for laser-heat of the TRPM3 channel was higher than the threshold for TRPV1, a bigger proportion of peripheral input containing this receptor might end in dorsal horn laser sensitive HTM neurons than in laser sensitive WDR neurons.

The differences in laser-heat sensitive and mechanosensitive receptive field sizes might be explained at least in part by differences in peripheral input converging on those neurons. Moreover, differences in the proportions of neurons expressing TRPM3 and/or TRPV1, and possibly even other heat sensitive ion channels, could be responsible for those differences in receptive field size. Since the threshold for laser-heat activation of the TRPM3 channel is higher than the threshold for TRPV1, a greater proportion of peripheral neurons containing this receptor might end in dorsal horn laser sensitive HTM neurons than for laser sensitive WDR neurons. Those neurons may or may not contain the TRPV1 channel.

5 SUMMARY

This study investigates peripheral transduction mechanisms for short noxious heat stimuli and the processing of them within the central nervous system. Noxious heat is a natural stimulus that activates peripheral sensory neurons expressing heat-gated ion channels. Recently, the TRPM3 channel has emerged as a noxious heat sensor independent of the well-known TRPV1 and evidence of a direct mechanism involving activation of the MOR regulating TRPM3 channel activity upon chemical stimulation with the neurosteroid PS has been described. Thus, the submitted thesis investigated mechanisms of heat-induced nociception using near-infrared laser stimulation as a rapid, accurate and appropriate way to apply noxious heat. Responses to laser-heat were analyzed at two different levels: *in vitro* by functional assays on heterologous expression systems and primary culture of sensory neurons and *in vivo* by behavioral experiments and electrophysiological recordings at the dorsal horn of the spinal cord in response to peripheral laser-heat stimulation.

The main findings of this study are the following:

1) Laser-heat activates the TRPV1 and the TRPM3 ion channel in heterologous expression systems with activation thresholds of about 574 µJ and 615 µJ.

2) Response amplitudes of TRPM3 upon chemical activation with 50 µM PS exceeded those of maximum laser stimulation (1.5 ± 0.003 of the ratio 340/380 versus 0.66 ± 0.011; n= 30 and 49, $p < 0.001$, Mann-Whitney Test).

3) Both chemical- and thermal- induced activity of the TRPM3 channel in heterologous expression systems co-expressing the MOR was significantly reduced with DAMGO. This inhibition consisted of 63.4% of agonist-induced responses and 44.5% of laser-heat-induced responses ($p < 0.001$, Mann-Whitney Test).

4) In cultured primary sensory neurons of rats, 15-25% of all neurons analyzed (n= 550) functionally co-expressed TRPV1 and TRPM3 receptors, 38% of the neurons analyzed expressed the TRPV1 receptor independent of TRPM3, 7-8% expressed the TRPM3 but not TRPV1, and 30-41% did not respond to either stimulus.

5) As in the expression system, native DRG neurons of rats displayed a direct inhibition by 18 ± 4.1 and $23 \pm 3\%$ when co-applying the MOR agonist DAMGO with PS ($p < 0.001$ for each compared to vehicle, non-significant differences between them, Mann-Whitney Test).

6) DAMGO did not influence the proportion of neurons responding to capsaicin (10 µM). However, the proportions of neurons co-expressing TRPV1 and TRPM3 were different between vehicle-treated cells (25%) and DAMGO-treated cells (15%).

In conclusion, TRPM3 is an additional neuronal detector for noxious heat stimuli that may be pharmacologically affected via peripherally expressed MOR and thus, by strictly peripherally applied opioids. Therefore, these results suggest new targets for the development of pharmacological treatments of acute and inflammatory pain without inducing the unwanted side-effects of the existing systemic opioid therapy.

In a second part, this thesis investigated the properties of spinal dorsal horn neurons responding to peripherally applied laser-heat. The processing of peripheral, contactless noxious heat stimulation was carried out by a subset of WDR and HTM dorsal horn neurons. The main characteristics of the laser-sensitive neurons were:

1) Laser heat stimuli sufficiently induced pain in animals *in vivo.*

2) All neurons that responded to suprathreshold laser-heat stimulation were nociceptive ones, including one third of the WDR neurons and half of HTM neurons investigated. No laser-heat responses of LTM neurons were found upon laser-heat stimulations confirming the noxious nature of the laser stimulator used.

3) Laser sensitive neurons were found at all depths of the dorsal horn including all laminae I to VI of the spinal cord. Recording depths of laser sensitive neurons ranged between 120-820 μm

4) The peripheral input of those dorsal horn neurons was composed of both, C- and A- fibers; however, laser-heat induced responses were exclusively transmitted by C-fibers.

5) The heat-sensitive receptive fields were smaller than their mechanosensitive receptive field and always located inside mechanosensitive receptive fields. The sizes of the heat receptive fields ranged between 10% and 60% of the mechanical receptive field.

6) The number of AP following laser stimulation was slightly higher in HTM neurons compared to WDR neurons (14 ± 0.7 vs 9 ± 4.3), however not significant, and the latencies after onset of the laser stimulation were 266 ± 16 ms and 308.3 ± 55. These latencies did not significantly change among neuron types.

7) The estimated temperature threshold for these laser sensitive WDR neurons and HTM neurons (40.1 °C versus 43.3 °C; n.s., Mann-Whitney Test) was comparable to the mean heat withdrawal threshold in awake rats (41 °C).

In response to laser-heat stimulation, heat-gated ion channels in primary sensory neurons act in a collaborative way, generating the transduction process which lead to transmission of action potential discharges to WDR and HTM laser sensitive neurons.

The differences in laser-heat sensitive and mechanosensitive receptive field sizes might be explained at least in part by differences in peripheral input converging on those neurons. Moreover, differences in the proportions of neurons expressing TRPM3 and/or TRPV1, and possibly even other heat sensitive ion channels, could be responsible for those differences in receptive field size.

Since the threshold for laser-heat activation of the TRPM3 channel is higher than the threshold for TRPV1, a greater proportion of peripheral neurons containing this receptor might end in dorsal horn laser sensitive HTM neurons than for laser sensitive WDR neurons. Those neurons may or may not contain the TRPV1 channel.

6 REFERENCES

1. Kandel, ER, Schwartz, JH, Jessell, TM: *Principles of neural science,* New York, McGraw-Hill, Health Professions Division, 2000.

2. Treede, RD: Neurophysiological studies of pain pathways in peripheral and central nervous system disorders. *Journal of neurology,* 250**:** 1152-1161, 2003.

3. International Association for the Study of Pain: *IASP Taxonomy.* 2017. Online: https://www.iasp-pain.org/Education/Content.aspx?ItemNumber=1698&navItemNumber=576, Stand: 14.12.2017.

4. Cohen, M, Quintner, J, van Rysewyk, S: Reconsidering the International Association for the Study of Pain definition of pain. *PAIN Reports,* 3**:** e634, 2018.

5. Julius, D, Basbaum, AI: Molecular mechanisms of nociception. *Nature,* 413**:** 203-210, 2001.

6. Scholz, J, Woolf, CJ: Can we conquer pain? *Nature neuroscience,* 5 Suppl**:** 1062-1067, 2002.

7. Todd, AJ: Neuronal circuitry for pain processing in the dorsal horn. *Nature reviews Neuroscience,* 11**:** 823-836, 2010.

8. Messlinger, K: [What is a nociceptor?]. *Der Anaesthesist,* 46**:** 142-153, 1997.

9. Treede, RD, Meyer, RA, Raja, SN, Campbell, JN: Evidence for two different heat transduction mechanisms in nociceptive primary afferents innervating monkey skin. *J Physiol,* 483 (Pt 3)**:** 747-758, 1995.

10. Treede, RD, Meyer, RA, Campbell, JN: Comparison of heat and mechanical receptive fields of cutaneous C-fiber nociceptors in monkey. *J Neurophysiol,* 64**:** 1502-1513, 1990.

11. Wooten, M, Weng, HJ, Hartke, TV, Borzan, J, Klein, AH, Turnquist, B, Dong, X, Meyer, RA, Ringkamp, M: Three functionally distinct classes of C-fibre nociceptors in primates. *Nature communications,* 5**:** 4122, 2014.

12. D'Mello, R, Dickenson, AH: Spinal cord mechanisms of pain. *British journal of anaesthesia,* 101**:** 8-16, 2008.

13. Vriens, J, Voets, T: Sensing the heat with TRPM3. *Pflugers Archiv : European journal of physiology*, 2018.

14. Vriens, J, Nilius, B, Voets, T: Peripheral thermosensation in mammals. *Nat Rev Neurosci,* 15**:** 573-589, 2014.

15. Julius, D: TRP channels and pain. *Annual review of cell and developmental biology,* 29**:** 355-384, 2013.

16. Liao, M, Cao, E, Julius, D, Cheng, Y: Structure of the TRPV1 ion channel determined by electron cryo-microscopy. *Nature,* 504**:** 107-112, 2013.

17. Bevan, S, Quallo, T, Andersson, DA: Trpv1. *Handbook of experimental pharmacology,* 222**:** 207-245, 2014.

18. Elitt, CM, Malin, SA, Koerber, HR, Davis, BM, Albers, KM: Overexpression of artemin in the tongue increases expression of TRPV1 and TRPA1 in trigeminal afferents and causes oral sensitivity to capsaicin and mustard oil. *Brain Res,* 1230**:** 80-90, 2008.

19. Bae, YC, Oh, JM, Hwang, SJ, Shigenaga, Y, Valtschanoff, JG: Expression of vanilloid receptor TRPV1 in the rat trigeminal sensory nuclei. *J Comp Neurol,* 478**:** 62-71, 2004.

20. Kobayashi, K, Fukuoka, T, Obata, K, Yamanaka, H, Dai, Y, Tokunaga, A, Noguchi, K: Distinct expression of TRPM8, TRPA1, and TRPV1 mRNAs in rat primary afferent neurons with adelta/c-fibers and colocalization with trk receptors. *J Comp Neurol,* 493**:** 596-606, 2005.

21. Binzen, U, Greffrath, W, Hennessy, S, Bausen, M, Saaler-Reinhardt, S, Treede, RD: Co-expression of the voltage-gated potassium channel Kv1.4 with transient receptor potential channels (TRPV1 and TRPV2) and the cannabinoid receptor CB1 in rat dorsal root ganglion neurons. *Neuroscience,* 142**:** 527-539, 2006.

22. Caterina, MJ, Leffler, A, Malmberg, AB, Martin, WJ, Trafton, J, Petersen-Zeitz, KR, Koltzenburg, M, Basbaum, AI, Julius, D: Impaired nociception and pain sensation in mice lacking the capsaicin receptor. *Science,* 288**:** 306-313, 2000.

23. Voets, T, Droogmans, G, Wissenbach, U, Janssens, A, Flockerzi, V, Nilius, B: The principle of temperature-dependent gating in cold- and heat-sensitive TRP channels. *Nature,* 430**:** 748-754, 2004.

24. Nilius, B, Talavera, K, Owsianik, G, Prenen, J, Droogmans, G, Voets, T: Gating of TRP channels: a voltage connection? *J Physiol,* 567**:** 35-44, 2005.

25. Brandt, MR, Beyer, CE, Stahl, SM: TRPV1 Antagonists and Chronic Pain: Beyond Thermal Perception. *Pharmaceuticals,* 5**:** 114-132, 2012.

26. Ramsey, IS, Moran, MM, Chong, JA, Clapham, DE: A voltage-gated proton-selective channel lacking the pore domain. *Nature,* 440**:** 1213-1216, 2006.

27. Amaya, F, Shimosato, G, Nagano, M, Ueda, M, Hashimoto, S, Tanaka, Y, Suzuki, H, Tanaka, M: NGF and GDNF differentially regulate TRPV1 expression that contributes to development of inflammatory thermal hyperalgesia. *Eur J Neurosci,* 20**:** 2303-2310, 2004.

28. Hara, T, Chiba, T, Abe, K, Makabe, A, Ikeno, S, Kawakami, K, Utsunomiya, I, Hama, T, Taguchi, K: Effect of paclitaxel on transient receptor potential vanilloid 1 in rat dorsal root ganglion. *Pain,* 154**:** 882-889, 2013.

29. Davis, JB, Gray, J, Gunthorpe, MJ, Hatcher, JP, Davey, PT, Overend, P, Harries, MH, Latcham, J, Clapham, C, Atkinson, K, Hughes, SA, Rance, K, Grau, E, Harper, AJ, Pugh, PL, Rogers, DC, Bingham, S, Randall, A, Sheardown, SA: Vanilloid receptor-1 is essential for inflammatory thermal hyperalgesia. *Nature,* 405**:** 183-187, 2000.

30. Ta, LE, Bieber, AJ, Carlton, SM, Loprinzi, CL, Low, PA, Windebank, AJ: Transient Receptor Potential Vanilloid 1 is essential for cisplatin-induced heat hyperalgesia in mice. *Molecular pain,* 6**:** 15, 2010.

31. Luo, H, Xu, IS, Chen, Y, Yang, F, Yu, L, Li, GX, Liu, FY, Xing, GG, Shi, YS, Li, T, Han, JS, Wan, Y: Behavioral and electrophysiological evidence for the differential functions of TRPV1 at early and late stages of chronic inflammatory nociception in rats. *Neurochemical research,* 33**:** 2151-2158, 2008.

32. Ruparel, S, Green, D, Chen, P, Hargreaves, KM: The cytochrome P450 inhibitor, ketoconazole, inhibits oxidized linoleic acid metabolite-mediated peripheral inflammatory pain. *Molecular pain,* 8**:** 73, 2012.

33. Martinez-Rojas, VA, Barragan-Iglesias, P, Rocha-Gonzalez, HI, Murbartian, J, Granados-Soto, V: Role of TRPV1 and ASIC3 in formalin-induced secondary allodynia and hyperalgesia. *Pharmacol Rep,* 66**:** 964-971, 2014.

34. Christoph, T, Bahrenberg, G, De Vry, J, Englberger, W, Erdmann, VA, Frech, M, Kogel, B, Rohl, T, Schiene, K, Schroder, W, Seibler, J, Kurreck, J: Investigation of TRPV1 loss-of-function phenotypes in transgenic shRNA expressing and knockout mice. *Molecular and cellular neurosciences,* 37**:** 579-589, 2008.

35. Ha, TH, Ryu, H, Kim, SE, Kim, HS, Ann, J, Tran, PT, Hoang, VH, Son, K, Cui, M, Choi, S, Blumberg, PM, Frank, R, Bahrenberg, G, Schiene, K, Christoph, T, Frormann, S, Lee, J: TRPV1 antagonist with high analgesic efficacy: 2-Thio pyridine C-region analogues of 2-(3-fluoro-4-methylsulfonylaminophenyl)propanamides. *Bioorg Med Chem,* 21**:** 6657-6664, 2013.

36. Uchytilova, E, Spicarova, D, Palecek, J: TRPV1 antagonist attenuates postoperative hypersensitivity by central and peripheral mechanisms. *Molecular pain,* 10**:** 67, 2014.

37. Lima, CK, Silva, RM, Lacerda, RB, Santos, BL, Silva, RV, Amaral, LS, Quintas, LE, Fraga, CA, Barreiro, EJ, Guimaraes, MZ, Miranda, AL: LASSBio-1135: a dual TRPV1 antagonist and anti-TNF-alpha compound orally effective in models of inflammatory and neuropathic pain. *PloS one,* 9**:** e99510, 2014.

38. Honore, P, Chandran, P, Hernandez, G, Gauvin, DM, Mikusa, JP, Zhong, C, Joshi, SK, Ghilardi, JR, Sevcik, MA, Fryer, RM, Segreti, JA, Banfor, PN, Marsh, K, Neelands, T, Bayburt, E, Daanen, JF, Gomtsyan, A, Lee, CH, Kort, ME, Reilly, RM, Surowy, CS, Kym, PR, Mantyh, PW, Sullivan, JP, Jarvis, MF, Faltynek, CR: Repeated dosing of ABT-102, a potent and selective TRPV1 antagonist, enhances TRPV1-mediated analgesic activity in rodents, but attenuates antagonist-induced hyperthermia. *Pain,* 142**:** 27-35, 2009.

39. Kitagawa, Y, Tamai, I, Hamada, Y, Usui, K, Wada, M, Sakata, M, Matsushita, M: Orally administered selective TRPV1 antagonist, JTS-653, attenuates chronic pain refractory to non-steroidal anti-inflammatory drugs in rats and mice including post-herpetic pain. *J Pharmacol Sci,* 122**:** 128-137, 2013.

40. Varga, A, Nemeth, J, Szabo, A, McDougall, JJ, Zhang, C, Elekes, K, Pinter, E, Szolcsanyi, J, Helyes, Z: Effects of the novel TRPV1 receptor antagonist SB366791 in vitro and in vivo in the rat. *Neurosci Lett,* 385**:** 137-142, 2005.

41. Chizh, BA, O'Donnell, MB, Napolitano, A, Wang, J, Brooke, AC, Aylott, MC, Bullman, JN, Gray, EJ, Lai, RY, Williams, PM, Appleby, JM: The effects of the TRPV1 antagonist SB-705498 on TRPV1 receptor-mediated activity and inflammatory hyperalgesia in humans. *Pain,* 132**:** 132-141, 2007.

42. Maher, MP, Bhattacharya, A, Ao, H, Swanson, N, Wu, NT, Freedman, J, Kansagara, M, Scott, B, Li, DH, Eckert, WA, 3rd, Liu, Y, Sepassi, K, Rizzolio, M, Fitzgerald, A, Liu, J, Branstetter, BJ, Rech, JC, Lebsack, AD, Breitenbucher, JG, Wickenden, AD, Chaplan, SR: Characterization of 2-(2,6-dichloro-benzyl)-thiazolo[5,4-d]pyrimidin-7-yl]-(4-trifluoromethyl-phenyl) -amine (JNJ-39729209) as a novel TRPV1 antagonist. *Eur J Pharmacol,* 663**:** 40-50, 2011.

43. Mayorga, AJ, Flores, CM, Trudeau, JJ, Moyer, JA, Shalayda, K, Dale, M, Frustaci, ME, Katz, N, Manitpisitkul, P, Treister, R, Ratcliffe, S, Romano, G: A randomized study to evaluate the analgesic efficacy of a single dose of the TRPV1 antagonist mavatrep in patients with osteoarthritis. *Scand J Pain,* 17**:** 134-143, 2017.

44. Gavva, NR, Treanor, JJ, Garami, A, Fang, L, Surapaneni, S, Akrami, A, Alvarez, F, Bak, A, Darling, M, Gore, A, Jang, GR, Kesslak, JP, Ni, L, Norman, MH, Palluconi, G, Rose, MJ, Salfi, M, Tan, E, Romanovsky, AA, Banfield, C, Davar, G: Pharmacological blockade of the vanilloid receptor TRPV1 elicits marked hyperthermia in humans. *Pain,* 136**:** 202-210, 2008.

45. Gavva, NR, Bannon, AW, Surapaneni, S, Hovland, DN, Jr., Lehto, SG, Gore, A, Juan, T, Deng, H, Han, B, Klionsky, L, Kuang, R, Le, A, Tamir, R, Wang, J, Youngblood, B, Zhu, D, Norman, MH, Magal, E, Treanor, JJ, Louis, JC: The vanilloid receptor TRPV1 is tonically activated in vivo and involved in body temperature regulation. *J Neurosci,* 27**:** 3366-3374, 2007.

46. Krarup, AL, Ny, L, Gunnarsson, J, Hvid-Jensen, F, Zetterstrand, S, Simren, M, Funch-Jensen, P, Hansen, MB, Drewes, AM: Randomized clinical trial: inhibition of the TRPV1 system in patients with nonerosive gastroesophageal reflux disease and a partial response to PPI treatment is not associated with analgesia to esophageal experimental pain. *Scandinavian journal of gastroenterology,* 48**:** 274-284, 2013.

47. Manitpisitkul, P, Mayorga, A, Shalayda, K, De Meulder, M, Romano, G, Jun, C, Moyer, JA: Safety, Tolerability and Pharmacokinetic and Pharmacodynamic Learnings from a Double-Blind, Randomized, Placebo-Controlled, Sequential Group First-in-Human Study of the TRPV1 Antagonist, JNJ-38893777, in Healthy Men. *Clinical drug investigation,* 35**:** 353-363, 2015.

48. Chen, Y, Willcockson, HH, Valtschanoff, JG: Influence of the vanilloid receptor TRPV1 on the activation of spinal cord glia in mouse models of pain. *Exp Neurol,* 220**:** 383-390, 2009.

49. Vardanyan, A, Wang, R, Vanderah, TW, Ossipov, MH, Lai, J, Porreca, F, King, T: TRPV1 receptor in expression of opioid-induced hyperalgesia. *The journal of pain : official journal of the American Pain Society,* 10**:** 243-252, 2009.

50. Mitchell, K, Lebovitz, EE, Keller, JM, Mannes, AJ, Nemenov, MI, Iadarola, MJ: Nociception and inflammatory hyperalgesia evaluated in rodents using infrared laser stimulation after Trpv1 gene knockout or resiniferatoxin lesion. *Pain,* 155**:** 733-745, 2014.

51. Watanabe, M, Ueda, T, Shibata, Y, Kumamoto, N, Ugawa, S: The role of TRPV1 channels in carrageenan-induced mechanical hyperalgesia in mice. *Neuroreport,* 26**:** 173-178, 2015.

52. Woodbury, CJ, Zwick, M, Wang, S, Lawson, JJ, Caterina, MJ, Koltzenburg, M, Albers, KM, Koerber, HR, Davis, BM: Nociceptors lacking TRPV1 and TRPV2 have normal heat responses. *J Neurosci,* 24**:** 6410-6415, 2004.

53. Magerl, W, Fuchs, PN, Meyer, RA, Treede, RD: Roles of capsaicin-insensitive nociceptors in cutaneous pain and secondary hyperalgesia. *Brain : a journal of neurology,* 124**:** 1754-1764, 2001.

54. Greffrath, W, Nemenov, MI, Schwarz, S, Baumgartner, U, Vogel, H, Arendt-Nielsen, L, Treede, RD: Inward currents in primary nociceptive neurons of the rat and pain sensations in humans elicited by infrared diode laser pulses. *Pain,* 99**:** 145-155, 2002.

55. Treede, R-D, Lorenz, J, Baumgärtner, U: Clinical usefulness of laser-evoked potentials. *Neurophysiologie Clinique/Clinical Neurophysiology,* 33**:** 303-314, 2003.

56. Baumgartner, U, Greffrath, W, Treede, RD: Contact heat and cold, mechanical, electrical and chemical stimuli to elicit small fiber-evoked potentials: merits and limitations for basic science and clinical use. *Neurophysiol Clin,* 42**:** 267-280, 2012.

57. Vriens, J, Owsianik, G, Hofmann, T, Philipp, SE, Stab, J, Chen, X, Benoit, M, Xue, F, Janssens, A, Kerselaers, S, Oberwinkler, J, Vennekens, R, Gudermann, T, Nilius, B, Voets, T: TRPM3 is a nociceptor channel involved in the detection of noxious heat. *Neuron,* 70**:** 482-494, 2011.

58. Lechner, SG, Frenzel, H, Wang, R, Lewin, GR: Developmental waves of mechanosensitivity acquisition in sensory neuron subtypes during embryonic development. *EMBO J,* 28**:** 1479-1491, 2009.

59. Straub, I, Krugel, U, Mohr, F, Teichert, J, Rizun, O, Konrad, M, Oberwinkler, J, Schaefer, M: Flavanones that selectively inhibit TRPM3 attenuate thermal nociception in vivo. *Molecular pharmacology,* 84**:** 736-750, 2013.

60. Straub, I, Mohr, F, Stab, J, Konrad, M, Philipp, SE, Oberwinkler, J, Schaefer, M: Citrus fruit and fabacea secondary metabolites potently and selectively block TRPM3. *Br J Pharmacol,* 168**:** 1835-1850, 2013.

61. Held, K, Voets, T, Vriens, J: TRPM3 in temperature sensing and beyond. *Temperature (Austin),* 2**:** 201-213, 2015.

62. Lee, N, Chen, J, Sun, L, Wu, S, Gray, KR, Rich, A, Huang, M, Lin, JH, Feder, JN, Janovitz, EB, Levesque, PC, Blanar, MA: Expression and characterization of human transient receptor potential melastatin 3 (hTRPM3). *The Journal of biological chemistry,* 278**:** 20890-20897, 2003.

63. Suzuki, H, Sasaki, E, Nakagawa, A, Muraki, Y, Hatano, N, Muraki, K: Diclofenac, a nonsteroidal anti-inflammatory drug, is an antagonist of human TRPM3 isoforms. *Pharmacol Res Perspect,* 4**:** e00232, 2016.

64. Chen, L, Chen, W, Qian, X, Fang, Y, Zhu, N: Liquiritigenin alleviates mechanical and cold hyperalgesia in a rat neuropathic pain model. *Scientific reports,* 4**:** 5676, 2014.

65. Wagner, TF, Loch, S, Lambert, S, Straub, I, Mannebach, S, Mathar, I, Dufer, M, Lis, A, Flockerzi, V, Philipp, SE, Oberwinkler, J: Transient receptor potential M3 channels are ionotropic steroid receptors in pancreatic beta cells. *Nature cell biology,* 10**:** 1421-1430, 2008.

66. Law, PY, Wong, YH, Loh, HH: Molecular mechanisms and regulation of opioid receptor signaling. *Annual review of pharmacology and toxicology,* 40**:** 389-430, 2000.

67. Stein, C, Clark, JD, Oh, U, Vasko, MR, Wilcox, GL, Overland, AC, Vanderah, TW, Spencer, RH: Peripheral mechanisms of pain and analgesia. *Brain research reviews,* 60**:** 90-113, 2009.

68. Herlitze, S, Garcia, DE, Mackie, K, Hille, B, Scheuer, T, Catterall, WA: Modulation of Ca2+ channels by G-protein beta gamma subunits. *Nature,* 380**:** 258-262, 1996.

69. Bao, Y, Gao, Y, Yang, L, Kong, X, Yu, J, Hou, W, Hua, B: The mechanism of mu-opioid receptor (MOR)-TRPV1 crosstalk in TRPV1 activation involves morphine anti-nociception, tolerance and dependence. *Channels,* 9**:** 235-243, 2015.

70. Zhang, X, Bao, L, Li, S: Opioid receptor trafficking and interaction in nociceptors. *Br J Pharmacol,* 172**:** 364-374, 2015.

71. Spahn, V, Fischer, O, Endres-Becker, J, Schafer, M, Stein, C, Zollner, C: Opioid withdrawal increases transient receptor potential vanilloid 1 activity in a protein kinase A-dependent manner. *Pain,* 154**:** 598-608, 2013.

72. Endres-Becker, J, Heppenstall, PA, Mousa, SA, Labuz, D, Oksche, A, Schafer, M, Stein, C, Zollner, C: Mu-opioid receptor activation modulates transient receptor potential vanilloid 1 (TRPV1) currents in sensory neurons in a model of inflammatory pain. *Molecular pharmacology,* 71**:** 12-18, 2007.

73. Vetter, I, Wyse, BD, Monteith, GR, Roberts-Thomson, SJ, Cabot, PJ: The mu opioid agonist morphine modulates potentiation of capsaicin-evoked TRPV1 responses through a cyclic AMP-dependent protein kinase A pathway. *Molecular pain,* 2**:** 22, 2006.

74. Baillie, LD, Schmidhammer, H, Mulligan, SJ: Peripheral mu-opioid receptor mediated inhibition of calcium signaling and action potential-evoked calcium fluorescent transients in primary afferent CGRP nociceptive terminals. *Neuropharmacology,* 93**:** 267-273, 2015.

75. Nockemann, D, Rouault, M, Labuz, D, Hublitz, P, McKnelly, K, Reis, FC, Stein, C, Heppenstall, PA: The K(+) channel GIRK2 is both necessary and sufficient for peripheral opioid-mediated analgesia. *EMBO Mol Med,* 5**:** 1263-1277, 2013.

76. Cunha, TM, Roman-Campos, D, Lotufo, CM, Duarte, HL, Souza, GR, Verri, WA, Jr., Funez, MI, Dias, QM, Schivo, IR, Domingues, AC, Sachs, D, Chiavegatto, S, Teixeira, MM, Hothersall, JS, Cruz, JS, Cunha, FQ, Ferreira, SH: Morphine peripheral analgesia depends on activation of the PI3Kgamma/AKT/nNOS/NO/KATP signaling pathway. *Proc Natl Acad Sci U S A,* 107**:** 4442-4447, 2010.

77. Fields, HL: The doctor's dilemma: opiate analgesics and chronic pain. *Neuron,* 69**:** 591-594, 2011.

78. Fields, H: State-dependent opioid control of pain. *Nat Rev Neurosci,* 5**:** 565-575, 2004.

79. Johnson, JL, Hutchinson, MR, Williams, DB, Rolan, P: Medication-overuse headache and opioid-induced hyperalgesia: A review of mechanisms, a neuroimmune hypothesis and a novel approach to treatment. *Cephalalgia : an international journal of headache,* 33**:** 52-64, 2013.

80. Price, DDa, Iowast, Greenspan, JDb, Dubner, Rb: Neurons involved in the exteroceptive function of pain. *Pain,* 106**:** 215-219, 2003.

81. Christensen, BN, Perl, ER: Spinal neurons specifically excited by noxious or thermal stimuli: marginal zone of the dorsal horn. *J Neurophysiol,* 33**:** 293-307, 1970.

82. Woolf, CJ, Fitzgerald, M: Somatotopic organization of cutaneous afferent terminals and dorsal horn neuronal receptive fields in the superficial and deep laminae of the rat lumbar spinal cord. *J Comp Neurol,* 251**:** 517-531, 1986.

83. Kenshalo, DR, Jr., Leonard, RB, Chung, JM, Willis, WD: Responses of primate spinothalamic neurons to graded and to repeated noxious heat stimuli. *J Neurophysiol,* 42**:** 1370-1389, 1979.

84. Coghill, RC, Mayer, DJ, Price, DD: Wide dynamic range but not nociceptive-specific neurons encode multidimensional features of prolonged repetitive heat pain. *J Neurophysiol,* 69**:** 703-716, 1993.

85. Maixner, W, Dubner, R, Bushnell, MC, Kenshalo, DR, Jr., Oliveras, JL: Wide-dynamic-range dorsal horn neurons participate in the encoding process by

which monkeys perceive the intensity of noxious heat stimuli. *Brain Res,* 374**:** 385-388, 1986.

86. Price, DD, Hu, JW, Dubner, R, Gracely, RH: Peripheral suppression of first pain and central summation of second pain evoked by noxious heat pulses. *Pain,* 3**:** 57-68, 1977.

87. Greffrath, W, Schwarz, ST, Busselberg, D, Treede, RD: Heat-induced action potential discharges in nociceptive primary sensory neurons of rats. *J Neurophysiol,* 102**:** 424-436, 2009.

88. Lumpkin, EA, Caterina, MJ: Mechanisms of sensory transduction in the skin. *Nature,* 445**:** 858-865, 2007.

89. Arendt-Nielsen, L, Chen, AC: Lasers and other thermal stimulators for activation of skin nociceptors in humans. *Neurophysiol Clin,* 33**:** 259-268, 2003.

90. Churyukanov, M, Plaghki, L, Legrain, V, Mouraux, A: Thermal detection thresholds of Adelta- and C-fibre afferents activated by brief CO2 laser pulses applied onto the human hairy skin. *PloS one,* 7**:** e35817, 2012.

91. Tarkka, IM, Treede, RD: Equivalent electrical source analysis of pain-related somatosensory evoked potentials elicited by a CO2 laser. *Journal of clinical neurophysiology : official publication of the American Electroencephalographic Society,* 10**:** 513-519, 1993.

92. Treede, RD: Transduction and transmission properties of primary nociceptive afferents. *Rossiiskii fiziologicheskii zhurnal imeni IM Sechenova,* 85**:** 205-211, 1999.

93. Baumgartner, U, Cruccu, G, Iannetti, GD, Treede, RD: Laser guns and hot plates. *Pain,* 116**:** 1-3, 2005.

94. Dusch, M, van der Ham, J, Weinkauf, B, Benrath, J, Rukwied, R, Ringkamp, M, Schmelz, M, Treede, RD, Baumgartner, U: Laser-evoked potentials mediated by mechano-insensitive nociceptors in human skin. *European journal of pain,* 20**:** 845-854, 2016.

95. Meyer, RA, Walker, RE, Mountcastle, VB, Jr.: A laser stimulator for the study of cutaneous thermal and pain sensations. *IEEE transactions on bio-medical engineering,* 23**:** 54-60, 1976.

96. Treede, RD: Peripheral acute pain mechanisms. *Ann Med,* 27**:** 213-216, 1995.

97. Kalliomäki, J, Weng, H-R, Nilsson, H-J, Schouenborg, J: Nociceptive C fibre input to the primary somatosensory cortex (SI). A field potential study in the rat. *Brain Research,* 622**:** 262-270, 1993.

98. Shaw, F-Z, Chen, R-F, Tsao, H-W, Yen, C-T: A multichannel system for recording and analysis of cortical field potentials in freely moving rats. *Journal of Neuroscience Methods,* 88**:** 33-43, 1999.

99. Xia, XL, Peng, WW, Iannetti, GD, Hu, L: Laser-evoked cortical responses in freely-moving rats reflect the activation of C-fibre afferent pathways. *NeuroImage,* 128**:** 209-217, 2016.

100. Garcia-Larrea, L, Frot, M, Valeriani, M: Brain generators of laser-evoked potentials: from dipoles to functional significance. *Neurophysiol Clin,* 33**:** 279-292, 2003.

101. Jankovski, A, Plaghki, L, Mouraux, A: Reliable EEG responses to the selective activation of C-fibre afferents using a temperature-controlled infrared laser stimulator in conjunction with an adaptive staircase algorithm. *Pain,* 154**:** 1578-1587, 2013.

102. Bromm, B, Lorenz, J: Neurophysiological evaluation of pain. *Electroencephalography and clinical neurophysiology,* 107**:** 227-253, 1998.

103. Hansen, HC, Treede, RD, Lorenz, J, Kunze, K, Bromm, B: Recovery from brain-stem lesions involving the nociceptive pathways: comparison of clinical findings with laser-evoked potentials. *Journal of clinical neurophysiology : official publication of the American Electroencephalographic Society,* 13**:** 330-338, 1996.

104. Kazarians, H, Scharein, E, Bromm, B: Laser evoked brain potentials in response to painful trigeminal nerve activation. *The International journal of neuroscience,* 81**:** 111-122, 1995.

105. Bromm, B, Treede, RD: Laser-evoked cerebral potentials in the assessment of cutaneous pain sensitivity in normal subjects and patients. *Revue neurologique,* 147**:** 625-643, 1991.

106. Treede, RD, Lankers, J, Frieling, A, Zangemeister, WH, Kunze, K, Bromm, B: Cerebral potentials evoked by painful, laser stimuli in patients with syringomyelia. *Brain : a journal of neurology,* 114 (Pt 4)**:** 1595-1607, 1991.

107. Lankers, J, Frieling, A, Kunze, K, Bromm, B: Ultralate cerebral potentials in a patient with hereditary motor and sensory neuropathy type I indicate preserved C-fibre function. *Journal of neurology, neurosurgery, and psychiatry,* 54**:** 650-652, 1991.

108. Kochs, E, Treede, RD, Schulte am Esch, J, Bromm, B: Modulation of pain-related somatosensory evoked potentials by general anesthesia. *Anesthesia and analgesia,* 71**:** 225-230, 1990.

109. Bromm, B, Scharein, E, Treede, RD: Analgesic effect of acetylsalicylic acid and lithium as measured with the CO2-laser stimulator. *Pharmacopsychiatry,* 21**:** 109-111, 1988.

110. Treede, RD, Kief, S, Holzer, T, Bromm, B: Late somatosensory evoked cerebral potentials in response to cutaneous heat stimuli. *Electroencephalography and clinical neurophysiology,* 70**:** 429-441, 1988.

111. Bromm, B, Treede, RD: Pain related cerebral potentials: late and ultralate components. *The International journal of neuroscience,* 33**:** 15-23, 1987.

112. Bromm, B, Treede, RD: Human cerebral potentials evoked by CO2 laser stimuli causing pain. *Exp Brain Res,* 67**:** 153-162, 1987.

113. Bromm, B, Jahnke, MT, Treede, RD: Responses of human cutaneous afferents to CO2 laser stimuli causing pain. *Exp Brain Res,* 55**:** 158-166, 1984.

114. Bromm, B, Treede, RD: Nerve fibre discharges, cerebral potentials and sensations induced by CO2 laser stimulation. *Human neurobiology,* 3**:** 33-40, 1984.

115. Bromm, B, Neitzel, H, Tecklenburg, A, Treede, RD: Evoked cerebral potential correlates of C-fibre activity in man. *Neurosci Lett,* 43**:** 109-114, 1983.

116. Bromm, B, Treede, RD: CO2 laser radiant heat pulses activate C nociceptors in man. *Pflugers Archiv : European journal of physiology,* 399**:** 155-156, 1983.

117. Haimi-Cohen, R, Cohen, A, Carmon, A: A model for the temperature distribution in skin noxiously stimulated by a brief pulse of CO2 laser radiation. *J Neurosci Methods,* 8**:** 127-137, 1983.

118. Kenton, B, Coger, R, Crue, B, Pinsky, J, Friedman, Y, Carmon, A: Peripheral fiber correlates to noxious thermal stimulation in humans. *Neurosci Lett,* 17**:** 301-306, 1980.

119. Coger, R, Kenton, B, Friedman, Y, Crue, BL, Pinsky, JJ, Carmon, A: Characteristics of the event-related brain potential to noxious thermal stimulation in man. *Bull Los Angeles Neurol Soc,* 44**:** 102-116, 1979.

120. Valeriani, M, Pazzaglia, C, Cruccu, G, Truini, A: Clinical usefulness of laser evoked potentials. *Neurophysiol Clin,* 42**:** 345-353, 2012.

121. Garcia-Larrea, L: Objective pain diagnostics: clinical neurophysiology. *Neurophysiol Clin,* 42**:** 187-197, 2012.

122. Welch, AJ, Pearce, JA, Diller, KR, Yoon, G, Cheong, WF: Heat generation in laser irradiated tissue. *Journal of biomechanical engineering,* 111**:** 62-68, 1989.

123. Bashkatov, AN, Genina, EA, Kochubey, VI, Tuchin, VV: Optical properties of human skin, subcutaneous and mucous tissues in the wavelength range from 400 to 2000 nm. *Journal of Physics D: Applied Physics,* 38**:** 2543, 2005.

124. Schieke, SM, Schroeder, P, Krutmann, J: Cutaneous effects of infrared radiation: from clinical observations to molecular response mechanisms. *Photodermatol Photoimmunol Photomed,* 19**:** 228-234, 2003.

125. Tillman, DB, Treede, RD, Meyer, RA, Campbell, JN: Response of C fibre nociceptors in the anaesthetized monkey to heat stimuli: estimates of receptor depth and threshold. *J Physiol,* 485 (Pt 3)**:** 753-765, 1995.

126. Abraira, VE, Ginty, DD: The sensory neurons of touch. *Neuron,* 79**:** 618-639, 2013.

127. Kakigi, R, Shibasaki, H: Estimation of conduction velocity of the spino-thalamic tract in man. *Electroencephalography and clinical neurophysiology,* 80**:** 39-45, 1991.

128. Kakigi, R, Tran, TD, Qiu, Y, Wang, X, Nguyen, TB, Inui, K, Watanabe, S, Hoshiyama, M: Cerebral responses following stimulation of unmyelinated C-fibers in humans: electro- and magneto-encephalographic study. *Neuroscience research,* 45**:** 255-275, 2003.

129. Mitchell, K, Bates, BD, Keller, JM, Lopez, M, Scholl, L, Navarro, J, Madian, N, Haspel, G, Nemenov, MI, Iadarola, MJ: Ablation of rat TRPV1-expressing Adelta/C-fibers with resiniferatoxin: analysis of withdrawal behaviors, recovery of function and molecular correlates. *Molecular pain,* 6**:** 94, 2010.

130. Tzabazis, AZ, Klukinov, M, Crottaz-Herbette, S, Nemenov, MI, Angst, MS, Yeomans, DC: Selective nociceptor activation in volunteers by infrared diode laser. *Molecular pain,* 7**:** 18, 2011.

131. Greffrath, Wa, Nemenov, MIb, Schwarz, Sa, Baumgartner, Ua, Vogel, Ha, Arendt-Nielsen, Lc, Treede, R-Da, Iowast: Inward currents in primary nociceptive neurons of the rat and pain sensations in humans elicited by infrared diode laser pulses. *Pain,* 99**:** 145-155, 2002.

132. Pribisko, AL, Perl, ER: Use of a near-infrared diode laser to activate mouse cutaneous nociceptors in vitro. *J Neurosci Methods,* 194**:** 235-241, 2011.

133. Devor, M, Carmon, A, Frostig, R: Primary afferent and spinal sensory neurons that respond to brief pulses of intense infrared laser radiation: A preliminary survey in rats. *Experimental Neurology,* 76**:** 483-494, 1982.

134. Sikandar, S, Ronga, I, Iannetti, GD, Dickenson, AH: Neural coding of nociceptive stimuli-from rat spinal neurones to human perception. *Pain,* 154**:** 1263-1273, 2013.

135. Zhang, J, Cavanaugh, DJ, Nemenov, MI, Basbaum, AI: The modality-specific contribution of peptidergic and non-peptidergic nociceptors is manifest at the level of dorsal horn nociresponsive neurons. *The Journal of Physiology,* 591**:** 1097-1110, 2013.

136. Baumgartner, U, Tiede, W, Treede, RD, Craig, AD: Laser-evoked potentials are graded and somatotopically organized anteroposteriorly in the operculoinsular cortex of anesthetized monkeys. *J Neurophysiol,* 96**:** 2802-2808, 2006.

137. Bragard, D, Chen, AC, Plaghki, L: Direct isolation of ultra-late (C-fibre) evoked brain potentials by CO2 laser stimulation of tiny cutaneous surface areas in man. *Neurosci Lett,* 209**:** 81-84, 1996.

138. Cruccu, G, Iannetti, GD, Agostino, R, Romaniello, A, Truini, A, Manfredi, M: Conduction velocity of the human spinothalamic tract as assessed by laser evoked potentials. *Neuroreport,* 11**:** 3029-3032, 2000.

139. Iannetti, GD, Leandri, M, Truini, A, Zambreanu, L, Cruccu, G, Tracey, I: Adelta nociceptor response to laser stimuli: selective effect of stimulus duration on

skin temperature, brain potentials and pain perception. *Clinical neurophysiology : official journal of the International Federation of Clinical Neurophysiology,* 115**:** 2629-2637, 2004.

140. Lorenz, J, Hansen, HC, Kunze, K, Bromm, B: Sensory deficits of a nerve root lesion can be objectively documented by somatosensory evoked potentials elicited by painful infrared laser stimulations: a case study. *Journal of neurology, neurosurgery, and psychiatry,* 61**:** 107-110, 1996.

141. Olausson, B: Recordings of polymodal single C-fiber nociceptive afferents following mechanical and argon-laser heat stimulation of human skin. *Experimental Brain Research,* 122**:** 44-54, 1998.

142. Opsommer, E, Masquelier, E, Plaghki, L: Determination of nerve conduction velocity of C-fibres in humans from thermal thresholds to contact heat (thermode) and from evoked brain potentials to radiant heat (CO_2 laser). *Neurophysiol Clin,* 29**:** 411-422, 1999.

143. Spiegel, J, Hansen, C, Treede, RD: Clinical evaluation criteria for the assessment of impaired pain sensitivity by thulium-laser evoked potentials. *Clinical neurophysiology : official journal of the International Federation of Clinical Neurophysiology,* 111**:** 725-735, 2000.

144. Grynkiewicz, G, Poenie, M, Tsien, RY: A new generation of Ca^{2+} indicators with greatly improved fluorescence properties. *The Journal of biological chemistry,* 260**:** 3440-3450, 1985.

145. Zimmermann, M: Ethical guidelines for investigations of experimental pain in conscious animals. *Pain,* 16**:** 109-110, 1983.

146. Waynforth, HB, Flecknell, PA: *Experimental and Surgical Technique in the Rat*, Academic Press, 1992.

147. Lambertz, D, Hoheisel, U, Mense, S: Influence of a chronic myositis on rat spinal field potentials evoked by TTX-resistant unmyelinated skin and muscle afferents. *European journal of pain,* 12**:** 686-695, 2008.

148. Zhang, J, Mense, S, Treede, RD, Hoheisel, U: Prevention and reversal of latent sensitization of dorsal horn neurons by glial blockers in a model of low back pain in male rats. *J Neurophysiol,* 118**:** 2059-2069, 2017.

149. Hoheisel, U, Mense, S: Inflammation of the thoracolumbar fascia excites and sensitizes rat dorsal horn neurons. *European journal of pain,* 19**:** 419-428, 2015.

150. Hoheisel, U, Reuter, R, de Freitas, MF, Treede, RD, Mense, S: Injection of nerve growth factor into a low back muscle induces long-lasting latent hypersensitivity in rat dorsal horn neurons. *Pain,* 154**:** 1953-1960, 2013.

151. Dembla, S, Behrendt, M, Mohr, F, Goecke, C, Sondermann, J, Schneider, FM, Schmidt, M, Stab, J, Enzeroth, R, Leitner, MG, Nunez-Badinez, P, Schwenk, J, Nurnberg, B, Cohen, A, Philipp, SE, Greffrath, W, Bunemann, M, Oliver, D, Zakharian, E, Schmidt, M, Oberwinkler, J: Anti-nociceptive action of peripheral

mu-opioid receptors by G-beta-gamma protein-mediated inhibition of TRPM3 channels. *eLife,* 6, 2017.

152. Demirkhanyan, L, Uchida, K, Tominaga, M, Zakharian, E: TRPM3 gating in planar lipid bilayers defines peculiar agonist specificity. *Channels,* 10**:** 258-260, 2016.

153. Uchida, K, Demirkhanyan, L, Asuthkar, S, Cohen, A, Tominaga, M, Zakharian, E: Stimulation-dependent gating of TRPM3 channel in planar lipid bilayers. *FASEB J,* 30**:** 1306-1316, 2016.

154. Greffrath, W, Binzen, U, Schwarz, ST, Saaler-Reinhardt, S, Treede, RD: Co-expression of heat sensitive vanilloid receptor subtypes in rat dorsal root ganglion neurons. *Neuroreport,* 14**:** 2251-2255, 2003.

155. Vandewauw, I, De Clercq, K, Mulier, M, Held, K, Pinto, S, Van Ranst, N, Segal, A, Voet, T, Vennekens, R, Zimmermann, K, Vriens, J, Voets, T: A TRP channel trio mediates acute noxious heat sensing. *Nature,* 555**:** 662-666, 2018.

156. Jiang, B, Sun, X, Cao, K, Wang, R: Endogenous Kv channels in human embryonic kidney (HEK-293) cells. *Mol Cell Biochem,* 238**:** 69-79, 2002.

157. Salimi, P, Esmaeili, A, Hashemi, M, Behjati, M: Endogenous expression of the atypical chemokine receptor CCX-CKR (CCRL1) gene in human embryonic kidney (HEK 293) cells. *Mol Cell Biochem,* 412**:** 229-233, 2016.

158. Quallo, T, Alkhatib, O, Gentry, C, Andersson, DA, Bevan, S: G protein betagamma subunits inhibit TRPM3 ion channels in sensory neurons. *eLife,* 6, 2017.

159. Badheka, D, Yudin, Y, Borbiro, I, Hartle, CM, Yazici, A, Mirshahi, T, Rohacs, T: Inhibition of Transient Receptor Potential Melastatin 3 ion channels by G-protein betagamma subunits. *eLife,* 6, 2017.

160. Ji, RR, Zhang, Q, Law, PY, Low, HH, Elde, R, Hokfelt, T: Expression of mu-, delta-, and kappa-opioid receptor-like immunoreactivities in rat dorsal root ganglia after carrageenan-induced inflammation. *J Neurosci,* 15**:** 8156-8166, 1995.

161. Schmidt, Y, Gaveriaux-Ruff, C, Machelska, H: mu-Opioid receptor antibody reveals tissue-dependent specific staining and increased neuronal mu-receptor immunoreactivity at the injured nerve trunk in mice. *PloS one,* 8**:** e79099, 2013.

162. Krugel, U, Straub, I, Beckmann, H, Schaefer, M: Primidone inhibits TRPM3 and attenuates thermal nociception in vivo. *Pain,* 158**:** 856-867, 2017.

163. Henrich, F, Magerl, W, Klein, T, Greffrath, W, Treede, RD: Capsaicin-sensitive C- and A-fibre nociceptors control long-term potentiation-like pain amplification in humans. *Brain : a journal of neurology,* 138**:** 2505-2520, 2015.

164. Konig, C, Gavrilova-Ruch, O, von Banchet, GS, Bauer, R, Grun, M, Hirsch, E, Rubio, I, Schulz, S, Heinemann, SH, Schaible, HG, Wetzker, R: Modulation of mu opioid receptor desensitization in peripheral sensory neurons by phosphoinositide 3-kinase gamma. *Neuroscience,* 169**:** 449-454, 2010.

165. Nagy, I, Rang, H: Noxious heat activates all capsaicin-sensitive and also a sub-population of capsaicin-insensitive dorsal root ganglion neurons. *Neuroscience,* 88**:** 995-997, 1999.

166. Nagy, I, Rang, HP: Similarities and differences between the responses of rat sensory neurons to noxious heat and capsaicin. *J Neurosci,* 19**:** 10647-10655, 1999.

167. Jia, S, Zhang, Y, Yu, J: Antinociceptive Effects of Isosakuranetin in a Rat Model of Peripheral Neuropathy. *Pharmacology,* 100**:** 201-207, 2017.

168. Schwarz, S, Greffrath, W, Busselberg, D, Treede, RD: Inactivation and tachyphylaxis of heat-evoked inward currents in nociceptive primary sensory neurones of rats. *J Physiol,* 528**:** 539-549, 2000.

169. Price, DD, Browe, AC: Responses of spinal cord neurons to graded noxious and non-noxious stimuli. *Brain Res,* 64**:** 425-429, 1973.

170. Roudaut, Y, Lonigro, A, Coste, B, Hao, J, Delmas, P, Crest, M: Touch sense: functional organization and molecular determinants of mechanosensitive receptors. *Channels,* 6**:** 234-245, 2012.

171. Price, DD, Dubner, R: Neurons that subserve the sensory-discriminative aspects of pain. *Pain,* 3**:** 307-338, 1977.

172. Plaghki, L, Mouraux, A: How do we selectively activate skin nociceptors with a high power infrared laser? Physiology and biophysics of laser stimulation. *Neurophysiol Clin,* 33**:** 269-277, 2003.

7 APPENDIX

7.1 Laser-heat induced nociception, single cell laser stimulation

7.1.1 Calibration curves of laser intensities

The laser stimulator DL 1470 (Rapp Optoelectronics, Germany) was tested for single and repeated laser stimulations with the laser power sensor 30(150)A-LP1-18 (Ophir Photonics, USA). To achieve this, the laser sensor was located on top of the microscope plate, in order to receive the radiant light of the laser which is located under the plate. For the first experiment, 5 single pulses were applied in different areas inside the laser sensor at a rate of 0.017 Hz, and the laser intensity tested was 34% (139.37 W) of the setup intensity, testing stimulations with pulse durations of 100, 50, 25 and 5 ms width (Figure Appendix 1). The laser sensor detected accurately laser-pulses of 100 (red trace), 50 (orange trace) and 25 (yellow trace) duration times. At duration times below 25 ms the laser sensor was unable to detect the pulses (Figure Appendix 1A). The magnitudes measured by the laser sensor were stable among repetitions, however, they decreased by decreasing laser duration time (Figure Appendix 1B). This was something unexpected, since power measures should be stable over time, only energy should decrease when pulse width decreases, which is also the case in this experiment (Figure Appendix 1C). This phenomenon occurred due to the capacities of the laser detector, which is not made to detect power in such short time scales. Therefore, we decided to calibrate our laser pulses with the sensor by modifying the laser intensities and leaving the pulse width in open pass. Then, a direct relationship can be found between power detected and intensity of the laser, following the formula $Y = 4.1X - 0.03$. Based on this we were able to define the power magnitudes for the cellular experiments (Table Appendix 1).
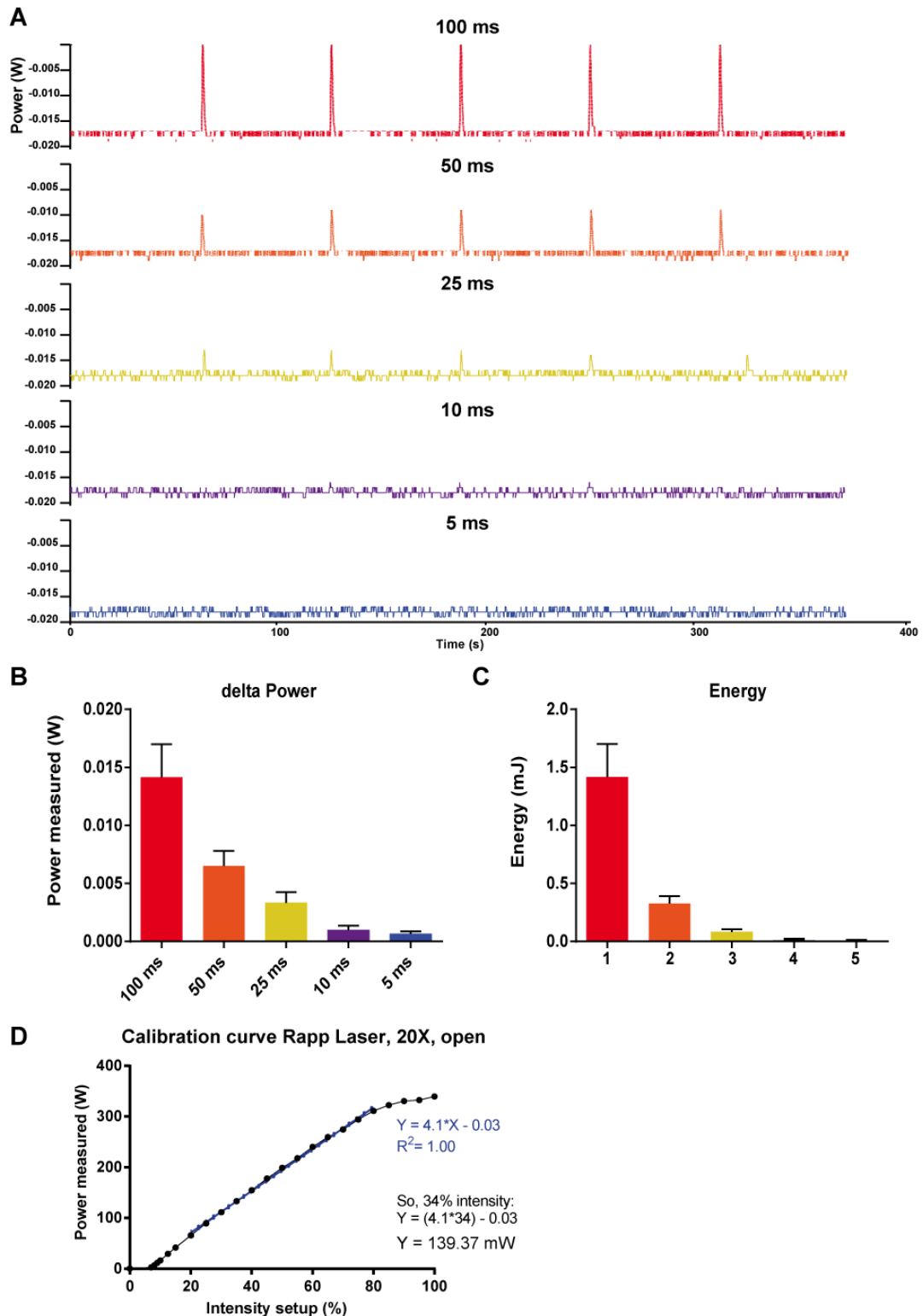
Figure Appendix 1: Calibration of the DL 1470 Rapp laser with a laser sensor. A) single responses and B) mean ± SEM of the change in power registered at 100 ms (red trace), 50 ms (orange trace), 25 ms (yellow trace), 10 ms (purple trace) and 5 ms (blue trace) laser stimulation duration time. Stimuli with duration time of 10 ms or below are not detected by the sensor. C) mean ± SEM of the energy applied on A). D) calibration curve at a magnification fold of the mocroscope of 20X. black dots: power magnitudes detected with the laser sensor. Blue line: linear regression of the values obtained between 20 and 80% of the laser intensity. The formula that describes the regression is shown in blue.

Table Appendix 1: Energy magnitudes used in single-cell laser stimulation experiments (Rapp laser)

Laser intensity setup (%)	Power (mW)[a]	Duration time (ms)	Energy (µJ)
18	73.77	5	368.85
19	77.87	5	389.35
20	81.97	5	409.85
21	86.07	5	430.35
22	90.17	5	450.85
23	94.27	5	471.35
24	98.37	5	491.85
25	102.47	5	512.35
26	106.57	5	532.85
27	110.67	5	553.35
28	114.77	5	573.85
29	118.87	5	594.35
30	122.97	5	614.85
31	127.07	5	635.35
32	131.17	5	655.85
33	135.27	5	676.35
34	139.37	5	696.85

35	143.47	5	717.35
36	147.57	5	737.85
37	151.67	5	758.35
38	155.77	5	778.85
39	159.87	5	799.35
40	163.97	5	819.85
45	184.47	5	922.35

a: Power was determined from Figure Appendix 1D.

7.1.2 Percentage of inhibition in DRG culture following chemical stimulation

DRG, chemical stimulation
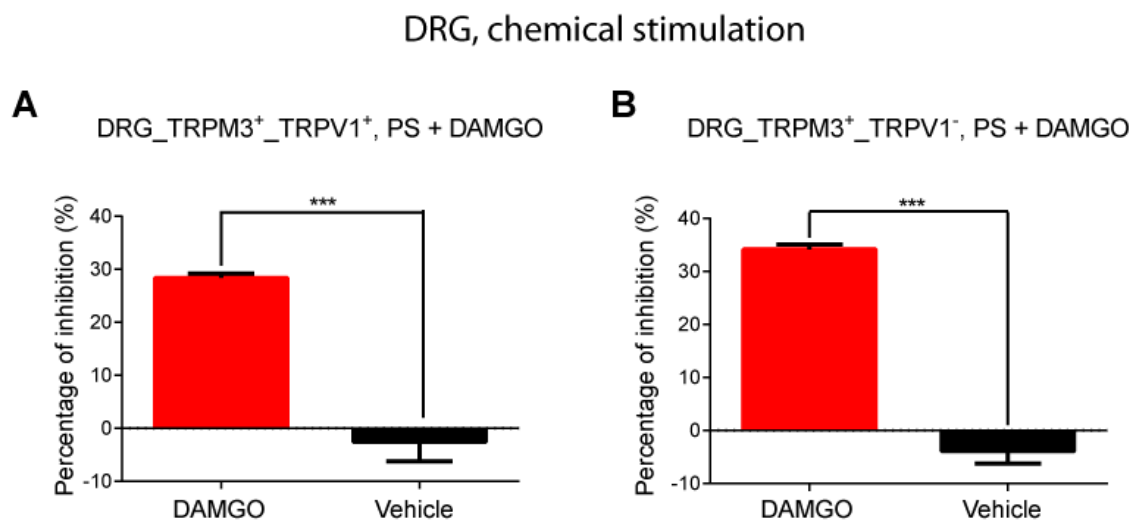
Figure Appendix 2: DRG sensory neurons responding to PS are inhibited by DAMGO. Percentage of inhibition of the chemical induced TRPM3 response mediated by addition of DAMGO during the second PS administration on DRG sensory neurons expressing the TRPM3 channel, sorted by co-expression of the TRPV1 channel.

7.2 Laser-heat stimulation in rat

7.2.1 Time to reach maximum temperature
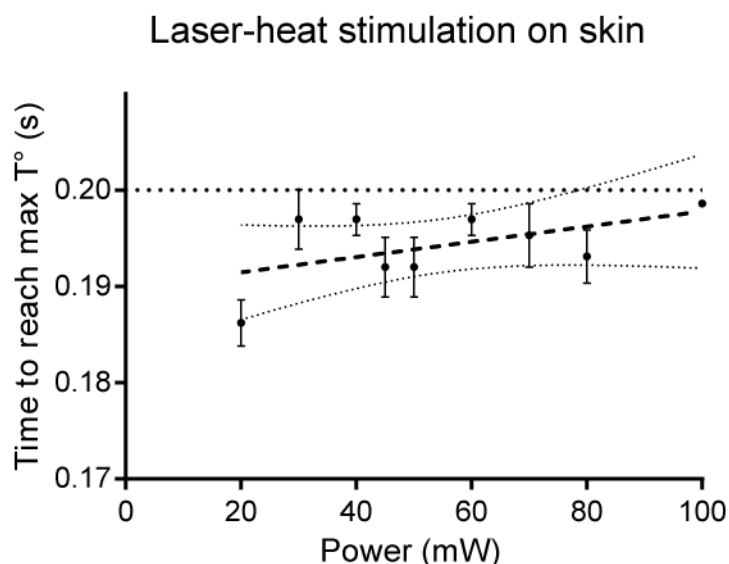
Figure Appendix 3: Non-linear relationship between power used on laser-heat stimulations and the time required reaching the maximum increase in skin temperature. In all cases, a 200 ms laser-heat pulse was used. Time required reaching the maximum increase in temperature in rat glabrous skin of a hind paw explant was always under 200 ms.

7.2.2 Alignment of electrophysiological recordings 1st effective LS

A Original recordings

WDR 1

WDR 2
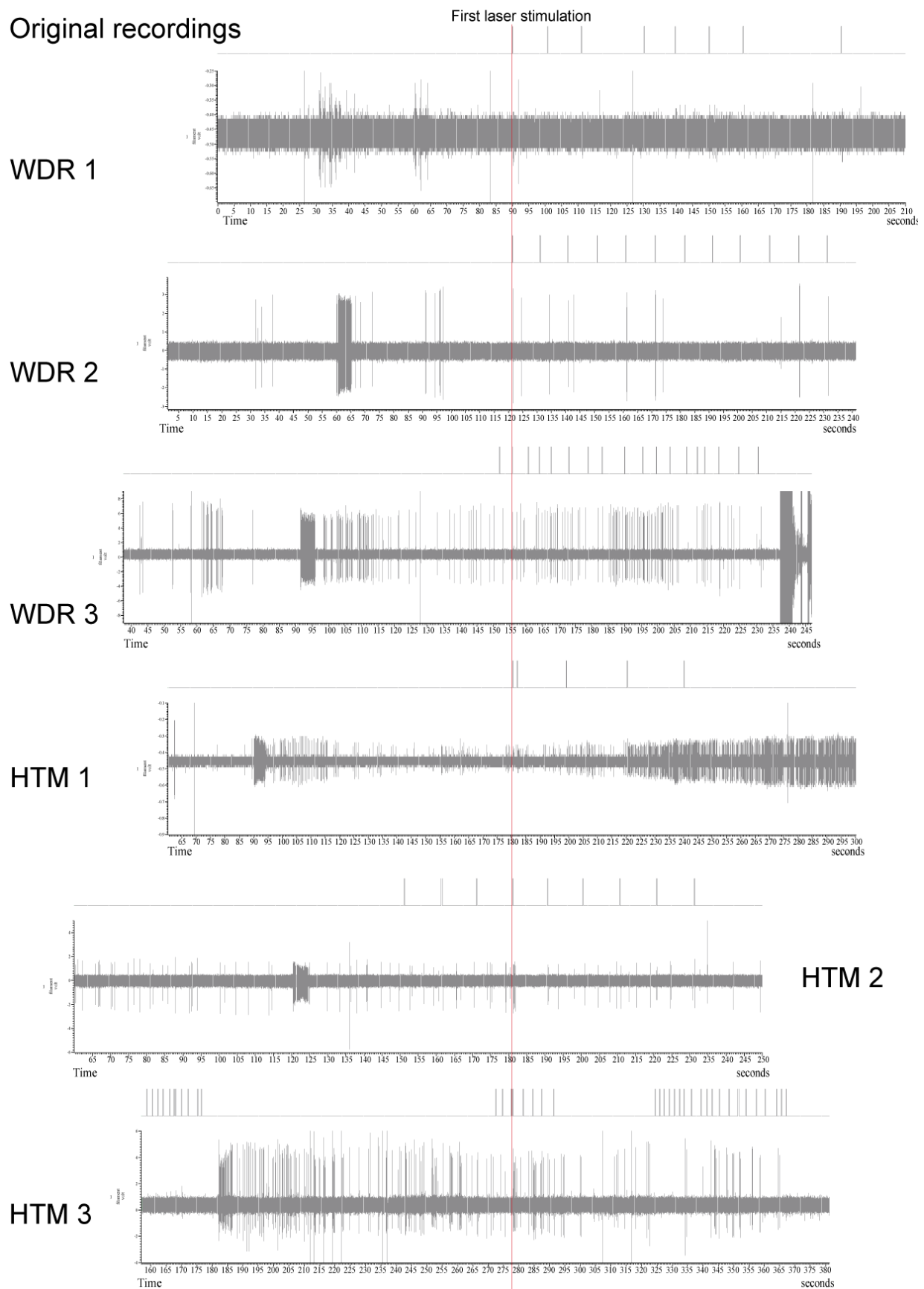
WDR 3

HTM 1

HTM 2

HTM 3

continues in next page

B Instantaneous frequencies

First laser stimulation

WDR 1
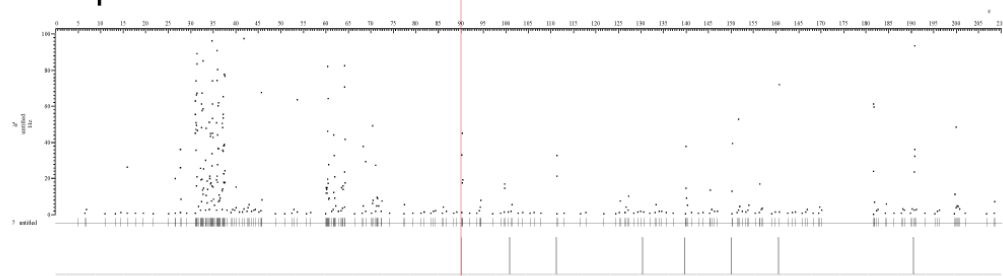
WDR 2
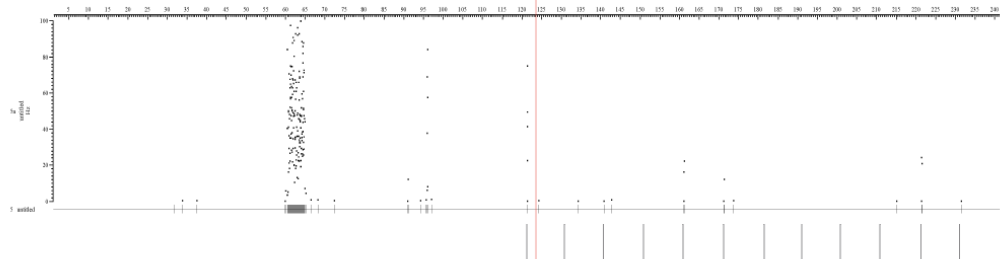
WDR 3
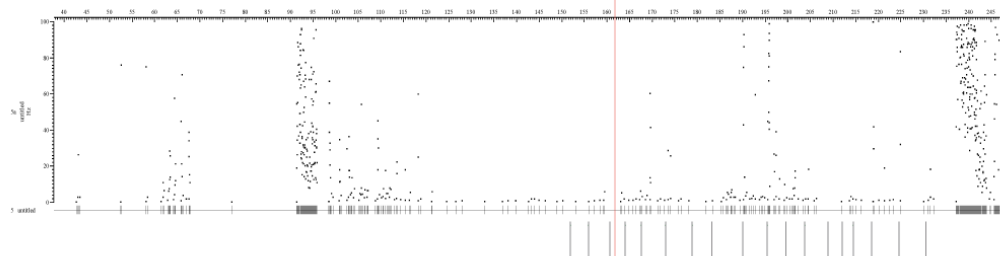
HTM 1
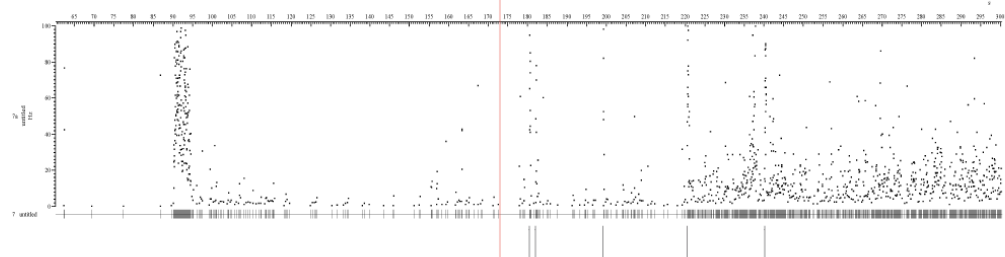
HTM 2
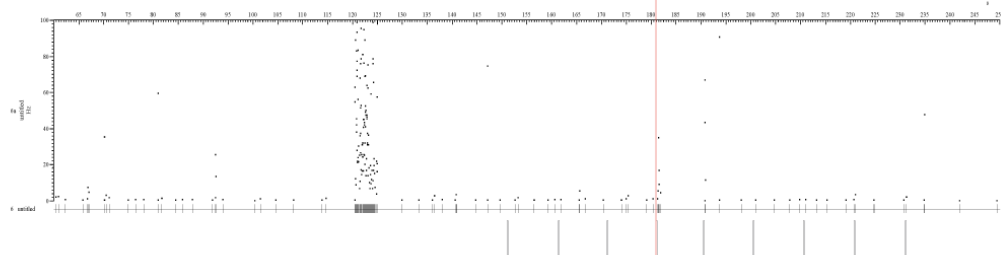
HTM 3
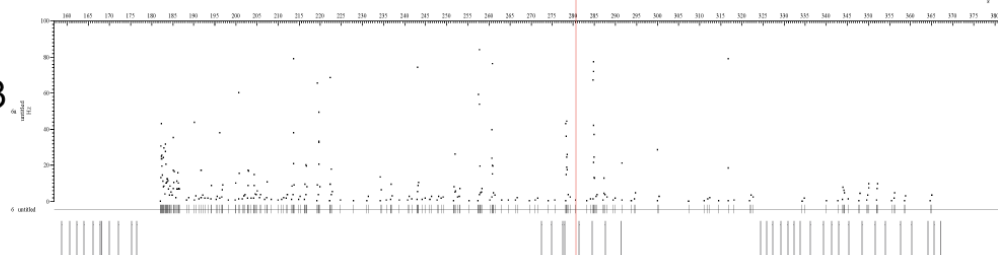
continues in next page

C Interval histogram 0.1 s bin
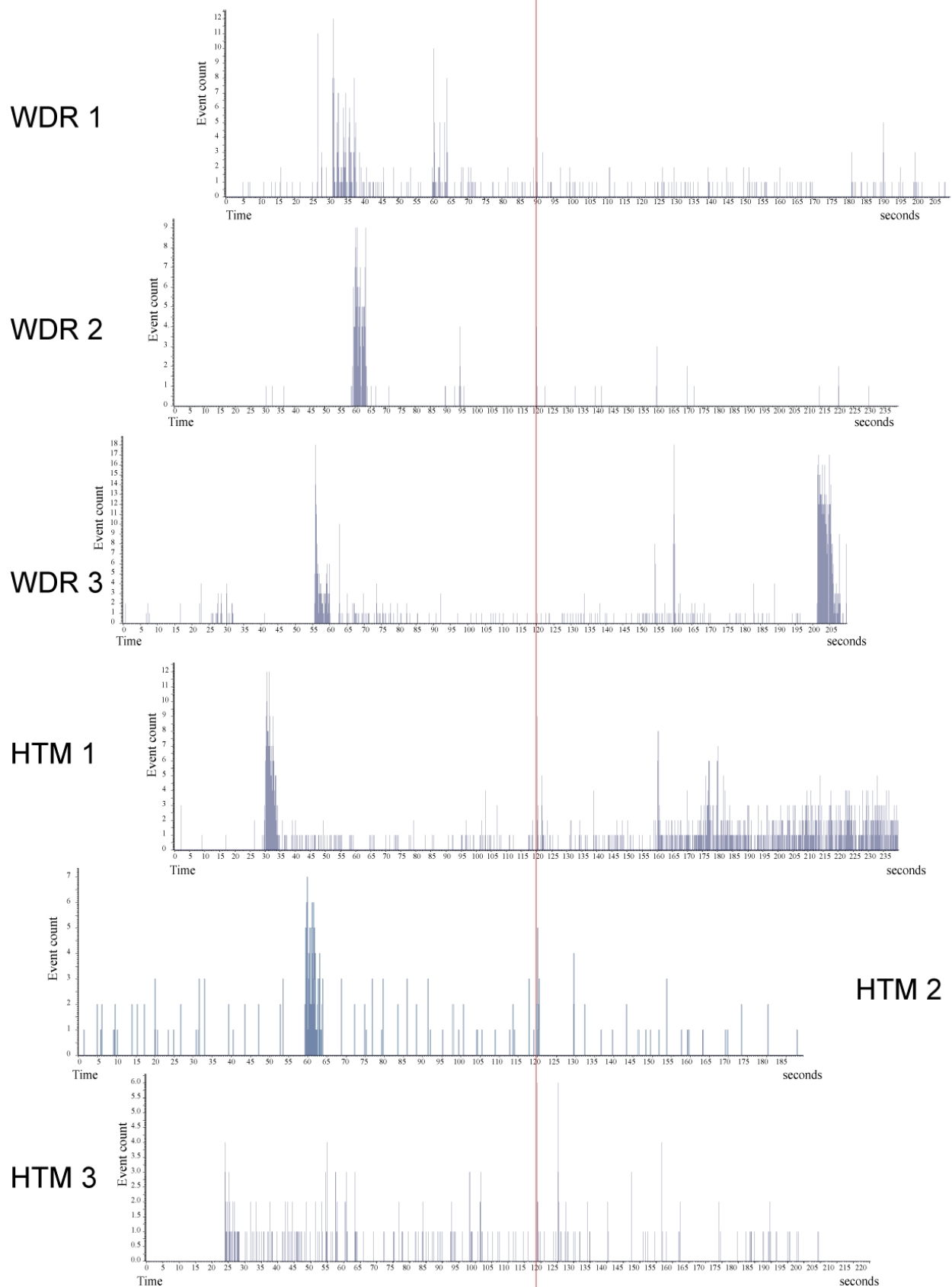
Figure Appendix 4: Responses (action potentials) of laser sensitive neurons aligned for the first effective laser stimulation. A) Original recordings, B) Instantaneous frequen-

cies and C) interval histograms of the laser sensitive neurons that were recorded concomitant with TTL signal. Responses to laser stimulation are depicted in Table 3.

8 CURRICULUM VITAE

PERSONAL DETAILS

Family name, given name:	Nuñez Badinez, Paulina
Date of birth:	April 1st, 1989
Place of birth:	Santiago de Chile
Marital status:	Single
Father:	Nuñez Morales, Ricardo
Mother:	Badinez Villegas, Victoria

SCHOOL EDUCATION

3/1997 – 11/2006	Colegio Alcázar de las Condes, Santiago, Chile
12/2006	Abitur (in Chile called *PSU*)

UNIVERSITY EDUCATION

Since 10/2015	Doctoral student at the University of Heidelberg, Medical Faculty Mannheim, Germany Mentor: Prof. Dr. med. Rolf-Detlef Treede
03/2012 – 04/2014	Master studies in Biotechnology at the Center for Biomedical Research of Universidad Andrés Bello, Santiago, Chile
02/2013 – 04/2013	Exchange program in the Neurophysiology department of the Medical Faculty Mannheim, University of Heidelberg, in frames of the Euro-Latin American Network on Diabetic Microangiopathy (EULAMDIMA) international research network sponsored by SP7 of European commission
03/2007 – 02/2012	Bachelor studies in Engineer in Biotechnology at Universidad Andrés Bello, Santiago, Chile
08/2011 – 02/2012	Studies abroad at Universidad Europea de Madrid, Spain

LANGUAGES

German   Fluently speaking and writing

English   Fluently speaking and writing

Spanish   Mother tongue

PUBLICATIONS THAT AROSE FROM THIS DOCTORAL THESIS

1.   Dembla, S, Behrendt, M, Mohr, F, Goecke, C, Sondermann, J, Schneider, FM, Schmidt, M, Stab, J, Enzeroth, R, Leitner, MG, **Nunez-Badinez, P**, Schwenk, J, Nurnberg, B, Cohen, A, Philipp, SE, Greffrath, W, Bunemann, M, Oliver, D, Zakharian, E, Schmidt, M, Oberwinkler, J: Anti-nociceptive action of peripheral mu-opioid receptors by G-beta-gamma protein-mediated inhibition of TRPM3 channels. eLife, 6, 2017.

2   **Nunez-Badinez, P**, Hoheisel, U, Treede, R.-D., Greffrath, W. Nociceptive spinal dorsal horn neurons of rats have smaller laser-heat sensitive than mechanosenstive receptive fields. Manuscript in process to be submitted to the Journal of Neurophysiology.

POSTER PRESENTATIONS THAT AROSE FROM THIS DOCTORAL THESIS

1.   02-05.03.2016: 95th Annual meeting of the Deutsche Physiologische Gesellschaft (DPG), Lübeck, Germany. Poster title: „Characterization of rat spinal dorsal horn neurons in response to laser-induced heat stimulation"

2.   26-30.09.2016, 16th World congress on Pain from the International Association for the Study on Pain (IASP), Yokohama, Japan: Poster title: "In the rat, laser–heat activated spinal dorsal horn neurons reveal smaller thermosensitive– than mechanosensitive–receptive fields"

3.   (in future) 12-16.09.2018, 17th World congress on Pain from the International Association for the Study on Pain (IASP), Boston, United States of America: Poster title: "Characterization of near IR diode laser stimulator activating nociceptors in the glabrous skin of rat hind paw and nociceptive dorsal horn neuron transmission properties to noxious laser-heat stimulation"

4.   (in future) 12-16.09.2018, 17th World congress on Pain from the International Association for the Study on Pain (IASP), Boston, United States of America: Poster title: "Modulatory effect of the µ-opioid receptor on TRPM3 channel-mediated responses might target differentially co-expressing TRPM3+ and TRPV1+ DRG neuron populations"

CONGRESSES ATTENDED

-14-17.10.2015, Deutscher Schmerzkongress from the *Deutsche Schmerzgesellschaft* (DGSS), Mannheim, Germany

-02-05.03.2016, 95th Annual meeting of the *Deutsche Physiologische Gesellschaft* (DPG), Lübeck, Germany

-26-30.09.2016, 16th World congress on Pain from the International Association for the Study on Pain (IASP), Yokohama, Japan

-19-22.10.2016, Deutscher Schmerzkongress from the *Deutsche Schmerzgesellschaft* (DGSS), Mannheim, Germany

PRIZES

-Reisekostenzuschuss DPG Jahrestagung Lübeck

-DAAD stipendium Funding program number 91525507-57048249

-Stürner Preis 2017 (Paper eLife)

CO-AUTHORSHIP OUTSIDE THE THESIS

1. **Nunez-Badinez, P**, Sepulveda, H, Diaz, E, Greffrath, W, Treede, RD, Stehberg, J, Montecino, M, van Zundert, B: Variable transcriptional responsiveness of the P2X3 receptor gene during CFA-induced inflammatory hyperalgesia. Journal of cellular biochemistry, 119: 3922-3935, 2018

9   ACKNOWLEDGMENTS